GROUND ICE CHARACTERISTICS IN PERMAFROST ON THE FOSHEIM PENINSULA, ELLESMERE ISLAND, N.W.T.

A STUDY UTILIZING GROUND PROBING RADAR AND GEOMORPHOLOGICAL TECHNIQUES

Peter Barry
Department of Geography
McGill University, Montreal
Autumn, 1992.

A Thesis submitted to the Faculty of Graduate Studies and Research in partial fulfillment of the requirements for the Degree of Master of Science.

ABSTRACT

This thesis investigates the nature and distribution of ground ice occurrences on the central Fosheim Peninsula, Ellesmere Island, and assesses the potential for thermokarst in light of possible climatic warming.

Field observations conducted in 1990 and 1991 involved geomorphological and cryostratigraphic examination of twenty-eight ground ice sections exposed in retrogressive thaw slumps and ground penetrating radar surveys of two of the thaw slumps. Samples were taken of ground ice and sediments exposed in thaw slump headwalls for laboratory analysis.

Samples were analyzed for moisture content, grain size distribution, and Atterberg limits. Gravimetric ice contents were calculated and an average ice content profile was constructed for the study area.

Ground ice was found to be an important component of permafrost on the Fosheim Peninsula and was widely associated with Holocene marine sediments. The ice occurred in two stratigraphic settings: from one to five meters in silt and clay, and at ten meters or deeper beneath marine silts. Ice contents were generally found to increase rapidly with depth down to three meters, where maximum ice content was stabilized.

Ground penetrating radar was found to be a useful tool for permafrost research, given its ability to discriminate between frozen and unfrozen soil, as well as between frozen and unfrozen water.

RÉSUMÉ

Le présent mémoire porte sur la distribution et la nature de la glace de sol dans le centre de la péninsule de Fosheim (île Ellesmere) ainsi que sur l'apparition probable de phénomènes de thermokarsts advenant un réchauffement climatique

Les travaux sur le terrain, effectués en 1990 et en 1991, comprennent des relevés géomorphologiques et cryostratigraphiques au droit de 28 coupes mises au jour par des affaissements causés par le dégel ainsi que les relevés géophysiques effectués au moyen d'un géoradar au droit de deux de ces affaissements Des échantillons de glace et de matériel minéral provenant de ces coupes ont fait l'objet de diverses analyses en laboratoire: contenu en eau, distribution de la taille des particules et limites d'Atterberg On a également déterminé le contenu en glace par gravimétrie puis un profil de la zone d'étude indiquant la valeur moyenne de contenu en glace

La glace de sol constitue une caractéristique importante des sédiments marins holocènes pergélisolés de la péninsule de Fosheim. Elle s'observe dans deux contextes stratigraphiques (1) dans des argiles et du limon, de 1 à 5 m de profondeur et (2) à plus de 10 m de profondeur, sous des argiles massives. On observe une augmentation rapide des concentrations en glace jusqu'à une profondeur de 3 mètres, où les valeurs se stabilisent.

L'utilité du géoradar en tant qu'outil de recherche en milieu de pergélisol, vu sa capacité de séparer la glace du matériel minéral et de l'eau, a été confirmée.

ACKNOWLEDGEMENTS

I would like to thank my supervisor Dr W H Pollard for his enthusiastic encouragement and generous support in the field and during the writing of this thesis

This project was supported by the Atmospheric Environment Service, Environment Canada, through their High Arctic Research Support Opportunity, the Association of Canadian Universities for Northern Studies (ACUNS) through the Eben Hopson Fellowship for Northern Studies, the Northern Scientific Training Programme (DINA), and the Polar Continental Shelf Project (Dr. Pollard) Thanks is also owed to Dr Alan Judge of the Terrain Sciences Division of the Geological Survey of Canada, EMR, for the use of the Pulse EKKO III ground probing radar, and for help with the data analysis; and to Dr Sylvia Edlund, also of Terrain Sciences, for support at the Hot Weather Creek Global Change Observatory The Pulse EKKO IV-H prototype GPR was generously lent by Dr Michel Allard of the Centre d'études nordique at Laval University.

Field assistance and technical help were offered by Mr Brian Moorman, Mr Craig Forcese, and Mr. Neil Comer, while technical support in Montreal was provided by Ms Paula Kestleman and Ms Lillian Lee of the McGill University Geography Department, and Mr Frank Caporuscio of the Geotechnical Research Centre, McGill University To these people I offer a sincere thank-you Thanks is also due the staff at Eureka weather station for their kind support and encouragement and great food.

I wish to thank my friends for their help (and commiseration), and my family for their patience and understanding while I worked on this thesis, none of this would have been possible without their support.

TABLE OF CONTENTS

ABSTRACT i
RESUMÉ ii

ACKNOWLEDGEMENTS iii

TABLE OF CONTENTS iv

PERSPECTIVE vi

CHAPTER 1 INTRODUCTION AND LITERATURE REVIEW 1

1 1 Thesis Objectives 1
1 2 Permafrost and Ground Ice 2
1 2 1 Origins of Ground Ice 6
1.3 Ground Ice Detection 6
1 3 1 Conventional Methods 7
1.3.2 Geophysical Techniques 9
1 4 Ground Probing Radar 10
1.4.1 Previous Work 13
1.4.2 Equipment 15
1 4.3 Radar Wave Propagation 16
1 4.4 Depth Determination 17
1 4.5 Depth of Penetration 22
1.4 6 Spatial Resolution 23
1 4 7 Data Processing 25
1.4 8 Interpretation 28
1.5 Effects of Climate Change on Permafrost 30
1.6 Summary 32

CHAPTER 2 STUDY AREA 34

2 1 The Fosheim Peninsula 34
2.1.1 Regional Setting 34
2.1 2 Bedrock Geology 34
2.1.3 Surficial Deposits 37
2.1.4 Physiography 38
2.1.5 Climatological and Glacial History 39
2.1 6 Modern Climate 41
2.2 Study Sites 45
2.2.1 Hot Weather Creek 45
2.2.2 Eureka 49
2.2.3 South Slidre 51
2.2.4 South Fosheim-1 51
2.2.5 South Fosheim-2 52
2.3 Summary 54

CHAPTER 3 METHODOLOGY 56

3.1 Introduction 56
3 2 Ground Probing Radar Survey Methodology 56
3 2 1 Preparation 58
3 2 2 Execution 59
3 2 3 Data Processing 61
3 3 Geological Survey Methodology 63
3 3 1 Field Program 63
3 3.2 Sample Moisture Contents and Chemistry 65
3 3.3 Atterberg Limits 66
3.3 4 Grain Size Analysis 68

CHAPTER 4 RESULTS 69

4.1 Organization of Results 69
4 2 Ground Probing Radar Surveys 69
4 2.1 Hot Weather Creek 1990 69
4 2 2 Eureka Oil Tank Farm 1991 78
4 2 3 Eureka Airstrip 1991 82
4.3 Geological Field Survey 87
4.3.1 Retrogressive Thaw Slumps 92
4.3.1 1 Past Thaw Slump Distribution 92
4.3 1 2 Present Thaw Slump Distribution 97
4.3 1 3 Thaw Slump Morphological Relationships 101
4.3.2 Ice Wedges 106
4.3.3 Soil Mechanics 108
4.3.4 Stratigraphic Relationships 109
4.3.5 Ice Content and Chemistry 114
4.4 Summary 120

CHAPTER 5 DISCUSSION AND CONCLUSIONS 121

5.1 Introduction 121
5.2 Ground Ice Abundance 121
5.2.1 Possible Consequences of Climate Change 123
5.3 Utility of Ground Probing Radar 125
5.4 Future Research 127

BIBLIOGRAPHY 129

"Lemme get this straight. You got a grant to go to the Arctic to look for *ice?* With a *RADAR?!*"

-- One of the author's gainfully unemployed friends.

CHAPTER 1 INTRODUCTION AND LITERATURE REVIEW

1.1 THESIS OBJECTIVES

The primary aim of this research project is to investigate the nature of near surface ground ice bodies, especially massive ground ice, on the Fosheim Peninsula using geological and geomorphological techniques and ground probing radar (GPR), a geophysical tool. It therefore has two basic thrusts, the detection of ground ice, and the analysis of its nature and distribution.

To achieve this aim, this project addresses two basic hypotheses:

1) Ground ice forms a common component of permafrost sediments on the Fosheim Peninsula below marine limit.

2) The physical differences between sediment and ice can be detected by ground probing radar, making it a useful and practical tool for permafrost investigations in this environment.

The first hypothesis is tested using information obtained during field investigations of ground ice exposures at locations on the Fosheim Peninsula. This includes the analysis of physiographic and stratigraphic relationships, macro-scale ice structure and ice chemistry. This section is based on field data collected in 1990 and 1991.

The second hypothesis is tested subjectively by comparing the quality of data returned versus the difficulties experienced using the GPR systems supplied by A. Judge (Terrain Sciences Division, Geological Survey of Canada), and M. Allard (Université Laval). A major consideration after the quality of output is the mechanical reliability of the equipment and its durability in the

face of long distance shipping. Two separate units are tested in different operating conditions.

1.2 PERMAFROST AND GROUND ICE

Permafrost is defined as ground which remains below 0°C for two or more years (Permafrost Subcommittee, 1988). It occurs in a large proportion of Canada as continuous or discontinuous coverage (Figure 1.1). As permafrost is defined in a purely thermal sense, there need actually be no ice in the ground for permafrost to exist. Ice occurring in any form in permafrost is referred to as ground ice. It can have many forms, from microscopic crystals between soil particles in ice bonded material, to massive ice bodies several cubic metres in volume. Common forms of ground ice in order of generally increasing size and expression are: ice lenses and veins, ice wedges, pingo ice, and massive ice beds which can range in size from a few metres to tens of metres in thickness and can extend over several kilometres.

Soil contains *excess ice* when the volume of moisture in the thawed soil is greater than the available pore space. Such soils are *thaw sensitive* because upon thawing, supernatant water is released causing subsidence of the surface proportional to the volume of the ice. When widespread, this effect is referred to as *thermokarst*, due to its superficial resemblance to limestone karst topography.

When the volume of ice is very high compared to that of the soil, it is

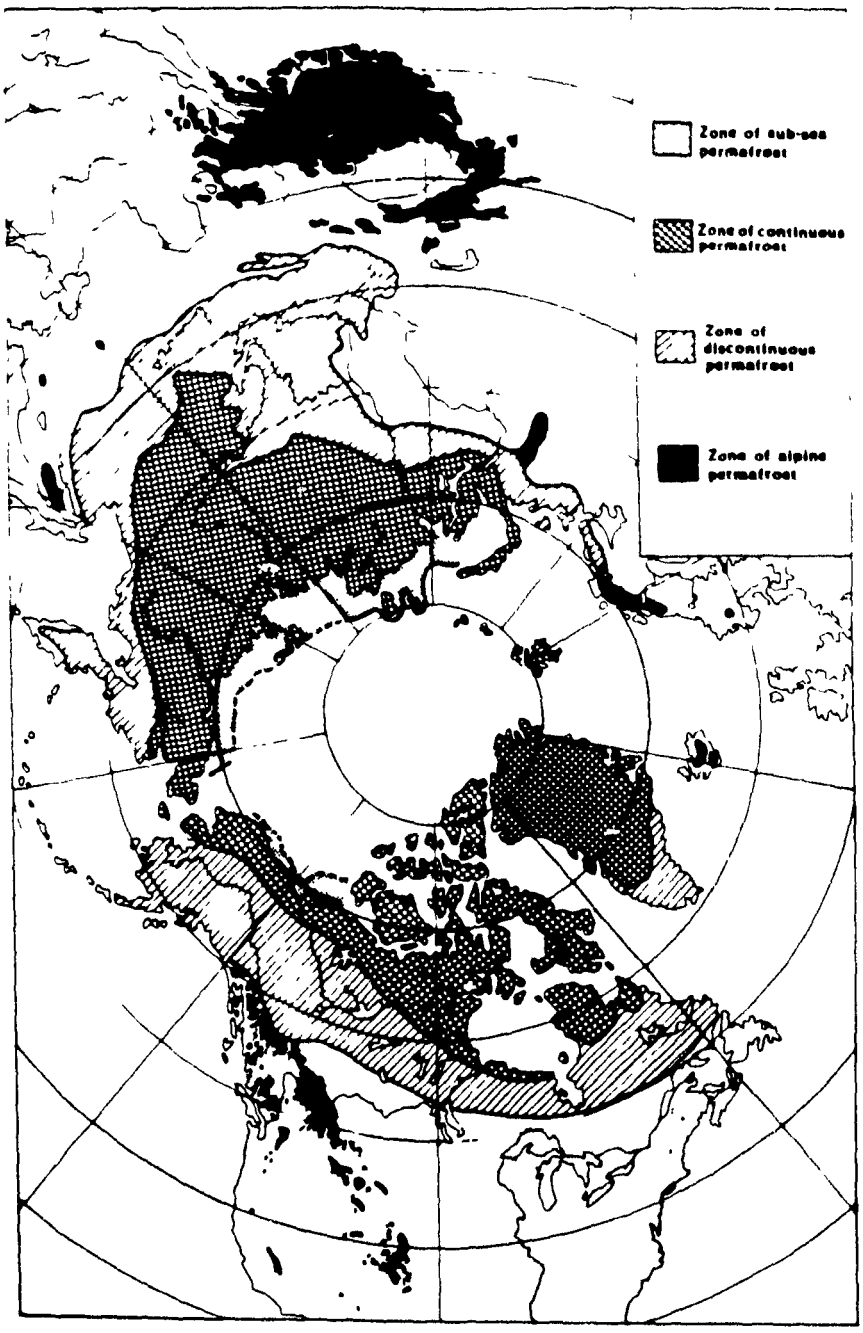

Figure 1.1 World distribution of permafrost. (Péwé, 1983)

termed *massive ice*. More specifically, massive ice is defined gravimetrically as ice content greater than 250% ice to dry weight of soil (Mackay, 1989, p.6).

The nature and distribution of ground ice in the High Arctic in general, and the Fosheim Peninsula in particular, is a subject which has received very little attention from researchers. In Canada, ground ice research has tended to be concentrated in the western Arctic, as this is where most development, especially petroleum exploration, has occurred. Recently, however, more work has been carried out in the islands of the Canadian Arctic Archipelago. Some of the most recent work has been spurred by concerns of global change and its potential impact on the high Arctic (Barry and Pollard, in press; Edlund *et al.*, 1989; Pollard, 1991) as has this project.

Ground ice research in the western Arctic focuses on defining different types of ground ice and assessing their distribution and abundances, as well as exploring mechanisms of formation. Mackay, a pioneer researcher in the field, has investigated the mechanics of pingo development, ice wedge formation, the effect of fire on active layer development, and the aggradation of permafrost into drained lakebeds (Mackay 1963, 1975b, 1977, 1982). His genetic system of ground ice classification divides ground ice into ten types formed by four basic mechanisms of moisture transfer (Mackay, 1972) (Figure 1.2). This classification system is used as the basis for Pollard and Dallimore's (1989) work utilizing crystal structure and orientation.

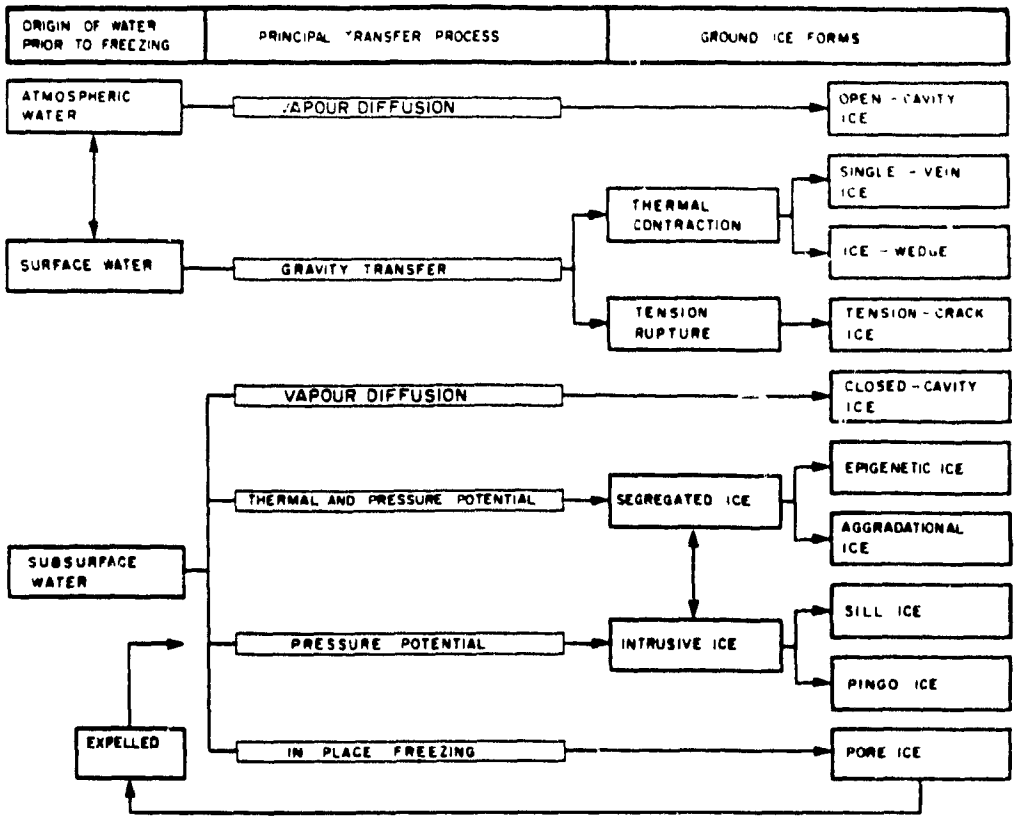

Figure 1.2 Ground ice classification scheme. (Mackay, 1972)

1.2.1 ORIGINS OF GROUND ICE

The origins of massive ground ice have been a topic of debate for several decades. A buried glacier ice origin has been argued by Russian researchers (Solomatin, 1986) based on evidence found in eastern and northern Siberia. Most North American researchers working in the western Arctic have suggested an ice segregation process which creates the ice *in situ* (Mackay, 1972). This argument is based on several forms of observation, including stratigraphy, upper and lower contacts, and geochemical analyses of ice masses. These observations show that most massive ice is conformable with surrounding sediments. Other features indicative of an ice segregation process are: inclusions in the ice of local material, including plant and root material; non glacially-deposited sediments containing massive ice; (Mackay, 1972, 1989); and ice crystallographic textures which are not consistent with buried glacier or snowbank ice (Pollard and Dallimore, 1989). However, recently some North American researchers have suggested that buried glacier ice may have a wider occurrence in the Canadian arctic than previously believed (French and Harry, 1991).

1.3 GROUND ICE DETECTION

Other than its origins, one of the major problems associated with ground ice is locating and delineating bodies of ice which have no obvious surface expression. These include massive segregated ice bodies, ice lenses, buried and/or inactive ice wedges, and areas of ice-rich permafrost. The fact that

these features can have significant effects on topography if they melt is especially important in areas of development, where construction and other human activities can drastically alter ground thermal characteristics.

1.3.1 CONVENTIONAL METHODS OF DETECTION

Brown (1974) presents airphoto interpretations of several permafrost and thermal erosion features, some of which can be used as clues to the existence of hidden ice forms. For example, retrogressive thaw slumps, which can easily be identified from airphotos, often are associated with massive segregated ice or ice-rich permafrost. This method is employed by Pollard (1991) and by Barry and Pollard for this and a related project. Unfortunately, the mechanisms of thaw slump initiation are not fully understood, and the absence of these features does not preclude the presence of ground ice.

Other features visible in airphotos include subsidence areas where ground ice has thawed, producing a chaotic terrain which is easily identified. While the absence of such features again does not preclude the existence of ground ice, they are of much greater spatial extent than retrogressive thaw slumps, and where they surround undisturbed terrain there is a good possibility that the terrain is ice-rich. Several undisturbed areas surrounded by chaotic terrain can be identified in airphotos of the study region and these appear to be residual plains. One of the larger areas was found in 1992 to have several massive ground ice exposures (Pollard, personal communication).

Drilling, especially shallow exploratory drilling, is a common method of locating massive ground ice. The greatest advantage to drilling is its ability to produce direct subsurface samples in the form of core or chips. This allows accurate measurements of ice content variations with depth and identification of soil or sediment type. The Mackenzie Valley Geotechnical Database (EBA, 1990) is an example of a computer based collection of shallow borehole records compiled over many years from the lower Mackenzie Valley and Delta area. Its usefulness for ground ice research has been demonstrated by Pollard and French (1980) in their estimation of the amount of ground ice in near surface sediments on Richards Island, N.W.T., and by Gowan and Dallimore (1990) in their investigation of the occurrence of massive ice in granular deposits.

The high quality of drill core data is offset by the difficulty in drilling, the environmental disruption (depending on the scale of drilling), the high cost, and the limited spatial relevance of what is essentially point source data. Unless one is prepared to drill a large number of holes, it is unrealistic to expect to make anything more than a statistical estimate of ground ice abundance. Ground ice bodies can be discrete, irregular, and limited in extent in such a way as to make interpolation between widely spaced boreholes extremely uncertain (Kovacs and Morey, 1979).

1.3.2 GEOPHYSICAL TECHNIQUES

Several geophysical techniques offer a promising alternative for detecting and delineating massive ground ice and icy permafrost. When used in conjunction with, or as a guide to, a drilling program, some of these methods can produce reliable data on ground ice conditions over a relatively large area (100s of metres) in a short time. Geophysical techniques can be used alone, but with less exact results, as they measure only the effects and not the substance of subsurface anomalies. If drill data is not available, then it may be possible to extrapolate from local natural exposures, such as stream banks or thaw slump faces. This method is employed in this project.

Gravity surveys were performed by Rampton and Walcott (1974) at Involuted Hill, N.W.T. Their results indicated the presence of massive ice bodies (later confirmed by drilling) which appeared as negative gravity anomalies due to their lower density relative to the surrounding sediments. Unfortunately, gravity surveys provide little or no information on depth or thickness of ice masses and require very precise topographical corrections, making them laborious and expensive to conduct. Thus the method is not widely used.

Another method which has been explored involves dual channel thermal infrared sensors mounted on an aircraft (Leschack *et al.*, 1973; Lougeay, 1973, Leschack and Del Grande, 1976), or satellite thermal imagery (Lougeay, 1981). These detect ground ice by sensing the reduced thermal emission of areas

underlain by ice. The system does not give information on ice thickness, but it might be useful for reconnaissance surveys to identify areas underlain by ice.

Resistivity and VLF surveys have been used to detect conductivity contrasts between ice and sediment as well as to detect freeze/thaw boundaries within sediments (Kinney, 1986; Mackay, 1975b). These surveys are ground based and can be carried out fairly easily, yielding data that is not difficult to interpret.

Reflection seismic methods are generally not used for shallow (< 100 m) investigations due to the relatively low frequencies of the energy sources used (50 - 150 Hz) and due to poor air/ground acoustic coupling. New energy sources such as high frequency sparkers may improve shallow performance in the near future if costs can be kept down (McCann *et al.*, 1988). In contrast, refraction seismic surveys (eg. hammer seismic) can be successful in detecting ground ice bodies at shallow depths (McCann *et al.*, 1988). An important advantage this system has over some electrical systems (including GPR) is that elevated soil moisture contents actually improve performance, instead of attenuating the signal and reducing penetration depths.

1.4 GROUND PROBING RADAR

Ground probing radar is used to detect and locate variations in dielectric properties beneath the ground. The method is similar to reflection seismic techniques, except that electromagnetic waves are used in place of mechanical

shock waves. A short, very high frequency electromagnetic pulse is transmitted into the ground. As it propagates downward, some of the energy is reflected back to the surface from boundaries of high dielectric contrast. The two-way travel time required for the transmitted pulse to be reflected back to the receiver on the surface is recorded and later converted to depth values. In a reflection survey, this procedure is repeated at regular intervals along a survey line to generate a profile of the underlying structure (Figure 1.3).

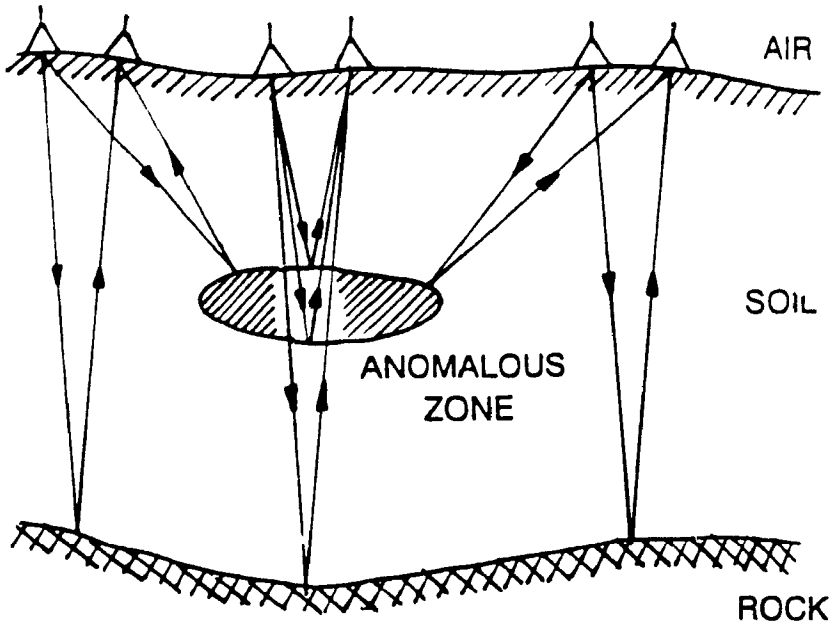

Figure 1.3 Ray paths for a hypothetical subsurface geometry (above) and the idealized results (below). (A Cubed, 1986)

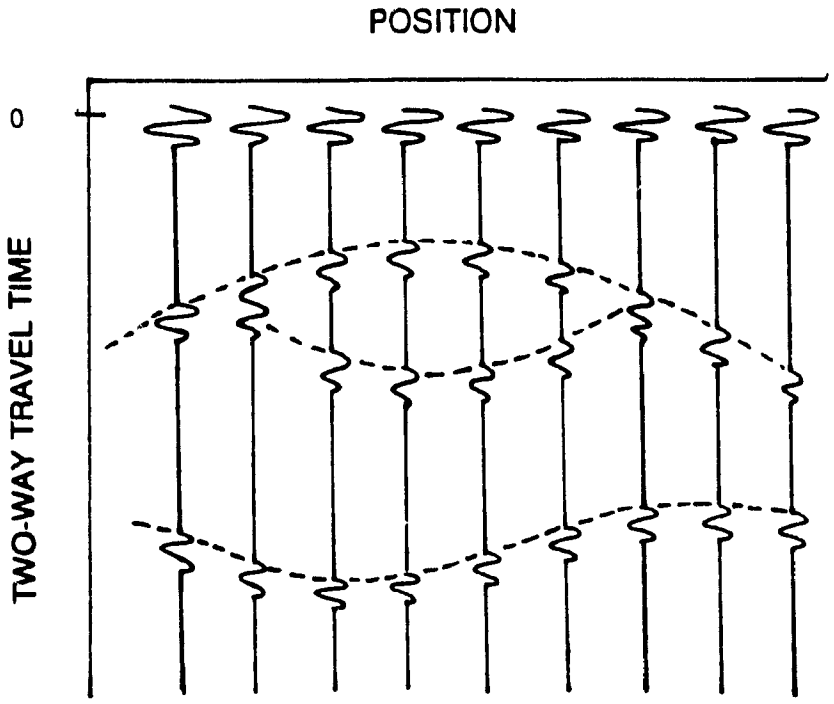

1.4.1 PREVIOUS WORK

Ground probing radar, both as airborne and ground based systems, has seen increased use in recent years. Airborne GPR has the advantage of large area coverage at high speeds over any terrain. However, airborne GPR lacks the horizontal location control of ground based systems, and suffers from a much greater degree of attenuation due to a large air/ground electrical mismatch (Hall *et al.*, 1980). This results in signal loss and reduced depth of penetration. Airborne surveys are also much more expensive to conduct than ground surveys due to aircraft costs.

Ground based GPR overcomes many of these difficulties. Developments in computers and electronics in the late 1980s have resulted in systems which are light, uncomplicated to operate, and portable (ie. a two person survey crew on foot). Some processing can be carried out in the field allowing for changes to be made to a survey or to a drilling program.

Ground probing radar investigations of permafrost and, in particular, of massive ground ice have been carried out sporadically throughout the 1970s and 1980s. The principle research groups have been the Geological Survey of Canada and the Cold Regions Research and Engineering Laboratory (CRREL) of the US Army Corps of Engineers. Most of the work has been carried out in the western Canadian Arctic and in Alaska in connection with petroleum exploration and related development.

In 1976, Davis *et al.* conducted some of the earliest GPR surveys in

permafrost with an analogue impulse radar system. They attempted to map massive ground ice bodies at Involuted Hill near Tuktoyaktuk, N.W.T. They found that radar wave penetration was reduced by the presence of a surface layer of conductive clay. Where this clay was intersected by ice wedges, however, penetration was greatly enhanced, and they were able to detect massive ice bodies beneath the clay. Their conclusion was that ice wedges can act as windows through radar-opaque materials. This phenomenon was also observed at Hot Weather Creek in 1990. Penetration at 50 MHz was enhanced over ice wedges, increasing penetration from 10 metres down to 15 metres.

Kovacs and Morey (1979) used an analogue GPR to map the presence of massive ground ice along the Alyeska pipeline in Alaska, where they were able to detect the tops and bottoms of ice bodies at up to 10 metres depth. The GPR data was found to be consistent with nearby shallow borehole logs. This study illustrated the early potential of GPR as an investigative tool for engineering.

Ulriksen (1982) investigated various civil engineering applications of GPR for his Doctoral thesis at Lund University in Sweden. His studies included profiling soils and bedrock, peat, ice and snow, as well as locating buried pipes and cables and detecting hidden damage in roads. He also offers an overview of the principles behind GPR. In his work with snow and ice, Ulriksen found that radar wave velocity increases with snow or ice density and decreases drastically with increased unfrozen water content.

Similar findings are reported by Patterson and Smith (1981) in Time Domain Reflectometry (TDR) laboratory experiments. Their findings indicate that since ice and soil particles do not differ greatly in their dielectric constants ($K_{a\,ice}$ = 3.2, $K_{a\,soil}$ = 2.2-3.5) when compared to that of water ($K_{a\,water}$ = 80), it is the unfrozen water content which most strongly influences radar wave velocity, and not the ratio of ice to soil. Thus a change in grain size resulting in a variation in unfrozen water content can produce a stronger reflection than a soil/ice interface. Nevertheless, strong reflections have been recorded at soil/ice interfaces (Dallimore and Davis, 1987).

GPR investigations of massive ice in clayey sands near Rae, N.W.T. by LaFleche and others (1988) provided valuable data for roadway repairs. Using a Pulse EKKO III digital GPR (the same unit which was used for this project at Hot Weather Creek in 1990), massive ground ice was detected within three metres of the surface. Stratigraphic structure was also delineated in conditions similar to those at Hot Weather Creek. A six metre borehole was used to confirm the GPR findings.

1.4.2 EQUIPMENT

A typical GPR system includes a transmitting unit, a receiving unit, and a recording and display unit. The transmitting unit generates a high voltage, short duration (1-20 ns) electromagnetic pulse and transmits it through a broadband antenna. The receiving unit picks up the reflected pulse using either

the same antenna (in a monostatic system), or a separate one (in a bistatic system). This unit measures the signal amplitude versus the delay time counted from the transmit pulse. The trace of the reflected signal is then displayed on a screen or as a hardcopy, and is saved to a storage medium (tape or disk) for later processing and analysis (A Cubed Inc., 1986).

Ideally, antennas should have a flat frequency response across at least a bandwidth equal to the centre frequency, but this is almost impossible to achieve in a field-use antenna. Most GPRs use resistively loaded dipole antennas. These antennas are not very efficient, but they are robust, light-weight, easy to manufacture, and have a reasonably flat frequency response (A Cubed Inc., 1986).

Centre frequency is controlled by dipole length, with shorter antennas yielding higher frequencies.

Antenna coupling with the ground is one of the weaknesses of GPR. This problem is reduced in ground based systems where the maximum transferal of energy into the ground is attained when the antennas are kept within a tenth of a wavelength of the surface (A Cubed Inc., 1986).

1.4.3 RADAR WAVE PROPAGATION

Once the transmitted radio pulse leaves the antenna and enters the ground, it is attenuated by wavefront spreading and ohmic losses. Wavefront spreading losses are affected by variations in EM wave velocities in the

subsurface which cause refraction. If the velocities increase substantially with depth, the radar waves will be refracted away from the vertical. This will increase the illuminated area and reduce the intensity of the reflected signal (Ulriksen, 1982).

Ohmic losses are more significant and occur when the pulse passes through a conductive material, such as saline ground water. This creates electrical eddy currents which drain energy from the pulse. Saline or marine clays and fine silts are thus a major impediment to GPR surveys (Jensen, personal communication).

1.4.4 DEPTH DETERMINATION

Since ground probing radar data is recorded as signal strength versus two way travel time, the radar in the reflection mode does not provide any information on the actual depths of the reflectors.

Radar waves propagate through a material at a velocity related to the dielectric constant as shown in equation 1.1 (Annan & Davis, 1976).

$$V = c / \sqrt{K_a} \qquad [1.1]$$

where K_a = apparent dielectric constant

$c = 0.3$ m/ns

Once dielectric properties are known and the radar wave velocities calculated, reflector depths can be found using the following equation (Kovacs & Morey, 1979).

$$D = V t_d/2 \qquad [1.2]$$

where D = depth (m)

V = effective velocity (m/ns)

t_d = two-way travel time (ns)

Velocity and dielectric values must be deduced from drill core data, or from Wide Angle Reflection and Refraction (WARR) or Common Mid Point (CMP) surveys. WARR and CMP surveys allow one to estimate the bulk dielectric properties of the subsurface without drilling holes by comparing radar wave travel times from a given reflector as antenna separation is increased (Annan *et al.*, 1975).

A CMP survey is carried out in a representative level area with relatively flat underlying strata. The survey is begun with the transmitter and the receiver antennas adjacent to each other. They are then moved apart at a constant rate as pulses are transmitted into the ground. The path from the transmitter to the reflecting layer and back to the receiver is well defined and varies predictably as the antennas are moved. The data is recorded as two-way travel time versus antenna separation (Figure 1.4). Waves which travel directly from the transmitter to the receiver generate a straight line of arrival times, the slope of which is inversely proportional to the velocity.

Since the speed of electromagnetic waves in air is precisely known, the exact antenna separation is found from the arrival time at the receiver of the transmitted air wave through the following equation (Annan *et al.*, 1975).

$$t_a = x/c \qquad [1.3]$$

where t_a = arrival time of air wave (ns)

c = speed in air (m/ns)

x = antenna separation (m)

The near surface ground wave velocity is related to the antenna separation through equation 1.4 (Annan *et al.*, 1975).

$$t_g = x/V_g \qquad [1.4]$$

where t_g = direct ground wave arrival

V_g = effective velocity in ground

From equation 1.1, equation 1.5 is derived which gives the apparent dielectric constant near the surface:

$$K_a = c^2/V_g^2 \qquad [1.5]$$

where K_a = apparent bulk dielectric constant

For reflected pulses, arrival times generate a hyperbolic curve. Arrival time squared is plotted versus the square of antenna separation (T^2 vs X^2), resulting in a straight line, the slope of which is inversely proportional to the square of the velocity at that depth. The procedure is repeated for each deeper layer to create a velocity profile for the area which can be used to assign depth values to the reflection profiles (A Cubed, 1986).

A major drawback to this system is that a thin layer of material with very different electrical characteristics will bias the average ground velocity (Annan *et al.*, 1975). For example, a thin layer of clay (high K_a) over the target site will

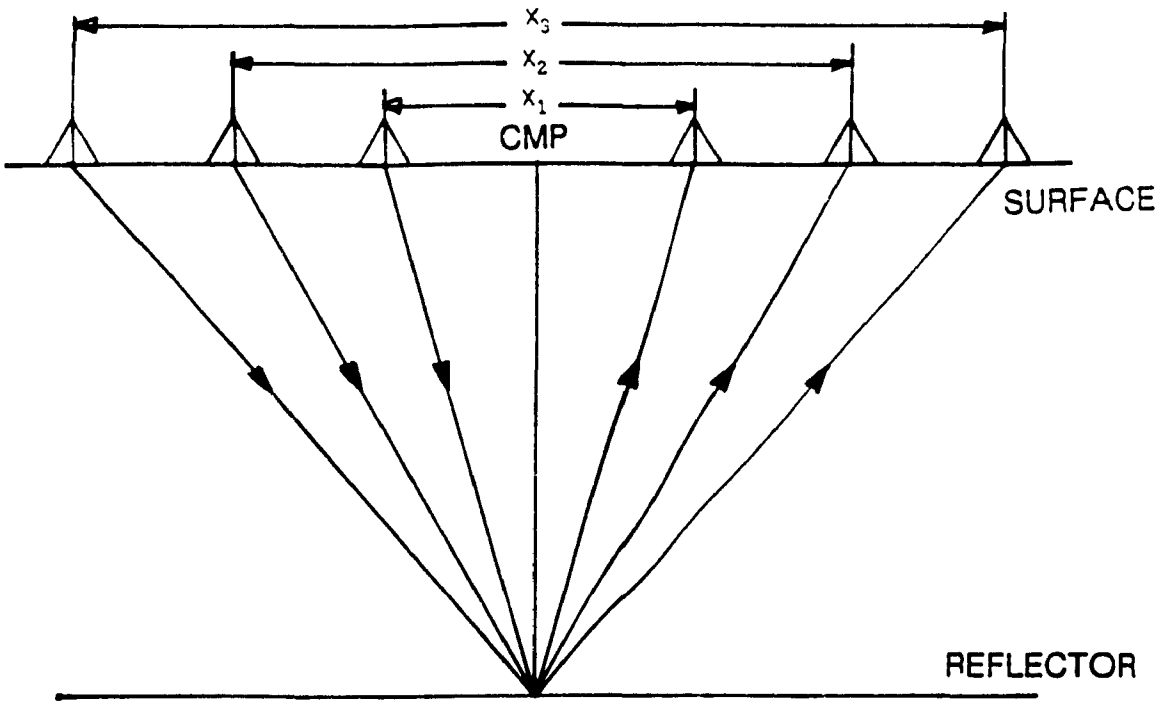

Figure 1.4a Widening ray paths for a CMP survey. (A Cubed,1986)

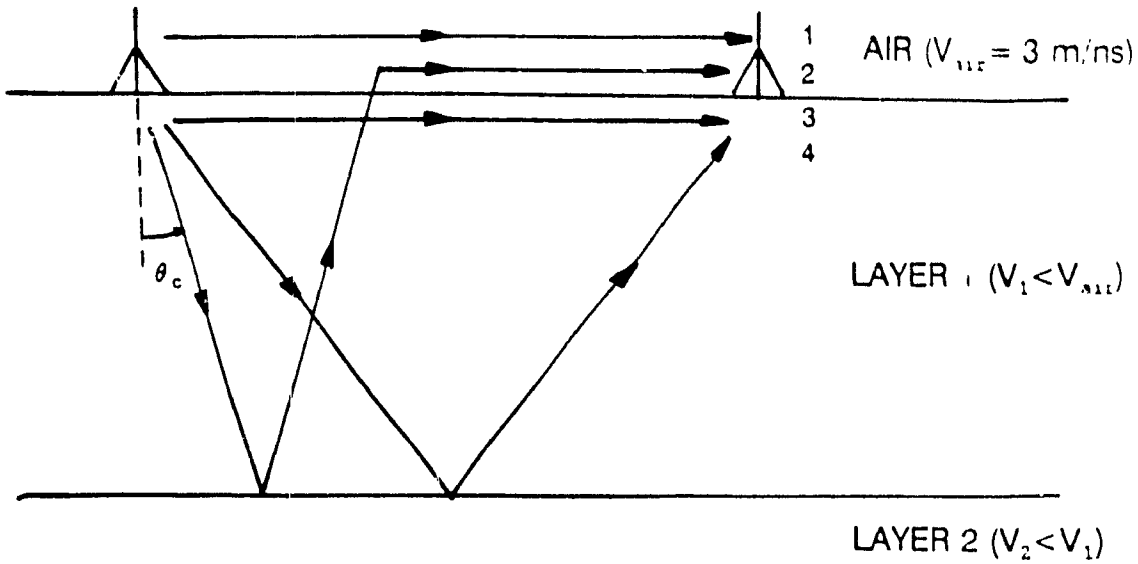

Figure 1.4b Possible ray paths between transmitting and receiving antennas.
1 - Direct air wave
2 - Critically refracted wave
3 - Direct ground wave
4 - Reflected ground wave
(A Cubed, 1986)

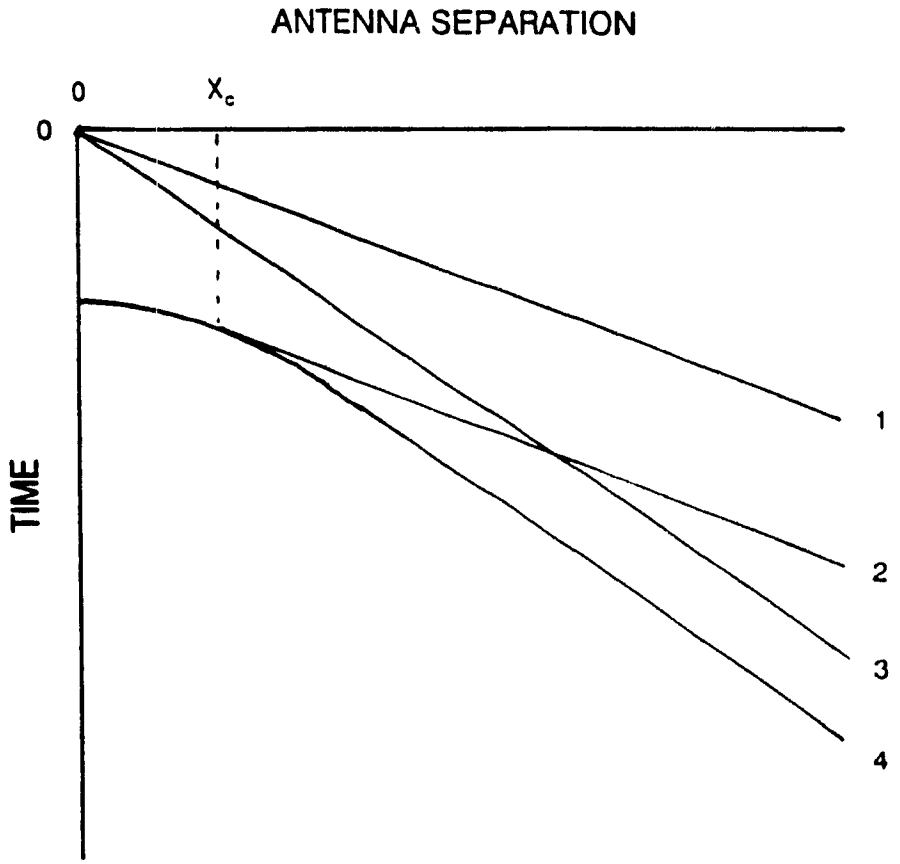

Figure 1.4c Idealized CMP results showing effects of four wave paths in Figure 1.4b. X_c - Critical antenna separation for refraction. (A Cubed, 1986)

artificially reduce the velocity and cause reflector depths to be underestimated.

Errors in CMP surveys increase with depth and with a decrease in transmitted frequency. Lower radar frequencies penetrate more deeply into the ground, but their longer wave length makes defining the leading edge of the pulse difficult. This creates uncertainties in determining event times (Annan *et al.*, 1975).

1.4.5 DEPTH OF PENETRATION

Radar wave ground penetration is enhanced by utilizing lower radar frequencies. Terrains with high conductivity and electrical permeability decrease penetration, as do those with low dielectric constant. Radar frequency is the only parameter controllable by the surveyor, thus it is an important consideration when setting up a survey. Also, as lower frequencies require larger antennas, field conditions become an important consideration in system set-up for ground based GPR.

Attenuation can also result from scattering by, for example, snow crystals. Backscattering near the surface by multiple point sources attenuates the pulse as well as severely cluttering the signal. It is often reduced by using a bistatic system instead of a single transmit/receive antenna. Backscattered pulses usually reflect directly back to the transmitting antenna. If the receiving antenna is located away from it as in a bistatic set up, signal cluttering is reduced (Ulriksen, 1982). This phenomenon was apparent in some of the early

data collected at Eureka in October, 1991. The problem was partially resolved by increasing the antenna separation.

1.4.6 SPATIAL RESOLUTION

The resolving power of the radar is dependant on both the radar system and on ground conditions. Resolution is usually quoted in terms of vertical and horizontal resolution, as these are dependant on different parameters.

Vertical resolution is determined by the frequency and the length (duration) of the transmitted pulse, as well as on the velocity of the pulse in the ground. As a general rule, vertical resolution increases with frequency. For a given frequency, the vertical resolution can not be less than the distance travelled by the pulse in half the time of the pulse duration. If two reflectors are closer together in the vertical direction than half of the pulse length, they will be merged together on the radar display. Thus, the optimum vertical resolution for a given frequency is defined in equation 1.6.

$$R_v = t\,V/2 \qquad [1.6]$$

where t = pulse duration (ns)

V = velocity in ground (m/ns)

Vertical resolution is related to the apparent bulk dielectric constant by combining equation 1.6 with equation 1.5 in the following:

$$R_v = t\,c\,/\,2\sqrt{K_a} \qquad [1.7]$$

A pulse length of 10 ns, for example, results in an optimum vertical resolution

of 84 cm in ice (K_e = 3.2). At lower frequencies this figure is increased, as it becomes more difficult to accurately identify the leading edge of the pulse. This results in a 'fuzzy' return, and produces errors in arrival time readings. These errors are usually small and inconsequential in regular profiles, but in CMP surveys they can cause errors of up to five percent in estimates of K_e (Annan *et al.*, 1975). Digital compression of the recorded data reduces the perceived pulse length and sharpens the image, reducing the error. Using a higher frequency also reduces error and improves resolution, but depth penetration suffers (A Cubed Inc., 1986).

Horizontal resolution is not strongly affected by subsurface characteristics, rather it is more a function of the distance between successive readings. GPR systems commonly employ a method called stacking whereby many repetitive pulses are transmitted and received and the average of the results is displayed and recorded (Hatton *et al.*, 1986). If the antennas are in motion, as in a continuous profile, then the averaged result includes data for a length along the traverse, not a point. Difficulties are increased when the speed of transit is not constant, as is common in ground based surveys in rough terrain.

Some of these problems are overcome by adopting a discrete profiling system whereby each reading is taken at a station, and the radar is moved a set distance between readings. This allows for more accurate positioning of the radar along the traverse line, as well as allowing the operator to carefully

position the antennas to ensure maximum coupling with the ground. This method is somewhat slower, but it greatly improves the quality of the data, especially on uneven terrain.

As explained earlier, subsurface electrical characteristics affect the lateral spreading of the pulse through refraction. This influences the horizontal resolution by changing the illuminated area. Where velocity increases with depth (moist silt and clay overlying ice for example), the pulse is refracted outwards, increasing the illuminated area and reducing both the horizontal resolution and the strength of reflected signals. The reverse is true where velocity decreases with depth.

1.4.7 DATA PROCESSING

Radar data is recorded in the time domain. This creates some special problems which must be dealt with through processing before the data can be fully used.

Since the basic principles of GPR are similar to reflection seismic theory, GPR data can be processed using the same methods. There are several computer software packages available which allow the digital data to be processed quickly and accurately.

The time domain character of the data results in a variety of features in the images produced. Individual point reflectors, such as rocks or pipes lying at right angles across the survey line, produce inverted hyperbolic reflections

in the raw data, with the reflector position coinciding with the apex of the hyperbola. This effect is produced when radar (or seismic) pulses which propagate outwards as well as downwards encounter a reflector which is not directly below the transmitter (Figure 1.3 earlier page). The system records the reflected pulse as having come from directly below the transmitter. As one approaches, passes over, and leaves the reflector; subsequent traces show the reflector at increasingly shallow depths and then increasingly greater depths.

Such hyperbolas can be resolved into point reflectors through a process called migration. This converts the data from a temporal representation to a spatial one. Migration is defined as the correct lateral positioning of reflector elements (Prakla-Seismos, 1978). It employs wave propagation and reflection equations to interpret reflections and deduce the often complex geometries that created them.

Deconvolution is a process by which the signature of a theoretical radar pulse is mathematically removed from the reflection data (Hatton *et al.*, 1986). Ideally, a transmitted pulse should consist of a single sharp spike of extremely short duration, but this is usually not the case. Overlap and interference between reflected pulses with multiple spikes obscures the record of the boundaries of changing dielectric character in the earth. These boundaries become clearer if an idealized pulse (not a single spike, but one which is generated by a transmitter under ideal conditions) is subtracted from each point in the reflection trace. This deconvolution leaves the original characteristic

trace of the subsurface reflector, assuming that the transmitter created a near ideal pulse in the first place (Hatton *et al.*, 1986).

Filtering is a very important tool in data enhancement. Typically, signal to noise ratios are reduced at very low and very high frequencies. Digital filters can be used to remove these portions of the reflected spectrum to improve the image. High frequency noise can be smoothed by averaging over a window containing several points and moving the window down each trace. Notch filters, which remove a specific frequency (or a very narrow bandwidth) can be used to remove specific noise events. These can result from ringing with railway tracks or overhead power lines, for example (Hatton *et al.*, 1986). Low frequency interference is removed by a process called *de-wowing*. Other simple techniques can be used to emphasize certain features in a profile. For example, comparing adjacent traces or averaging across several traces enhances horizontal features. Similarly, plotting the differences between adjacent traces enhances steeply inclined features.

Since attenuation usually increases with depth, radar systems often employ "time variable gain" or automatic gain control (AGC) instead of a constant gain function Signals reflected from greater depths arrive after a greater time delay, so these signals are amplified more than those which arrive earlier. This serves to reduce the dynamic range of signal strengths to a range that the digital recording system can display (Annan & Davis, 1976). AGC gain is also used to enhance later reflectors without overpowering the early ones;

however, information on relative reflector strengths is lost. Constant gain functions multiply all points on a trace by the same selected value, thereby preserving relative reflector strengths.

Beyond filtering and gain application, displaying only selected parts of the traces greatly aids interpretation. For example, if a high frequency record with traces from zero to 128 ns is plotted on paper or on a screen, fine details near the surface are usually lost. However, if only points from zero to 40 ns are displayed, the image is "stretched", revealing the details. This function also speeds processing, as filters and gain need only be applied to the selected segment.

1.4.8 INTERPRETATION

Pure massive ice bodies appear "clear" to radar and are easily detected. Impurities in the ice, such as sediment layers or air bubbles, affect the electrical characteristics of the ice. Annan and Davis (1976) conducted CMP surveys at Involuted Hill, N.W.T. They found the dielectric constant for the massive ground ice to be 2.6 instead of 3.2, the expected value. Inspection of recovered drill core revealed a high bubble content in the ice, which reduced its bulk density to .67 g/cm^3 from .92 g/cm^3. These results agreed with the empirical relation (Annan & Davis, 1976; after Robin *et al.*, 1969):

$$K_a = 1 + 2.36\rho \qquad [1.9]$$

where ρ = bulk density of ice

It can be seen then, that in some instances, the presence of air bubbles throughout ground ice bodies could lead to significant errors in velocity estimates and depth plots. This could result in the overestimation of the thickness and therefore the volume of ground ice. Again the need for drill core data is underlined.

As was mentioned earlier, frequency affects depth of penetration as well as vertical resolution. The frequency chosen should reflect the aim of the survey. For example, to gain information on the tops of ground ice bodies near the surface (ie. those susceptible to thermokarst erosion), a high frequency (200 MHz) is suitable. This results in increased resolution near the surface, and reduced transmitter washout. That is, events closer to time zero can be recorded at higher frequencies without being overpowered by the transmitted pulse. At low frequencies (25 MHz), this becomes a problem, thus these frequencies are more suitable for deeper investigations. This is especially true in view of the increased depth of penetration at these frequencies. Multiple surveys at different frequencies over the same area are useful in maximizing the information returned, but are time consuming.

The most important stage of interpretation is the visual inspection of the GPR profiles. This step can be something of an artform, and requires experience and at least a basic understanding of the local geology to be done well. It is at this stage that other data from the investigated site, such as drill cores, becomes important. While one can infer something about what kinds of

materials give rise to specific radar reflections from their shape or relation to each other, GPR does not actually identify what is creating the reflections.

1.5 EFFECTS OF CLIMATE CHANGE ON PERMAFROST

Potential changes in permafrost conditions due to possible climatic warming have been investigated to some extent in the western Canadian Arctic and Alaska, but little has been done in the high Arctic. Edlund and others (1989) offer the increased incidence of active layer detachment slides and the reactivation of ground ice slumps observed during the abnormally warm summer of 1988 as possible consequences of global warming.

Mackay (1975a) suggests that past climatic fluctuations have left observable features in permafrost such as truncated ice wedges, young thermokarst lakes, mass movements, cryoturbation features, etc. Gold and Lachenbruch (1973) show from deep borehole temperature profiles of the North Slope of Alaska that ground temperatures have increased by about 2°C in the last century. A similar study on the Fosheim Peninsula, Ellesmere Island, suggests an increase of 2° to 5°C in ground temperatures since the Little Ice Age, and a 4.2°C increase between about the 1870s and 1971 (Taylor, 1991).

Osterkamp (1984) estimates that a 3°C increase in mean annual air and ground temperatures in Alaska will result in thawing of permafrost in the discontinuous zone, and in widespread changes in the continuous zone in Alaska. Goodwin, Brown, and Outcalt (1984) employ Stefan's solution in a

model to estimate the effects of both a 3°C and a 6°C increase in mean annual air temperatures at Fairbanks and at Barrow, Alaska. They calculate that a 3°C temperature rise would result in a 41% increase in active layer depth and a 110 metre decrease in permafrost thickness at Barrow over a period of ten years.

In contrast to these researchers, Shamanova and Parmuzin (1988) in Russia state that climate change serves only as a backdrop against which local variations in heat exchange between the ground and the atmosphere (caused by changes in vegetation, snow depth, etc.) are the driving forces behind thermokarst. Their work is based in the Kolyma lowlands of northeastern Siberia. It should be noted that they do not include thaw slumps or active layer detachments as thermokarst because they are small, transient features. Rather, they are concerned with larger-scale phenomena like thaw lakes, alas landscapes, and major taliks; features which have not been widely observed or at least described in the Canadian high Arctic. This position is supported by Smith and Riseborough (1983) whose computer models suggest that site factors such as precipitation (especially snow cover), soil moisture, vegetation, lithology, etc., can be as important as climate in determining ground temperature and permafrost response to climate variability.

1.6 SUMMARY

A pressing need for more research into ground ice conditions and the potential for thermal degradation exists in the high Arctic, especially in view of possible climate change. Specifically, the distribution and abundance of ground ice should be explored to gain insight into mechanisms of its formation. Airphoto surveys can be used to identify areas likely to be underlain by ground ice, but they give little information on the depth and thickness of the ice. Several techniques for detecting ground ice in local area surveys currently exist, but none have been developed to the point where synoptic scale surveys could be carried out reliably and affordably. Until they are, knowledge of ground ice conditions in the high Arctic will likely remain limited.

Ground probing radar is a useful geophysical tool for shallow subsurface investigations where it compliments other types of subsurface information, such as drill core logs. The technology and the techniques are continuing to evolve, and GPR has the potential to become an indispensable part of geomorphological research in general, and of permafrost research in particular. Recent developments in antenna design will make higher frequencies available to users, resulting in much higher spatial resolution and allowing detailed studies of the active layer. The regional coverage possible with airborne GPR may be combined with the penetration and resolution of ground based systems in the near future as the technology improves. Synoptic scale coverage may also one day be available if an orbit based system is developed. Such a system

would allow widespread monitoring of changes in permafrost and active layer conditions. For the present, ground probing radar remains a valuable site investigative tool to be used in conjunction with other techniques of permafrost research.

CHAPTER 2 STUDY AREA

2.1 THE FOSHEIM PENINSULA

The Fosheim Peninsula is located on the west central side of Ellesmere Island, N.W.T., in the Canadian Arctic Archipelago (Figure 2.1). The peninsula is approximately 150 km along its northwest - southeast axis and is bounded by Eureka Sound to the west and southwest, by Greely Fiord to the north, by Bay Fiord to the south, and by Canon Fiord to the east. The peninsula has a surface area of approximately 11 000 km^2.

Like all of the Queen Elizabeth Islands, Ellesmere lies well within the zone of continuous permafrost. Thermal measurements from three boreholes within 100 km of Eureka indicate that permafrost extends to about 500 m depth (Judge *et al.*, 1981).

The study area , within a 30 km radius of Slidre Fiord and was selected for its high Arctic location, the reported presence of ground ice exposures (Edlund *et al.*, 1989; Pollard, 1991), and the proximity of logistical and technical support through the Eureka weather station and the GSC camp at Hot Weather Creek.

2.1.1 REGIONAL SETTING

The northwest and central Fosheim Peninsula, containing the study area, is located in the northern Sverdrup Basin on the Queen Elizabeth Islands Subplate while the southeast portion extends onto the Franklinian Geosyncline

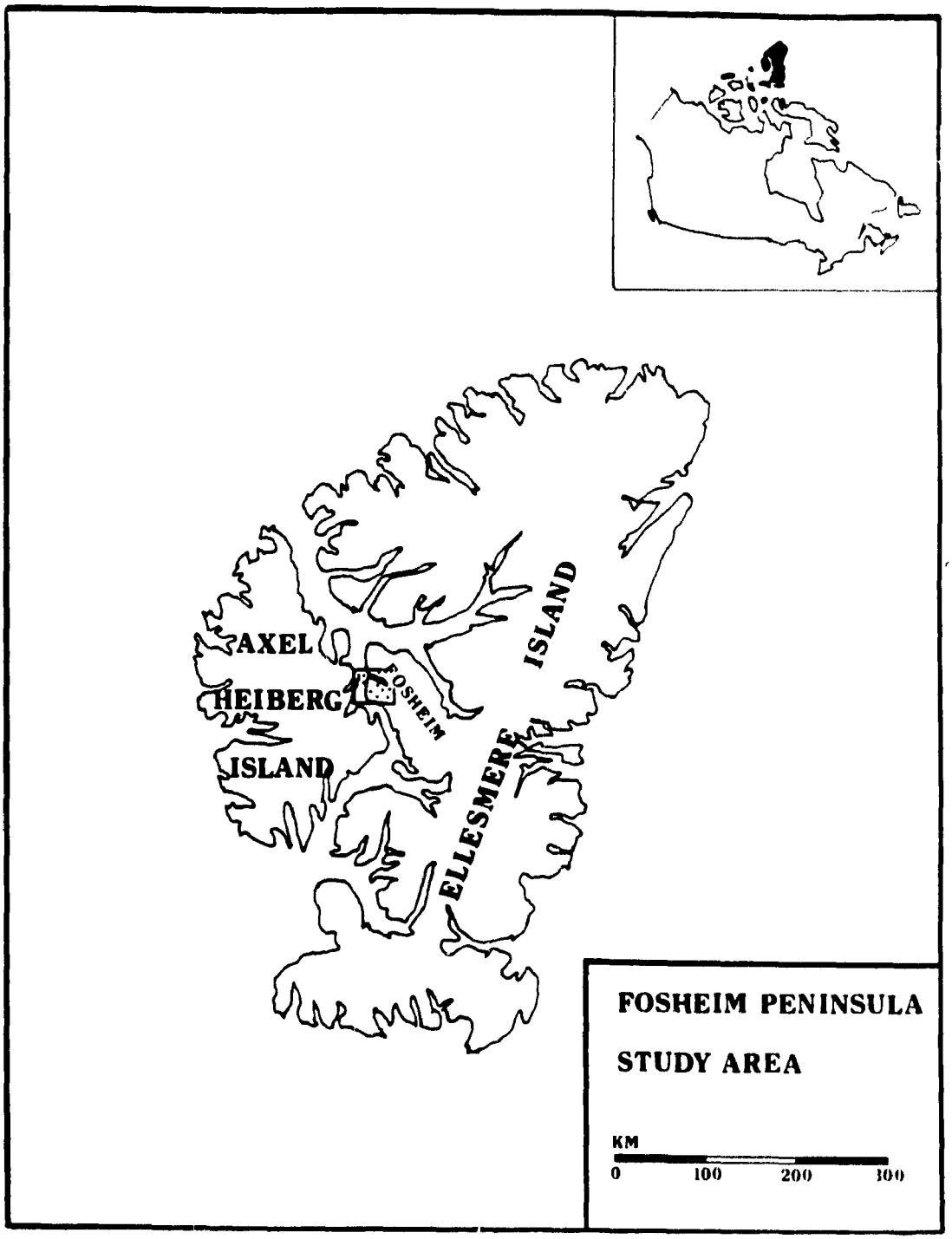

Figure 2.1 Location map of study region.

(Kerr, 1981). The Sverdrup Basin is marginal to the northwestern Canadian Arctic and contains up to 13 000 metres of mostly conformable sediments of lower Carboniferous to upper Cretaceous age. The structural axis matches the depositional axis fairly closely, but there is evidence that the basin was deformed during the Eureka Orogeny after the deposition of Cenozoic sediments (Thorsteinsson and Tozer, 1970).

2.1.2 BEDROCK GEOLOGY

There is some question as to whether or not ground ice exists in any significant quantity within the bedrock of this area. Thus far, none has been reported in the literature; however, observations by Pollard in 1992 (personal communication) confirm its presence. The area is underlain by mostly conformable, poorly lithified clastic units which strike roughly north to south with late Cretaceous to Tertiary rocks of the eastwardly dipping Eureka Sound Group located to the east of Slidre Fiord. To the west, centred on Slidre Fiord and separated from the Eureka Sound Group by the Black Top Anticline, lie older sediments of Triassic and Jurassic age surrounding younger rocks of Jurassic and Cretaceous age located in the Weather Station Syncline (Thorsteinsson, 1971).

2.1.3 SURFICIAL DEPOSITS

Subsurface units are mostly overlain by a relatively thin layer of colluvial silts and fine sands developed from weathered bedrock. Weathering proceeds through the physical breakup of the parent material by frost action and possibly by the growth of segregated ice below the frost table. Bedrock is often weathered to several metres depth, indicating that weathering occurs below the active layer, or that the active layer was once much thicker and that glaciation did not erode the weathered rock as deeply in some areas as in others (Hodgson, 1989a). Detailed mapping of surficial geology in this area has not yet appeared in the literature, but an unpublished map of surficial deposits at 1:250 000 scale has been compiled by Bell (1992) which indicates the widespread presence of marine sediments as a thin veneer over bedrock and as delta, beach, and nearshore deposits in much of the study area.

A large portion of the Fosheim Peninsula was submerged during the late Pleistocene and early Holocene. According to the literature (Hodgson, 1989a), marine sediments deposited during Pleistocene transgressions form the only widespread non-glacial deposits. However, recent evidence discovered by Bell suggests a wider distribution of Holocene marine sediments (Pollard, personal communication).

Low areas near coasts may show beach deposits from marine off lap composed of coarse sand and gravel. These tend not to extend to marine limit as initial emergence was rapid and beaches had little time to form. The low

level of wave activity due to the probable presence of shorefast ice through much of the year would also have limited beach formation. Regressive sequences comprised of silt or silt and clay up to 30 metres thick locally are often overlain by shallow water facies of sand and gravel up to 10 metres thick near deltas. Where upland sources are composed of very fine textured rock, the shallow facies are difficult to distinguish from deep water facies. Transgressive sequences, though expected, have yet to be identified (Hodgson, 1989a).

Glacial deposits occur locally, usually proximal to existing glaciers which are known to have been active in the early Holocene. It has been suggested that the past glaciations may only have deposited a thin, discontinuous layer of material which is indistinguishable from weathered bedrock, or that such a layer has been largely eroded since deglaciation (Hodgson, 1989a).

2.1.4 PHYSIOGRAPHY

Most of the peninsula is composed of ridge and valley terrain and dissected plateaus (Bostock, 1970 GSC map 1245A). These plateaus may represent an erosional surface underlying beds of Miocene age on western Ellesmere and eastern Axel Heiberg Islands. This surface lies between 150 and 700 metres elevation, while the inter island channels are 200 to 500 m deep (Hodgson, 1989b, after Balkwill and Bustin, 1975, and Bustin, 1982). Minor lowlands are generally restricted to coastal areas and to an area south east of

Slidre Fiord. The Sawtooth Mountains form a glaciated highland to the south east which runs NNE - SSW and features peaks up to 1200 m high. Other highlands with ridges up to 640m - 760+ m high define the northern and western edges of the peninsula. Between the highlands lies a rolling lowland cut by many short river channels and ice wedge polygons.

2.1.5 CLIMATOLOGICAL AND GLACIAL HISTORY

The marine limit in the central Fosheim near Slidre Fiord is estimated to be approximately 140 metres above sea level, but this area lies beyond (to the west of) the maximum ice extent of the late Wisconsin glaciation at about 8700 - 8800 BP (Hodgson, 1985). Areas north west and south east of the peninsula show evidence of lower marine limits, possibly indicating that the Fosheim was ice free while the rest of the area was still being glaciated. Uplift would then have started earlier in the central region which shows a typical high Arctic reemergence curve: rapid and then diminishing uplift (Hodgson, 1985).

Earlier models of glacial extent based on emergence rates of the eastern Queen Elizabeth Islands postulated the existence of an archipelago-wide Innuitian ice sheet which broke up about 5000 BP (England, 1976 after Blake, 1970). However, England maintains that crustal depression can be caused by local ice masses, such that several independent ice caps could produce the observed emergence record. Changes in the Greenland ice sheet would also be reflected on Ellesmere Island. Tectonic uplift related to any of the several rifts

in the Arctic would obscure isostatic rebound signatures as well (England, 1983). Therefore the emergence record is misleading. England proposes that the increased growth of the Laurentian Ice Sheet 33 000 to 28 000 BP would have created a topographic barrier to southerly cyclonic air flow, starving the Arctic ice mass of moisture (England and Bradley, 1978). This would lead to a reduction in ice mass to form the convergent but not coalescent Franklin Ice Complex of the late Wisconsin (England, 1976). Evidence of such an event may be seen in the presence of lake sediments dating from 20 000 BP in central Ellesmere Island which would not have survived a widespread ice sheet, and the presence of heavily weathered moraines and Greenland erratics on northeastern Ellesmere Island (England, 1978).

Warm periods six and four thousand years ago are proposed by Stewart and England (1983) to explain maximum driftwood penetrations of fiords on Ellesmere Island. A warmer period might have resulted in a larger seasonally ice free area, allowing driftwood from Arctic rivers to penetrate the fiords.

Oxygen isotope ratios from a 1979 core on the Agassiz Ice Cap indicate that temperatures 800 to 100 years ago during the Little Ice Age were 2-3°C lower than today. This agrees with temperature-depth measurements from boreholes within 160 km of the corehole which suggest ground temperature increases of 2-5°C since the Little Ice Age. This discrepancy is likely due to an air temperature increase of 2-3°C coupled with increased snowfall which would tend to insulate the ground from the winter cold (Taylor, 1991).

Other apparent evidence of past ground temperature fluctuations were observed as thermal erosional surfaces (thaw unconformities) in ground ice exposures on the Fosheim Peninsula in 1990 and 1991. These features are characterized by abrupt, non-conformable changes in ice texture and in soil volumetric ice content and were observed as much as three metres below the surface. Depth variations in some of the thaw erosional surfaces over only a few metres distance imply that they may have been caused by local effects, instead of regional climate changes.

2.1.6 MODERN CLIMATE

The Fosheim Peninsula enjoys warmer average summer temperatures than the surrounding regions, giving rise to the motto of Eureka Weather Station: "Garden Spot of the Arctic". (The station staff especially enjoy hearing the weather reports from the sister station Mould Bay on Prince Patrick Island which is *not* known for its sun bathing weather.) Eureka is located on the north shore of Slidre Fiord at 80°00'N 85°56'W. The average annual air temperature at Eureka is -19.7°C (for 1951 to 1980) while the average daily temperature in July is 5.4°C. The station experiences an average 100 day long melt season ($T_{max} > 0°C$) and 299 days of frost ($T_{min} < 0°C$) (Edlund, 1983, after AES, 1975). As the station is located on the shore of the fiord at an altitude of only 10 metres, a low altitude thermal inversion in the summer (due possibly to cold air drainage) results in these temperatures being somewhat

TABLE 2.1
FOSHEIM PENINSULA CLIMATE DATA

	MEAN MONTHLY AIR TEMPERATURE (°C)			
	February	July	Year	Source
Eureka (1951-1980)	-38.0	5.4	-19.7	AES, 1982
Hot Weather Creek				
1988	--	12.7	--	AES,
1989	-38.5	6.5	-16.0	courtesy
1990	--	8.3	--	Edlund.

lower than the inland temperatures. This is especially true on calm, sunny days when temperatures one to two kilometres inland may be as much as five to ten degrees warmer. At the Hot Weather Creek Geological Survey of Canada camp 30 km to the east, for example, the average daily temperature for July 1988 was 5.5°C warmer than the same period at Eureka (Edlund *et al.*, 1989), and for 1989 and 1990 was 2.3° and 2.7°C warmer respectively (AES, courtesy of Edlund). Not all inland temperatures are warmer, however Broad upland plains to the south of Slidre Fiord can be colder and windier than Eureka, likely due to their greater altitude and lack of wind breaks. While no temperature records exist for these areas, field observations made in June and July of 1991 recorded snow on days that Eureka recorded rain, and ventifacts were found to be plentiful in rocky areas. Also, some of these areas were observed to have large deflation surfaces indicative of a dry, windy environment

The relatively warm temperatures at Eureka resulted in active layer depths of between 30 and 60 cm in early July 1991, while ice wedge tops were measured at depths of 40 to 60 cm, which are consistent with active layer observations made in 1992 (Pollard, personal communication). Active layer thicknesses of between 50 and 80 cm for most areas near Hot Weather Creek were measured in early July 1990 while extreme active layer depths of 100 cm were recorded in moist, low lying areas and thaw slump floors. At Hot Weather Creek in July, 1990, tops of ice wedges exposed in stream banks were measured at 50 cm depths, corresponding to current average active layer

Figure 2 2 Ice wedge top exposed at Eureka showing shallower growth in recent times. The youngest part of the wedge in the centre is 30 cm below the surface while the older flanks are 40 cm deep This implies that average ground temperatures have decreased in recent decades

depths for that particular site, while ice wedge tops at Eureka were found at 30 cm depths in 1991. Given the semi-annual nature of ice wedge growth, these depths correspond to recent maximum active layer depths. Some ice wedges at Eureka showed tops at 40 cm depth with a central spike several centimetres across reaching 30 cm depth (Figure 2.2), indicating that thaw depths were greater in the recent past.

Precipitation at both Eureka and Hot Weather Creek is very limited, Eureka receives an average of 64 mm per year, 44.1 mm as snow and 23.4 mm as rain (AES, 1982). Summer precipitation events tend to be isolated with only an average of 16 days out of June, July and August having rain or snow.

2.2 STUDY SITES

The study area is divided into five sections (Figure 2.3): Hot Weather Creek, Eureka, South Slidre, and South Fosheim-1 and -2. In all, 28 sites were investigated, with ground probing radar surveys carried out at Hot Weather Creek and Eureka.

2.2.1 HOT WEATHER CREEK

The 1990 study site at Hot Weather Creek (79°58'N, 84°28'W) is characterized by rolling lowlands with above average temperatures and by relatively lush vegetation (Edlund *et al.*, 1989). It is the location of a Global Change Terrestrial Observatory operated by the Terrain Sciences Division of the

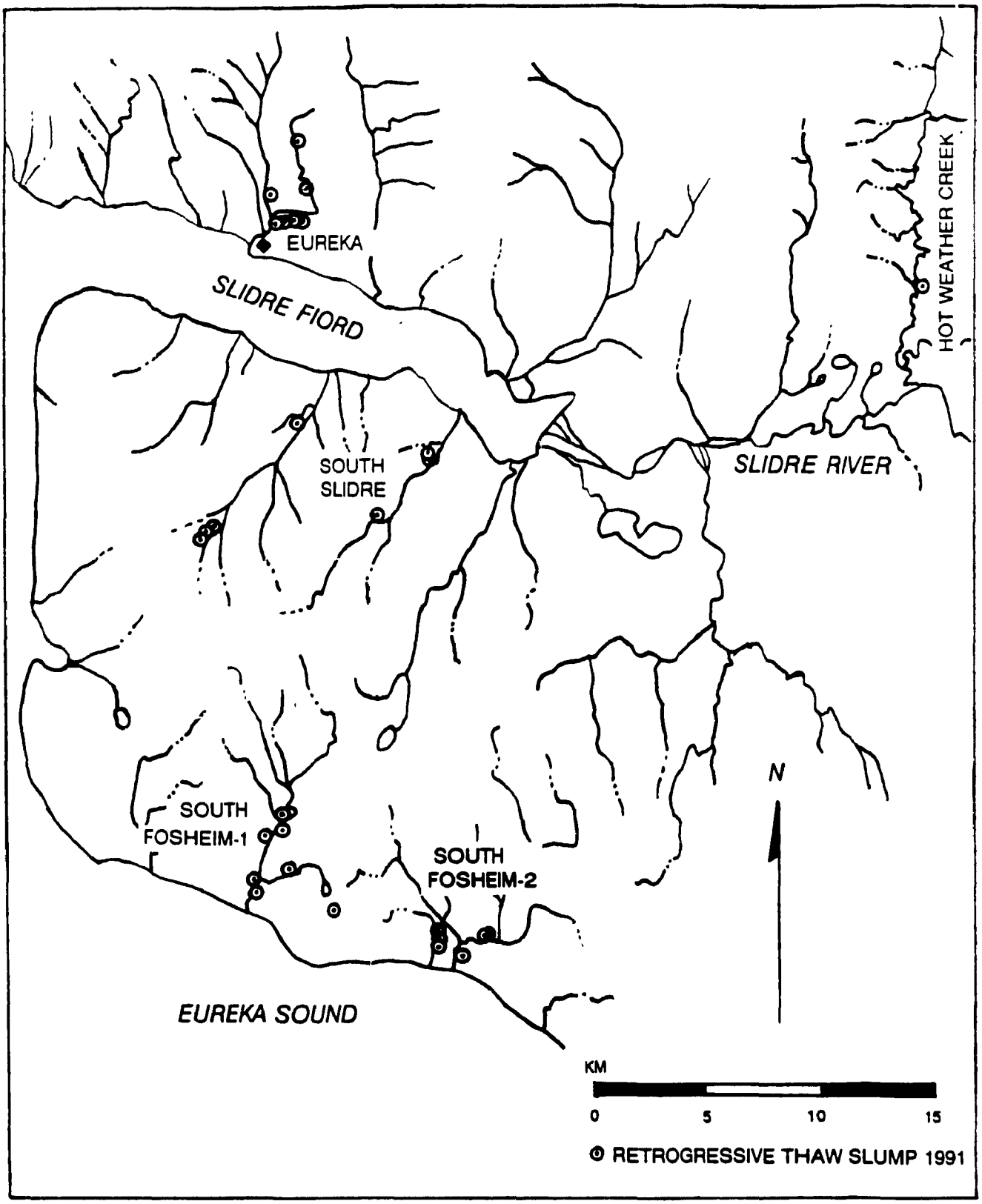

Figure 2.3 Study region showing five study areas and location of thaw slumps active in 1991.

Figure 2.4 The thaw slump at Hot Weather Creek lies within an older, stabilized slump with an eroded headwall (marked)

Figure 2.5 Close-up of headwall ice at Hot Weather Creek showing banded ice and silt

Geological Survey of Canada.

Two points of investigation were a bimodal thaw slump and a small thaw depression.

The bimodal retrogressive thaw slump (described in Edlund *et al.*, 1989) is located within what appears to be the stabilized scar of an older thaw slump (Figure 2.4). It was the main target of field studies carried out at Hot Weather Creek. The active slump and the stabilized scar occur on the outer bank of a meander in the creek. Other thermal erosion features on the outer bank in this area included exposed ice wedges and a thermal erosional niche at the base of the stream bank.

Massive ground ice and icy sediments were exposed in the headwall of the retrogressive thaw slump. In June 1990, the east bowl of the active slump displayed a three meter headwall showing silty-sand overlying 1.6-1.9+ m of massive ice containing silty bands. In places the banding was contorted and faulted. The contact between the massive ice and overlying clay was abrupt and unconformable. It truncated ice/sediment bands and elongated gas bubbles which were cloudy in appearance (Pollard, 1990) (Figure 2.5).

Ice wedges up to 1.7 m wide and 3 m deep outcropped at various locations in the side of the stream channel and in the slump headwall. These displayed relatively flat tops at depths of about 50 cm.

The small sedge and cottongrass-filled thaw depression is located about 25 metres south west of the Hot Weather Creek automatic weather station on

an elevated plain just west of the creek valley. The area features high centred ice wedge polygons five to ten metres in diameter and is somewhat windier and cooler than the slump site according to field observations.

Ground ice conditions described at Hot Weather Creek are similar to those encountered at most of the other study sites, except that this site is relatively small and isolated.

2.2.2 EUREKA

The area in the vicinity of the Eureka study site features a gently southward sloping plain which is cut by several southward flowing streams, of which Station Creek and Black Top Creek are the largest. As is seen at lower elevations elsewhere on the Fosheim, marine silts and fine sands form a blanket over poorly consolidated bedrock below 137 to 152 m (450 to 500 feet) elevation. It is within this blanket that ground ice has been most frequently observed (Figure 2.6).

Most of the eight exposures of icy sediments and massive ice at Eureka occur on the shallow, north facing slope of an asymmetrical valley just north of the AES airstrip, unofficially named Strip Creek. These exposures occur in relatively shallow thaw slumps which, given the local abundance of vehicle tracks and scarring by bulldozers, may be anthropogenically induced.

The largest active slumps in this study area occur on Station Creek and farther north on Strip Creek. These are located on steep southwest and east

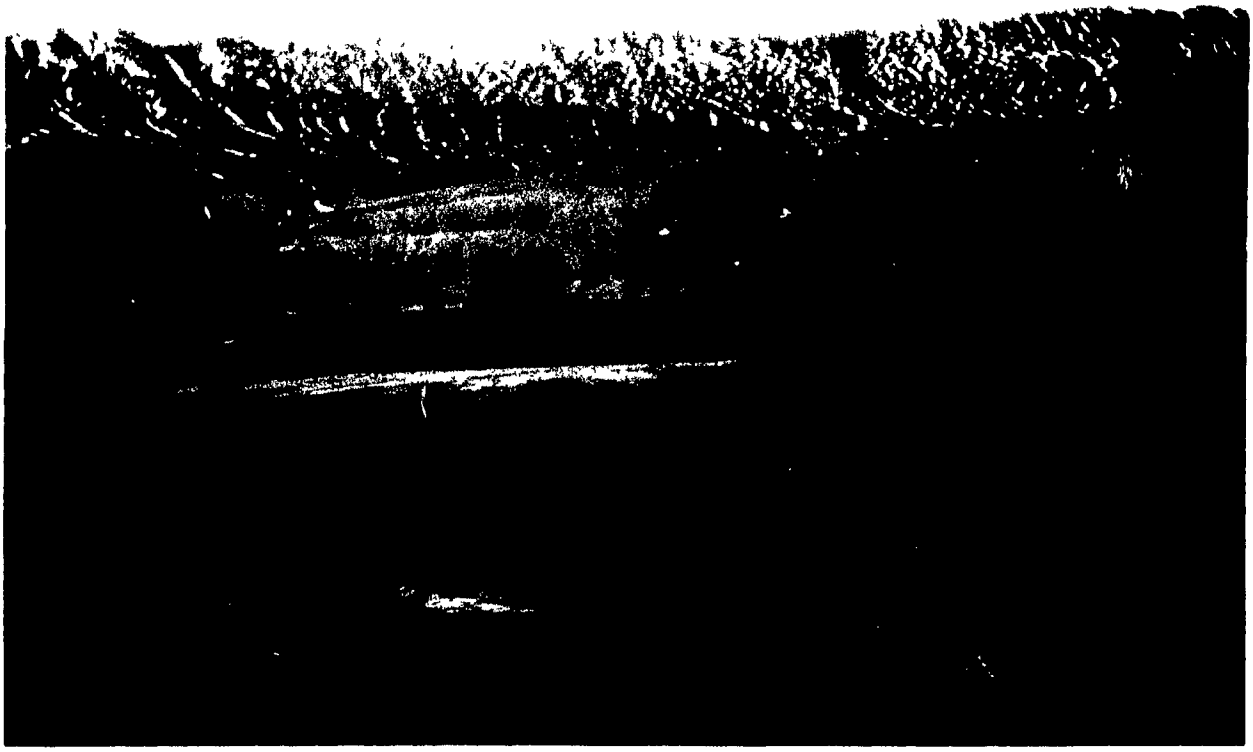

Figure 2.6 Two thaw slumps in the Eureka area which is characterized by rolling lowlands cut by asymmetrical valleys Black Top Ridge, a local landmark, lies in the background.

facing slopes in areas undisturbed by vehicles. However, in all cases, the presence of the streams nearby suggests that fluvial erosion may play a part in slump initiation.

No ground ice exposures were observed more than a few kilometres from Eureka, despite extensive ground and air reconnaissance north of the whole length of the fiord. The elevations of these sites range from 29 to 82 m a.s.l., averaging 48 m a.s.l.

2.2.3 SOUTH SLIDRE

Seven ground ice sections were identified on two northward flowing creeks on the sloping plains south of Slidre Fiord. These exposures faced roughly east and north of east, and lay on the steep slopes of two asymmetrical valleys between 61 m and 98 m a.s.l., averaging 84 m a.s.l. Several inactive slumps (displaying headwalls but no active thaw) and slump scars (with stabilized headwalls and floors) were also seen on other steep creek banks in the vicinity of the active slumps, indicating that fluvial erosion may expose icy sediments, leading to thermal erosion.

2.2.4 SOUTH FOSHEIM-1

This area is characterized as a rolling lowland cut by deep and often asymmetrical valleys controlled in part by the underlying geological structure. A sediment blanket of variable thickness covers poorly consolidated bedrock

below about 150 m a.s.l. Surficial materials consist of fine sand and silt with shell fragments in several locations. Beach deposits of silts and rounded pebbles form terraces up to one kilometre inland at altitudes of up to 110 m a.s.l. (Figure 2.7). These deposits merge with colluvial silts and boulders eroded from rocky ridges upslope.

Vegetation is generally sparse in this dry, windswept region. Locally, some valleys support relatively lush vegetation along their floors and on their shallower slopes. These areas are noticeably wetter and are quite hummocky.

Aerial and ground reconnaissance revealed seven active retrogressive thaw slumps and several stabilized slump scars of various sizes and orientations between 28 m and 101 m a.s.l., averaging 56 m a.s.l, and within five kilometres of the southern coast. Both the active and the stabilized slumps occurred in relatively steep creek banks, some of which showed signs of fluvial undercutting and bank collapse. In some areas, creek bank collapse was seen to increase bank slopes along extensive lengths. Thermal-erosional undercutting was not observed to be actively occurring in this area, however.

2.2.5 SOUTH FOSHEIM-2

This area is similar to South Fosheim-1 in terms of physiography, but it is slightly damper and hummocky vegetated areas are more widespread.

Six active and several inactive sites were identified within a few kilometres of the coast. Several of the stabilized slumps contained damp spots

Figure 2 7 View from a raised beach ridge located one kilometre inland and 110 metres above Eureka Sound in the South Fosheim-1 area Beach deposits slope straight down to sea level. Note distant river valley at lower left

Figure 2.8 A large (50 m wide) thaw slump in the SF-1 area showing ice rich silt overlying massive ice.

and were known to have been active in 1990 (Pollard, personal communication). In many cases, slumps may become stabilized for several years and then be reactivated or may show limited activity in late summer. The presence of damp spots or seepage indicates melting of icy material and a potential for massive ground ice. The active slumps were found between 41 and 60 m a.s.l. at an average altitude of 48 m a.s.l. on relatively steep valley slopes facing south and east.

Surprisingly, no thaw slumps or other ground ice exposures were seen in the extensive lowlands to the north of this area. As this area is geologically similar to where slumps have been seen, ground ice may be present but is not experiencing thaw. If so, this will bias any ground ice distribution survey that relies on naturally occurring thaw-related exposures.

2.3 SUMMARY

The Fosheim Peninsula features ridges and valleys with plateaus and minor lowlands blanketed by unconsolidated fine grained marine sediments of varying thickness. These overlie poorly consolidated fine grained clastic bedrock of Triassic to Jurassic age to the west, and of late Cretaceous to Tertiary age to the east. The area appears to have undergone deglaciation prior to surrounding regions, or to have escaped late Wisconsinan glaciation completely, which would imply a long period of cold conditions. Crustal depression due to ice masses adjacent to this area resulted in a present marine

limit at 137 m a.s.l. in the central Fosheim, with slightly lower values to the south.

This marine regression and the subsequent aggradation of permafrost to its present thickness of about 500 metres may have resulted in the widespread formation of ice rich sediment and massive ground ice in areas below 137 m elevation (Pollard, 1990).

Ground ice is exposed primarily by retrogressive thaw slumps which may be initiated by fluvial erosion or anthropogenic factors such as vehicle activity. Numerous active layer detachment slides may not be deep enough to initiate thaw slumping. Thus far, massive ground ice has been observed primarily in unconsolidated overburden, and only in one location in bedrock (Pollard, 1992, personal communication).

However, ground ice distribution has been mapped solely on the basis of natural exposures in features whose initiating factors are not clearly understood. Thus the present knowledge of ground ice distribution is biased by the distribution of retrogressive thaw slumps, so that only areas where ground ice is degrading have been identified.

CHAPTER 3 METHODOLOGY

3.1 INTRODUCTION

This project was primarily a field study supported by laboratory analysis. Field work was carried out over three periods in summer 1990 and 1991 and autumn 1991. Two complimentary survey methods were used in the field to gather data on ground ice. A geophysical method using ground probing radar (GPR) was employed at three sites in an effort to determine the local extent of ground ice and to evaluate the GPR system as a tool for high Arctic permafrost research. In conjunction with this survey technique, standard geological and geomorphological techniques were adopted to map ground ice occurrences and their stratigraphic relationships with the surrounding sediments. The methodology involved in the GPR surveys and data analysis is discussed in section 3.2 and the geological methods and lab procedures are described in section 3.3.

3.2 GROUND PROBING RADAR SURVEY METHODOLOGY

Ground probing radar surveys were performed at two sites at Hot Weather Creek in July 1990 using a Pulse EKKO III GPR unit (Figure 3.1) manufactured by A Cubed Inc. (now Sensors and Software Inc.) of Mississauga, Ontario. This survey was carried out in cooperation with the Terrain Science Division of the Geological Survey of Canada as a follow up to preliminary surveys carried out the year before. In October 1991, a site north

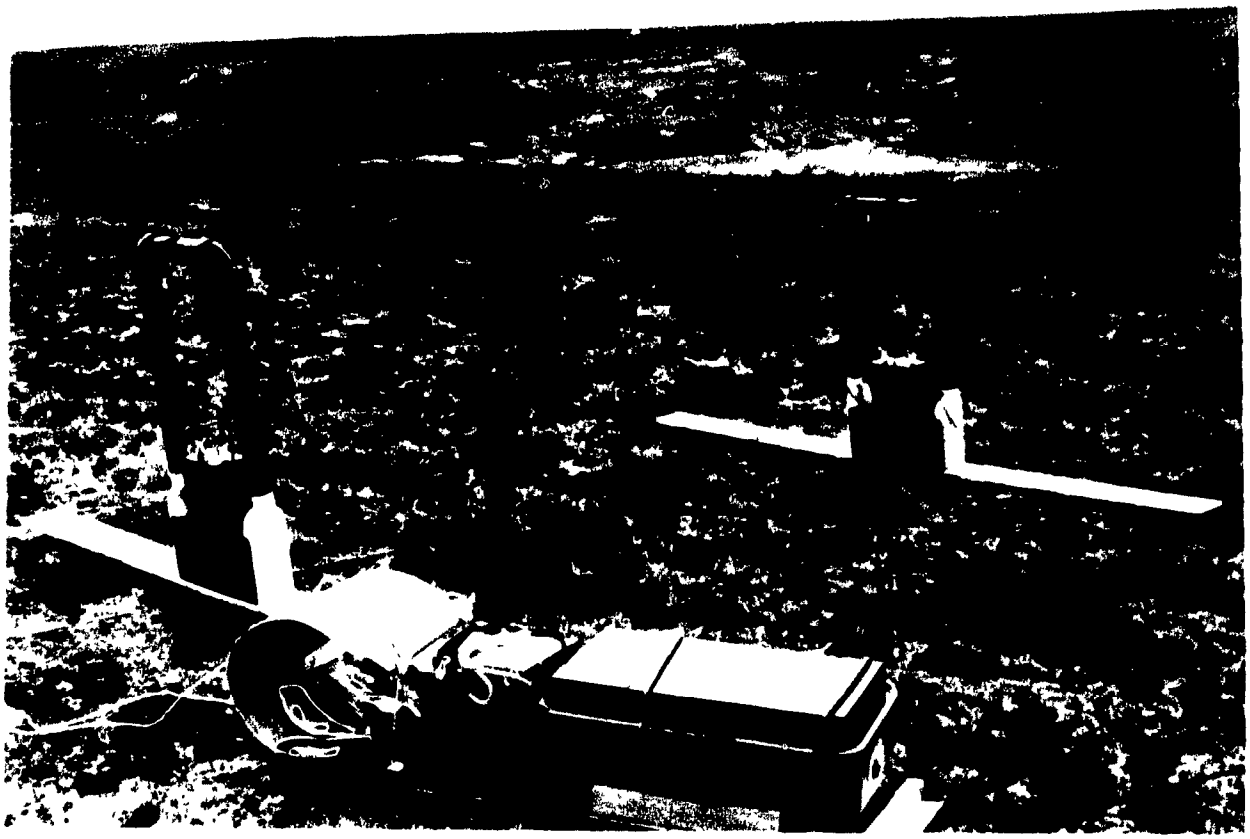

Figure 3 1 The Pulse EKKO III ground probing radar with two 50 MHz antennas (long white objects) to which are attached the transmitter and receiver, and the control unit (including tape storage device) with a 12 volt battery in the foreground The Pulse EKKO IV uses a laptop computer as a control console

of the Eureka air strip was investigated using a prototype Pulse EKKO IV-H borrowed from the Centre d'études nordique of Laval University in Quebec City.

3.2.1 PREPARATION

At Hot Weather Creek, two survey grids that incorporated the previous year's survey were laid out (1), near a retrogressive thaw slump and (2), on an undisturbed plain featuring ice wedge polygons. General topography of the grid was surveyed using a hand held Abney level, while the relative positions of the lines were surveyed using a plane table. Distances along the lines were measured with a nylon survey chain. Positions of the survey grids at Hot Weather Creek were fixed relative to the thaw slump using one metre square targets which were visible on low level aerial photography taken later in the summer.

One retrogressive thaw slump identified in July 1991 north of the Eureka air strip was selected for a GPR survey carried out in October 1991. Although October on Ellesmere Island was not considered to be the best time for a GPR survey in this environment, timing was determined by equipment availability and space on the Eureka supply flights from Resolute Bay.

A grid was laid out over snow of 5 to 30 cm depth surrounding the multiple lobes of the thaw slump, and was surveyed with an Abney level. Given the relative absence of surface variations in the vicinity of the slump and the extreme weather conditions, it was decided that absolute positioning at the

time of the survey was not critical. Visual estimates of line positions relative to each other and to the slump were made. Line distances were measured with a survey tape, and all intersection points were recorded. In 1992 a Magellan Global Positioning System accurate to within 30 m was used by Pollard to determine survey positions at this site. Site investigations included measurements of snow depths at various points along the survey lines. Permanent makers placed around the slump in the summer of 1991 to measure retreat rates were incorporated into the survey grid.

3.2.2 EXECUTION

At Hot Weather Creek, low frequency (25 and 50 MHz) surveys were carried out over a relatively large area to gain a general view of the stratigraphy to a depth of 15 to 25 meters. The 50 MHz antennas yielded medium vertical resolution (40-50 cm) images of the one to 15 meter depth range (assuming a radar wave ground velocity of .10 m/ns). These were used chiefly to identify and trace an ice-rich layer and to locate ice wedges. The 25 MHz surveys yielded low resolution (70-80 cm) images of the 4 to 25 meter depth range. These were useful in determining the deeper structure in the area, including local dips and strikes calculated from apparent dips visible on intersecting profiles.

Near surface studies were attempted by other researchers in 1989 using 100 MHz antennas, but "ringing" (repetitive reflections between two closely

space objects or boundaries) in the well-developed active layer and possibly between the antennas obscured most of the data. The 200 MHz antennas used in 1990 overcame much of this problem, and high resolution ($\approx$10 cm) images were obtained for the .25 to 2 meter depth range. These surveys were carried out on a closely spaced grid within the old slump scar in an attempt to map the top of the ice mass which was melting in the reactivated slump. More widely spaced surveys were carried out on the undisturbed plain at the Automatic Weather Station site in order to investigate active layer variations across a two year old active layer detachment slide scar and to image ice wedges near a developing thaw pond. Unfortunately, the equipment failed partway through this survey, ending the field season a day early.

At the Eureka air strip in 1991, two identical sets of 225 MHz high frequency surveys were conducted. The first survey experienced excessive noise introduced by faulty coaxial cable connectors between the control console and the antennas (a problem with the prototype which has since been corrected), and ringing between the antennas. The problems were remedied by modifying the antennae construction to increase their separation, and ensuring sufficient slack in the five meter connecting cable. Upon inspection of the second data set it was discovered that while previous problems had been solved, ringing was now occurring within the snow layer and between the antennas and the control unit or the twelve volt battery. After allowing sufficient slack in the cable to protect the connectors, the antenna-control unit

separation was only three and a half meters. Given the snow conditions at the air strip site, it was decided that another site some kilometres away might offer better results. Thus on the second to last day of the field period, after more modifications and repairs had been made to the unit and after a ninety minute trip across rough tundra in a tracked vehicle, a survey was started at a thaw slump identified as EU-9 from the summer study. The unit failed on the third trace, possibly due to the rough transport despite the extensive precautions taken to avoid damage.

3.2.3 DATA PROCESSING

Pulse EKKO III data was stored on cassette in the field by the radar unit. Upon return to the GSC offices in Ottawa, the data was transferred to diskette through a Hewlett-Packard computer using the program EKKO DISK by A Cubed Inc. The data records were edited at this point and bad traces discarded or replaced with traces of zero value. A descriptive header file for each data file was created at this stage. The Pulse EKKO IV system software allows this to be done in the field.

Further processing of the data was carried out at the same facilities using EKKO PLOT, also by A Cubed. This program was used to filter traces with a low pass filter, and to apply various gain functions to the displayed data without modifying the stored data. Hard copies of the radar profiles were produced using this program.

All of the Pulse EKKO III data was later converted to DOS format by GSC staff for use on more readily available IBM compatible PC desktop computers with the Pulse EKKO IV software by Sensors and Software Inc. This software package allows more complex filtering and enhancement, as well as editing and topographic corrections. Most of the data collected in 1991 was processed in the field with software similar to this.

Processing involved two main functions; filtering and gain application. A low pass filter was passed down each trace to remove high frequency noise and smooth the data. This filter was an N-point running average with a window length set by the user. In general, a window length of two points was used for the higher frequency data, while as many as ten points were averaged in the low frequency traces. Horizontal features in the profiles were enhanced by averaging a specified number of traces to either side of each trace. Usually no more than three traces were averaged together.

Both constant gain and automatic gain control functions were applied to the data. AGC was found to be more useful on profiles where interference from the radar hardware was a problem, as this method could be used to compensate for system noise. Constant gain functions were used more to enhance deeper reflectors in the low frequency surveys where system noise was less evident and relative reflector strengths were important.

Vertical enlargement of the high frequency profiles to enhance fine details in the top two to three metres greatly aided interpretation. This function

was used extensively with the October 1991 data, as a problem with the radar caused the first 60 ns of each trace to be repeated at 120 and 180 ns, thus overwriting the deeper reflections (ie. no data is available for depths greater than about three meters).

The results of the GPR surveys are presented in chapter four.

3.3 GEOLOGICAL SURVEY METHODOLOGY

This stage of the project involved a more conventional approach to ground ice investigation and focused mainly on retrogressive thaw slumps. The program involved reconnaissance by air and by land to identify potential study areas, measurement and sampling of the sites, some shallow drilling, and laboratory analysis of collected samples.

3.3.1 FIELD PROGRAM

In the summer of 1991, helicopter reconnaissance was conducted over the Fosheim Peninsula south and southeast from Slidre Fiord to Eureka Sound, and east about 25 km up the Slidre River valley. Several areas of active thermal erosion and thaw slumping were identified. Many of these sites were investigated on the ground over the following weeks.

Original plans for ground probing radar surveys of several of these sites had to be abandoned due to the unavailability of a GPR unit. Thus most sites were investigated using only conventional geological and geomorphological

techniques. Physical dimensions of the thaw slumps were measured with a survey tape and a Silva compass inclinometer. A surveying altimeter was used to fix site altitudes relative to sea level at the South Fosheim sites, and relative to Eureka air strip (elevation 78 m a.s.l.) in the Eureka area.

Soil and ice samples were collected for later analysis in Montreal. Surface soil samples were taken at many sites and selected thaw slump headwalls were sampled at regular intervals (typically 50 cm) down their faces to develop ice content profiles of representative stratigraphies. Samples were sealed in plastic bags and weighed in the field.

While drill data would have been a welcome addition to the collected information, no drilling program was planned for 1991. The reason for this omission is that this project is part of a larger study being carried out over three years which is only in its initial, reconnaissance phase. Therefore logistics and field schedules were designed such that a large number of sites might be investigated, a goal which was not compatible with a drill program.

Given the nature of the observed stratigraphic relationships of the ground ice, fairly deep holes (5 + m) must be drilled to sample through these ice layers. An entire field season should be dedicated to drilling with equipment capable of attaining these depths. Some drill core data is available from the 1990 season at Hot Weather Creek, as well as some 1973 core logs from a site near Eureka.

3.3.2 SAMPLE MOISTURE CONTENTS AND CHEMISTRY

Ice and icy soil samples collected in the field were tested for ice content. All samples were weighed in the field prior to shipment to Montreal. Upon arrival in Montreal, thawed samples were drained and the filtered supernatant water stored at 3° to 5°C for later analysis. The filters and the sediment were then oven dried to determine gravimetric moisture contents. These values were then converted to volumetric ice contents using Pollard and French's (1980) equations:

$$V_{ice} = MC\ (\rho)(1.09) \qquad [3.1]$$

where V_{ice} = ice %vol.

MC = gravimetric moisture (% dry wt.)

ρ = ave. bulk density (silt = 1.45 g/cm^3)

1.09 = volume change on freezing

$$V_{ice} = \frac{MC\ (1.09)}{MC\ (1.09) + (1/P)} \qquad [3.2]$$

where P = ave. particle density

Average particle density is assumed by Pollard and French (1980) to be equal to 2.6 g/cm^3 for sediments on Richard's Island, N.W.T. This value is used here as the sediments are similar.

Assuming that silt has 44% void space (Kezdi, 1974), when moisture content is 28% by weight, ice volume equals 44% from equation 3.1, indicating that all of the void space in the sample is filled with ice. Above 28%

moisture content, ice volume exceeds void space, and equation 3.1 no longer applies. Equation 3.2 is therefore used where excess ice exists (Pollard and French, 1980).

Filtered water from icy sediment and pure ice samples were tested for pH and Total Dissolved Solids (TDS) using the Hanna model 624-00 pHep meter and the model 661-10 DIST 1 ATC Dissolved Solids Tester. The pH meter has a precision of ±.2 while the TDS meter is rated at ±2%FS with all measurements automatically corrected to 20°C (lab temperature was 20°C to 21°C). Where TDS concentrations exceeded the 1990 ppm upper range of the tester, the samples were diluted with distilled water. The pH meter was periodically calibrated in a buffer solution of pH 7.0 to correct for instrument drift.

3.3.3 ATTERBERG LIMITS

The liquid limit of a soil is defined as the gravimetric moisture content (% dry weight) at the boundary between liquid and plastic states, while the plastic limit is defined as the moisture content at the boundary between solid and plastic states (Wray, 1986).

To determine the liquid limit, soil samples were crushed using a rubber-tipped pestle and mortar, and were moulded wet into the bowl of a Casagrande device with the surface of the sample parallel to the base of the instrument. A grooving tool was used to divide the sample into two sections. The bowl was repeatedly dropped a predetermined distance to the base until the two soil

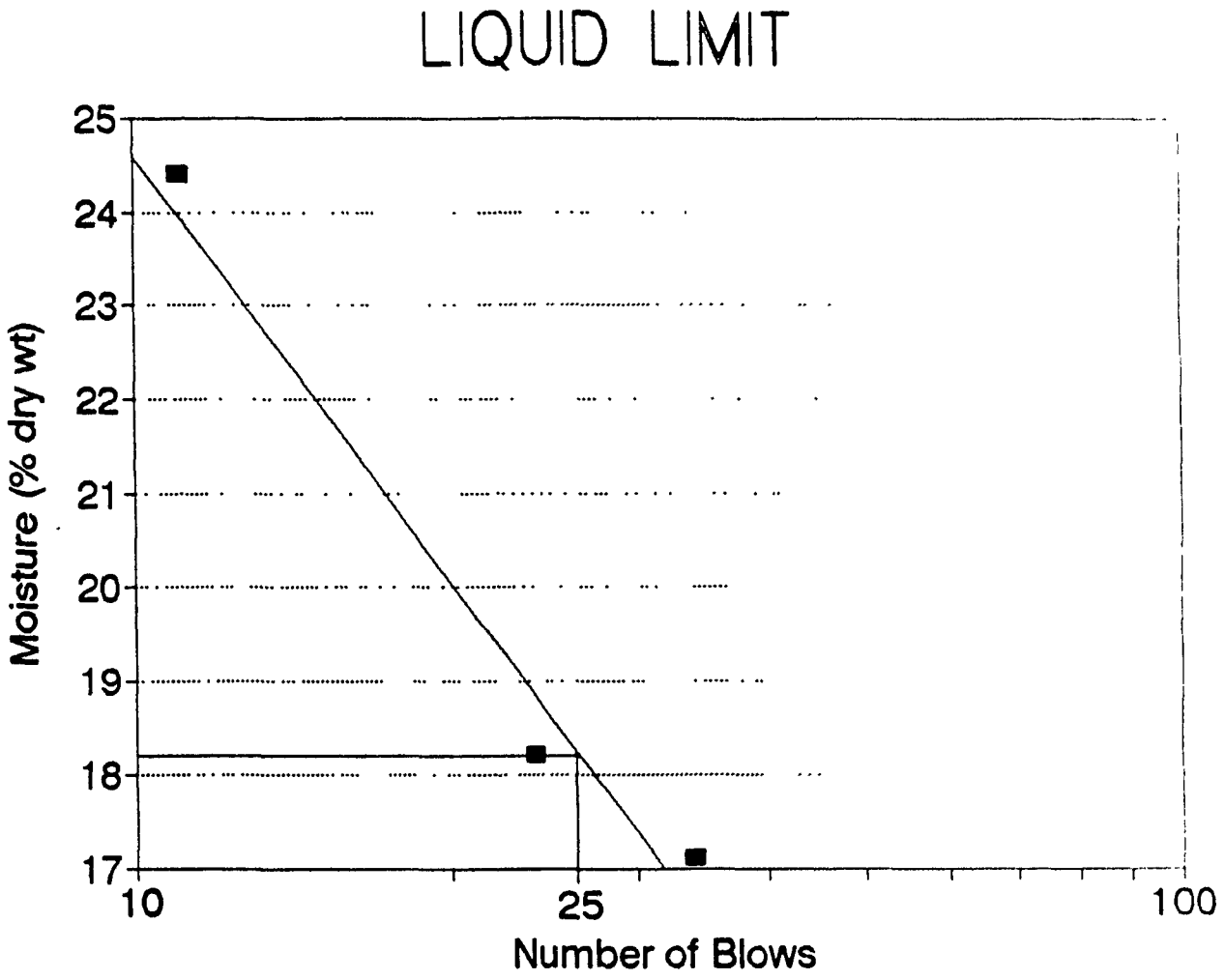

Figure 3.2 Example of Liquid Limit determination.

sections joined along a distance of at least 25 mm. If the number of blows was between 10 and 40, the sample was then weighed and oven dried to determine the moisture content. This process was repeated three times for each soil sample and the results plotted as gravimetric moisture content on an arithmetically scaled y-axis vs the number of drops or blows on a log x-axis. A line was fitted to the data and the liquid limit determined as the moisture content corresponding to the 25 blow value (Figure 3.2).

Plastic limits were then determined as the moisture content at which a sample could be rolled into a thread 3 mm in diameter without breaking. This process was repeated three times per sample and the average taken.

The Plasticity index was then determined for each sample by subtracting the value of the plastic limit from that of the liquid limit.

3.3.4 GRAIN SIZE ANALYSIS

Samples were crushed as above and were wet sieved through four sieves of openings 1.19, .597, .150, and .075 mm (ASTM # 16, 30, 100, and 200). The portion of the sample passing the # 200 sieve was analyzed by a hydrometer test using an ASTM 151H hydrometer. The procedures set out in Lambe (1951) and Wray (1986) were followed and the work was carried out at the McGill Geography Department and at the Centre for Geotechnical Studies laboratory, McGill University.

CHAPTER 4 RESULTS

4.1 ORGANIZATION OF RESULTS

Ground probing radar and stratigraphic survey results are presented separately so that differences between the information types may be clearly seen. GPR offers a less detailed view over a larger area while conventional methods provide locally detailed information which must then be extrapolated. Both methods compliment each other. Another reason for presenting the results separately is that the two methods were undertaken independently at different times and sites due to logistical limitations and the restricted availability of the radar equipment.

4.2 GROUND PROBING RADAR SURVEYS

The quality and value of GPR survey results varies greatly between Hot Weather Creek and Eureka due largely to differences in equipment and transmission centre frequencies. Ground conditions such as freeze/thaw state are also important, but are secondary in this particular instance, and lithological differences are relatively unimportant as both areas are similar.

4.2.1 HOT WEATHER CREEK 1990

Surveys were conducted at centre frequencies of 25, 50, and 200 MHz in 1990, and at 100 Mhz by other workers in 1989 (Figure 4.1). Attenuation of the higher transmitted frequencies was very pronounced due to the fine

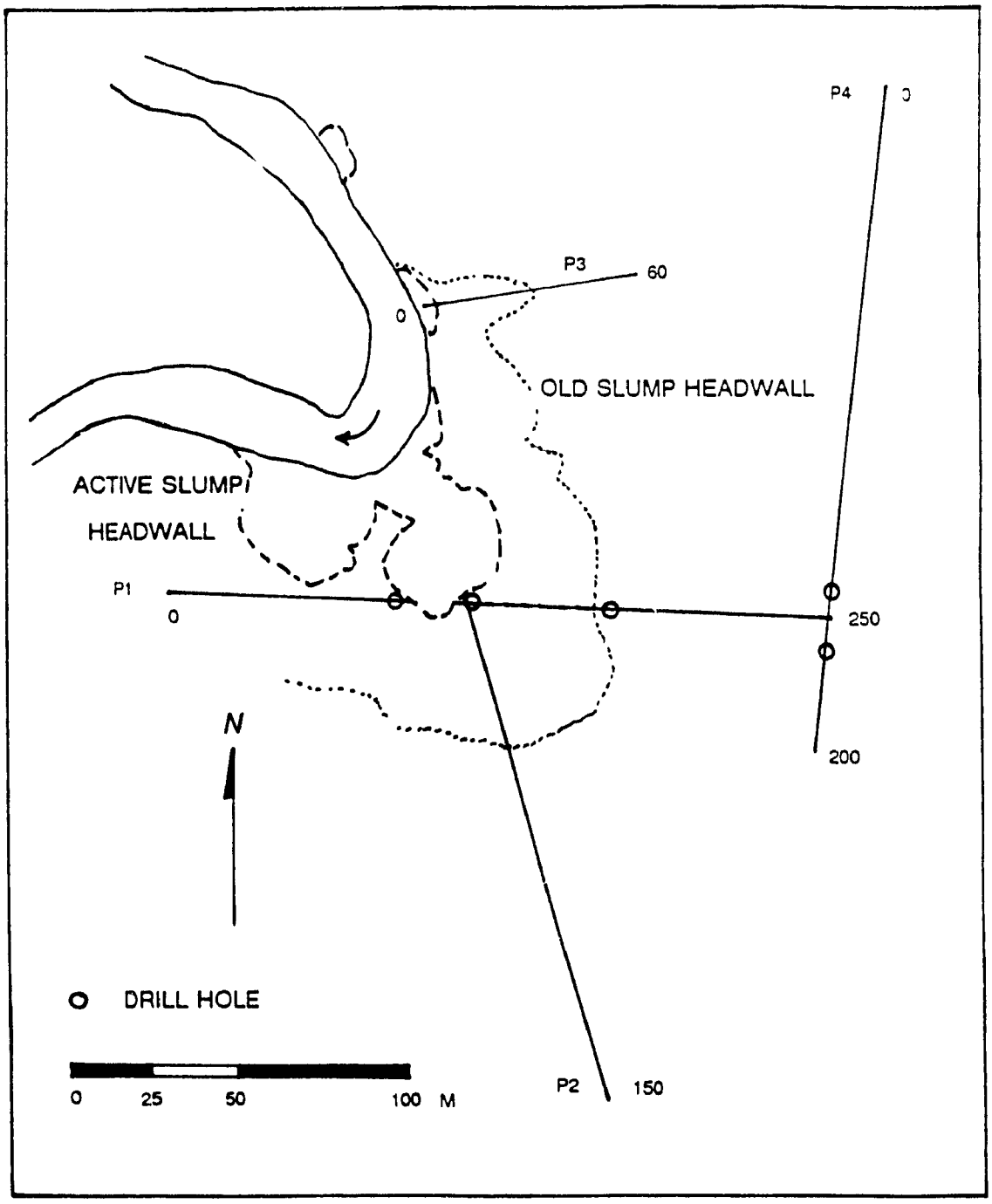

Figure 4.1 Hot Weather Creek GPR survey grid with drill hole locations relative to the July, 1990 headwall position. Numbers indicate Profile number and position.

grained nature of the soil and the high moisture content of the 50 cm to 80 cm thick active layer at Hot Weather Creek in July 1990, Thus, the 25 and 50 MHz profiles were more suitable for deeper profiling. Typical depths of penetration at 50 MHz were 10 to 15 metres assuming an average radar wave velocity of .10 meters per nanosecond (K_a=9.0). This velocity was derived from several common mid point (CMP) surveys conducted at 50 and 100 MHz. Figure 4.2 shows the results of one CMP survey and the derived velocity structure of the subsurface. The relatively high velocities of .15 and .16 m/ns below six and ten metres respectively are indicative of ice rich sediments with very little unfrozen water present. A value of .10 m/ns was chosen as a representative velocity to reflect the widespread presence of silt and clay in thaw slump exposures, as these materials display lower velocities.

Figure 4.3 shows a 50 MHz profile running from the active slump headwall on the left, up a gentle slope over the old slump headwall at station 125 (distances in metres), and onto an undisturbed plain of ice wedge polygons. The two reflectors at the top of the profile are respectively the air and direct ground wave signatures. In places where the ground wave velocity is high, the ground wave is lost in the air wave signature. This is more apparent on the second profile Figure 4.4 which is over level ground.

The stacked hyperbolic curves (Figure 4.3) from 150 to 250 ns at station 196 are typical of the reverberant trains created by the presence of ice wedges. Ice wedges 1.7 m wide and 3+ m deep were exposed by a stream bank

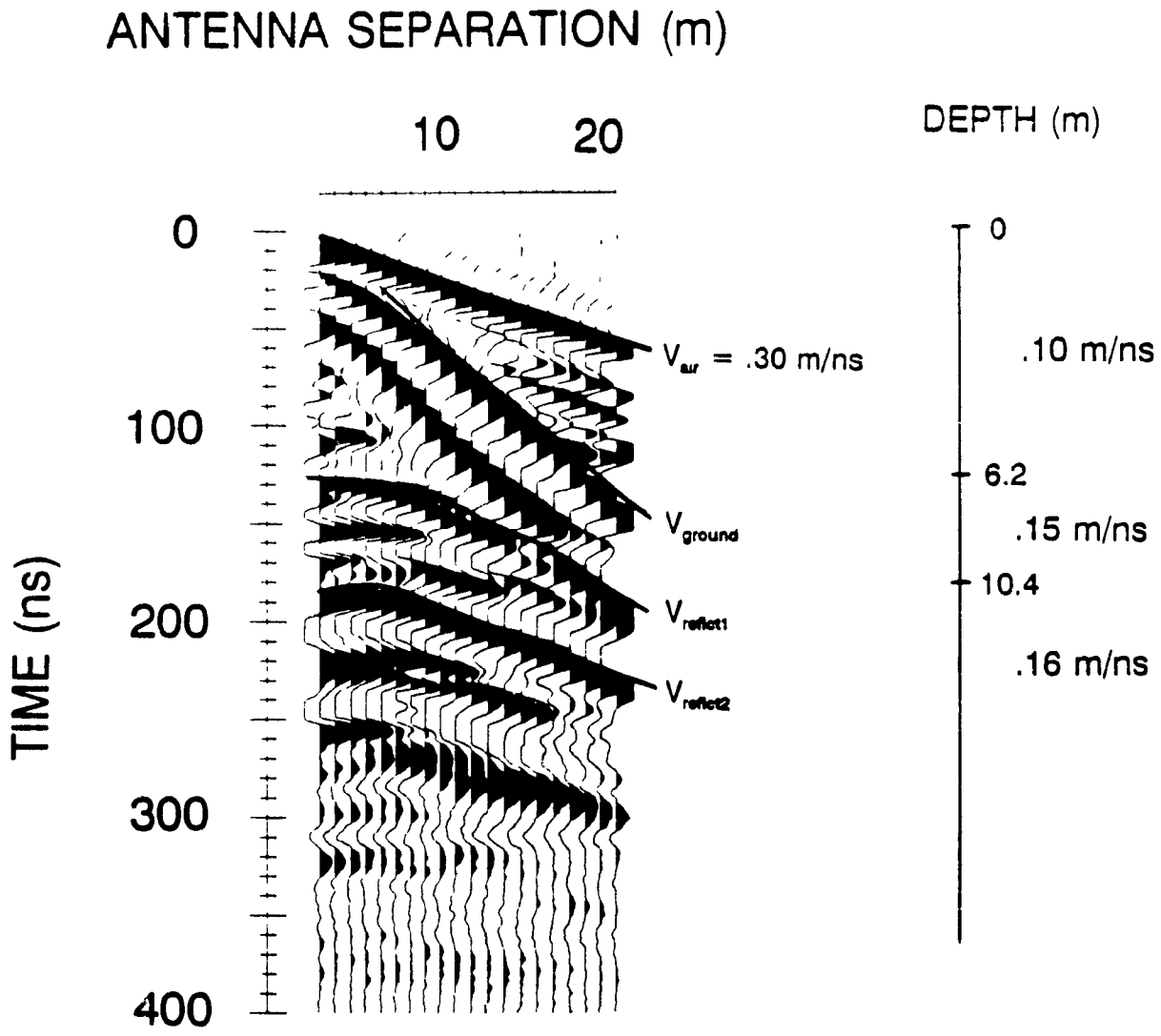

Figure 4.2a Results of a 50 MHz CMP survey at Hot Weather Creek showing the velocity structure of the subsurface.

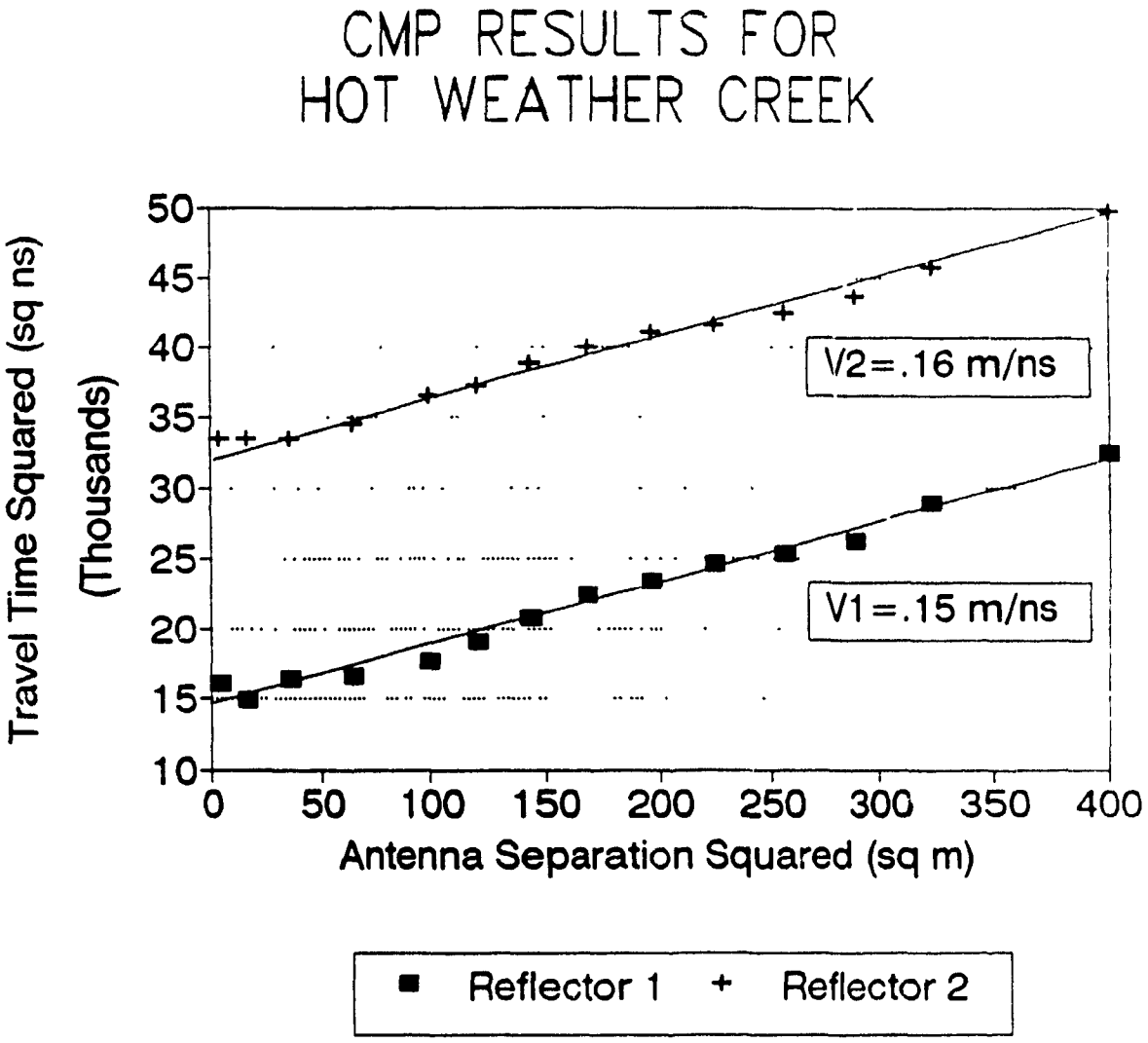

Figure 4.2b T^2 vs X^2 plot for previous CMP revealing velocities associated with two reflectors at 6.2 m and 10.4 m depths.

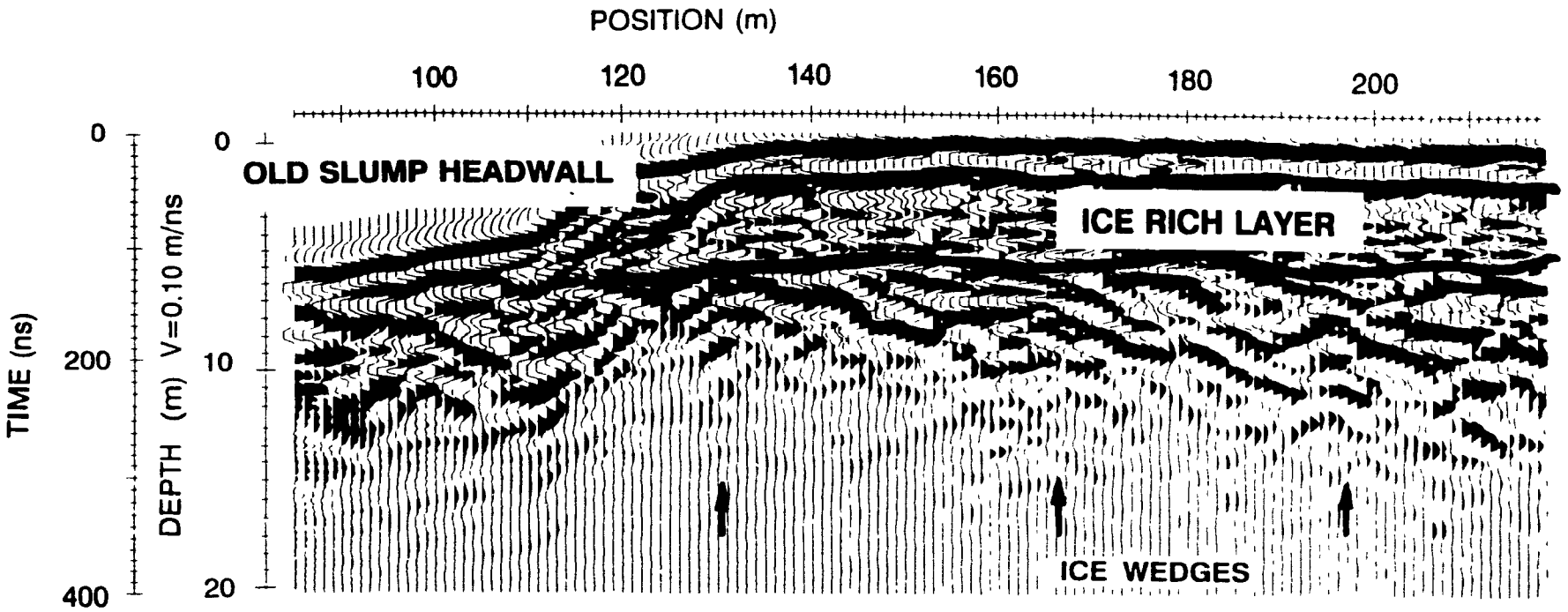

Figure 4.3 50 MHz profile Line 1 corrected for topography, showing a strong reflector at the top of the ice-rich layer which terminates at the old slump headwall.

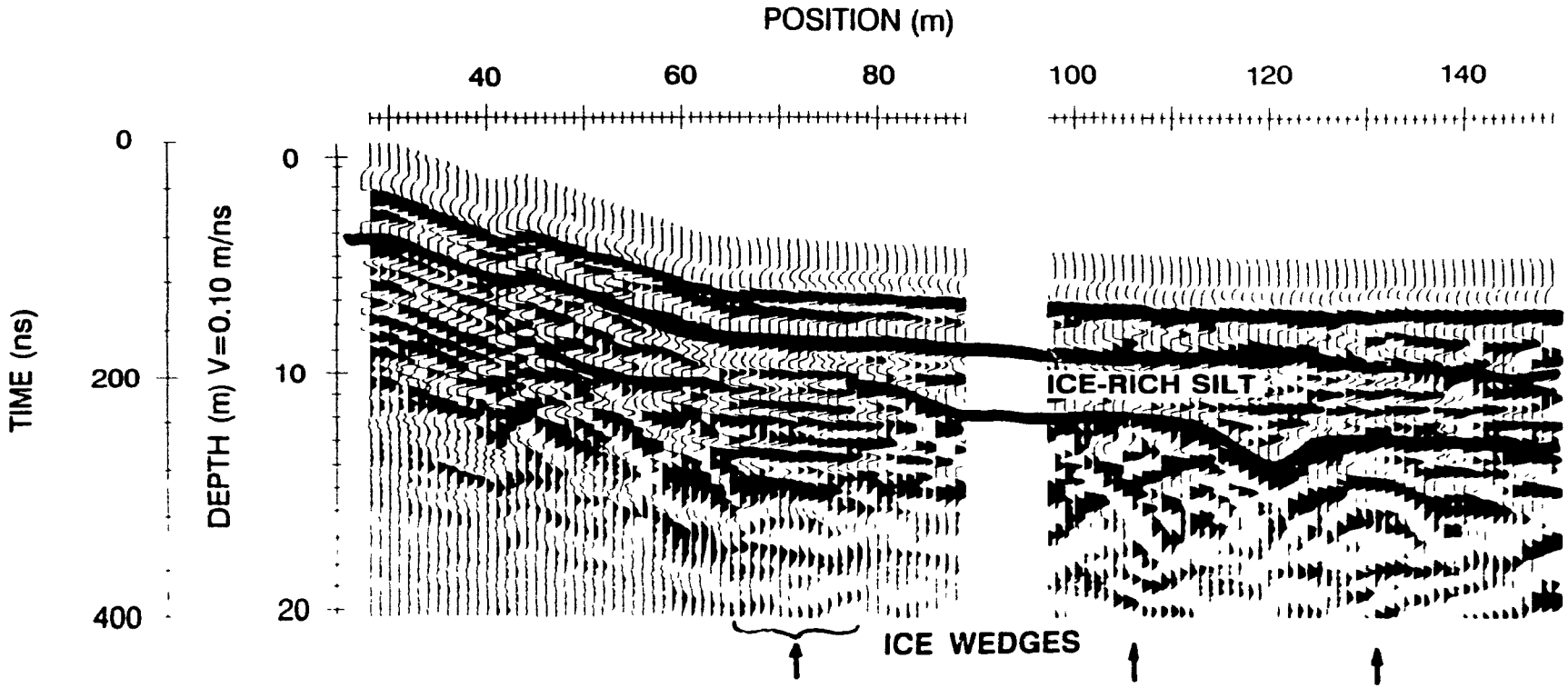

Figure 4 4 50 MHz profile Line 4 showing ice-rich layer and increased radar penetration through ice wedges.

collapse in this area. A surface trough characteristic of an ice wedge was recorded during the survey at this location. Similar features can be seen at stations 130 and 164. The latter station is located on a slope where no surface features indicative of an ice wedge were observed. Mackay (1963, p. 49) states that ice wedges can be obscured by the downslope movement of soil material without the destruction of the wedges themselves. Thus the GPR can be used to detect buried ice wedges. The late arrival of the reverberations must not be interpreted as the depth extent of the ice wedges. Internal reflections and scattering of the radar wave by the ice wedge results in these anomalous travel times (Arcone *et al.*, 1982).

On this and other 50 MHz surveys, areas of increased penetration can be seen where ice wedges occur. As mentioned earlier, Davis and others (1976) observed a similar phenomenon over ice wedges in clay till at Involuted Hill, N.W.T. The ice was found to act as a window through the radar-opaque material. At Hot Weather Creek, penetration was increased from 10 metres to between 15 to 20 metres. Increased penetration depths under ice wedges were also observed on the 25 MHz profiles, although to a more limited extent.

The strong reflector seen at about 40 ns (2 m depth) in Figure 4.3 is interpreted as being the top of a massive ice or continuous ice-rich layer extending to depths of six to eight metres. This layer appears to be free of any laterally extensive reflectors which can be imaged at 50 MHz. Given the continuous nature of the upper boundary of this layer, and its relatively

constant depth, it may represent a former thaw unconformity significantly below the present maximum thaw depths of about a half to one metre as indicated by nearby exposed ice wedge cross sections. This implies that the thaw unconformity and the ice-rich layer predate the currently active 1 to 2 metre wide ice wedges. The base of this layer appears to be discontinuous and undulating, possibly indicating a gradational boundary.

Strata observed in 50 MHz profiles on lines 1 and 4 with apparent dips to the north and east were calculated to dip about 10 degrees to the northeast.

Several shallow holes were drilled using a CRREL permafrost coring kit. These cores revealed the presence of ice-rich silt with clay and massive ice layers several centimetres thick. One hole was drilled in a high-centred ice wedge polygon at the intersection of profiles 1 and 4 which showed ice-bonded sand and detrital coal with minor silt displaying contorted lamina. Only minor amounts of ice were visible in this 2.23 m deep hole. While several holes were drilled, none were deep enough to sample the layer below the strong radar reflection. Since the radar data could not be processed in the field with the Pulse EKKO III system, coreholes were not targeted to any specific depth with the result that at least one hole appears to have stopped just short of a massive ice layer.

The termination of the layer at the old slump headwall indicates that it probably predates the slump. If it is an ice-rich layer, its melting likely contributed to the formation of the old slump.

Several surveys were also carried out at 25 MHz. This frequency provided very good results for deeper stratigraphic interpretation. Typical depths of penetration were 25 metres, again assuming an average velocity of 10 m/ns, with penetrations of up to 30 metres through ice wedges.

Figure 4.5 shows two profiles at 25 MHz. Fairly homogenous stratigraphy can be seen, displaying discontinuous lamina with no strong structural disconformities. The reflections may be due to variations in ice content, or in grain size such as clay layers in silt or sand. The apparent cross-bedded structure visible in some of the profiles suggests an alluvial environment of deposition.

The base of the ice-rich layer appears as a well defined, irregular reflector between 5 and 7 metres depth in these 25 MHz profiles. In contrast to the 50 MHz profiles, here the base of the icy layer appears sharper. However, it remains discontinuous and in places seems to cross-cut other reflectors.

4.2.2 EUREKA OIL TANK FARM 1991

A ground probing radar survey using a high frequency prototype radar unit was carried out over three weeks in September and October of 1991 at the Eureka weather station on Ellesmere Island, N.W.T. The aim of the survey was to assess the application of utilizing GPR to locate and track an oil spill as it dispersed down slope within the seasonally thawed layer of soil above permafrost. The spill occurred in early 1990, and involved several thousand

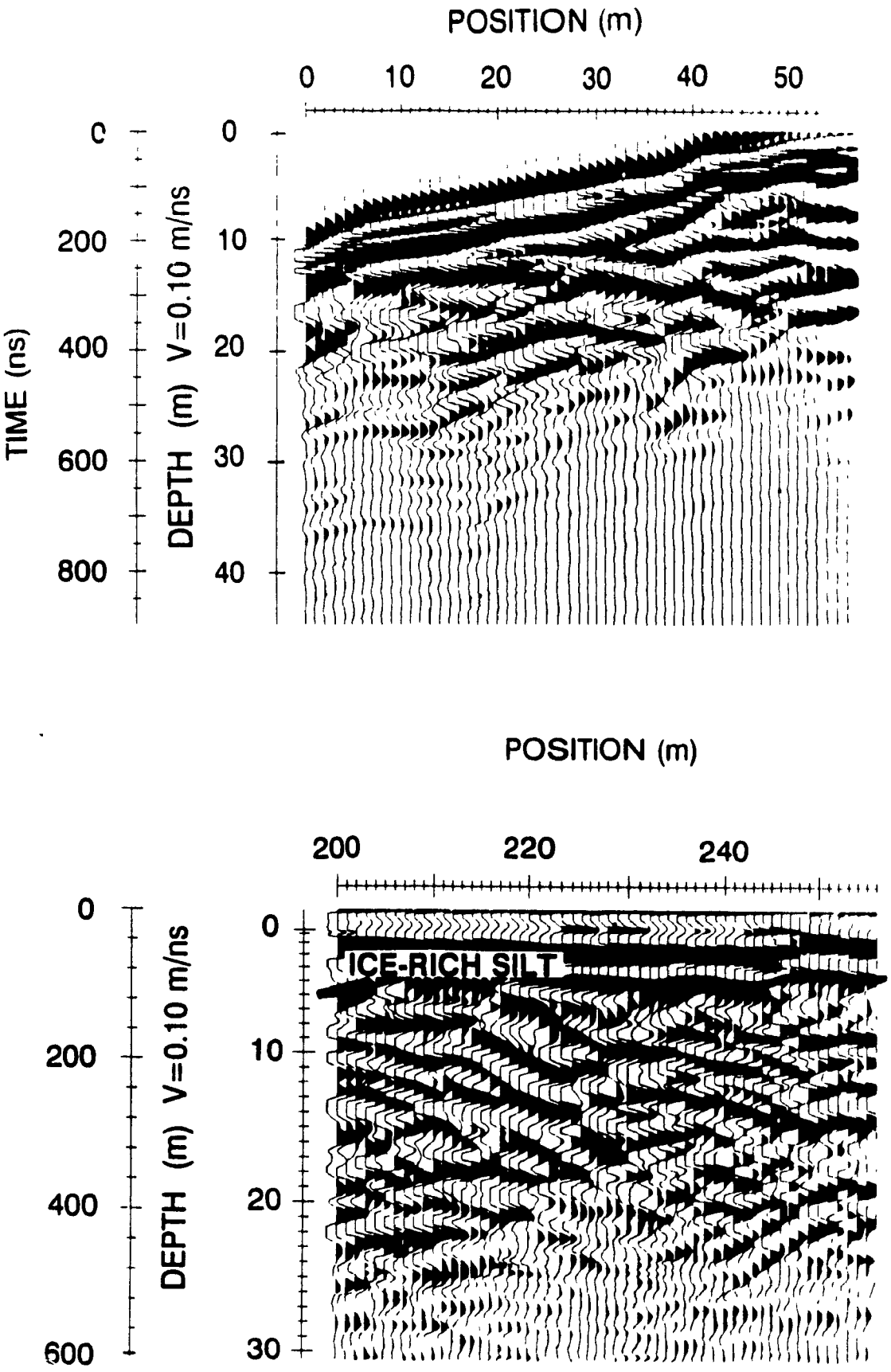

Figure 4.5 25 MHz profiles showing deeper cross-bedded structures in the sediment.

Figure 4.6 The Eureka tank farm survey was carried out to the west (left) of the tank assembly above the scarp The tank farm is to be replaced by a new assembly to the east of the current location, farther from the station's water supply which is located 150 m southwest of the present tank farm location.

litres of winter-grade diesel oil. Given the dielectric and phase properties of water and diesel oil, it was assumed that if the oil remained in the soil in any significant quantity, a geophysical method such as GPR would provide a quick and easy way to determine whether or not the oil mass threatened the station's drinking water supply located 100 to 150 metres down slope to the south west of the station tank farm. As of October, 1991, no evidence of the original oil spill was visible on the surface, thus the survey was arranged to intersect the oil as it migrated down slope from the tank farm (Figure 4.6).

Unfortunately, no oil was conclusively identified in the survey. One possible reason is that after a year and a half, the oil had dispersed and evaporated to the point where it was no longer concentrated enough to be detectable. In view of the fact that most of the contaminated soil was removed shortly after the spill (O'Connor Assc., 1990), this is the most likely possibility.

It should also be noted that difficulties were encountered with the GPR hardware and software. The system used for this survey was a prototype Pulse EKKO IV-H high frequency GPR with centre frequencies of 225, 450, and 900 MHz, which was being tested for Sensors and Software Inc. Being a prototype, there were several problems with the unit which resulted in poor quality data. These problems have since been dealt with by the manufacturer.

Despite these difficulties, some interesting features were seen in the near surface record. The Pulse EKKO IV-H system uses higher frequencies than the

Pulse EKKO IV unit, enabling it to detect shallow features with much greater detail. It is especially useful for active layer studies when the 900 MHz antennas are employed. No reflections from unfrozen pockets of the active layer were observed either in the area affected by oil or in an unaffected area, indicating that the oil had not prevented the freeze back of the soil. (The presence of oil was confirmed by a strong fuel odour in shallow (5 cm deep) holes which were dug at the time of the survey.)

That the oil did not appear to affect freezing characteristics concurs with observations made by Mackay and others (1979) concerning experimental spills of crude oil on both tundra and taiga soils. In that study, no change in the insulating characteristics were observed beyond those caused by the lowering of albedo by oil on the surface. The test spills were not large, on the order of 720 to 1800 litres. Active layer depths were also found to be unaffected after a 200 litre spill on tundra near Tuktoyaktuk (Mackay *et al.*, 1974).

4.2.3 EUREKA AIRSTRIP 1991

The hardware problems that plagued the Eureka tank farm survey also affected the airstrip survey which was carried out at the same time. This work was centred on slump EU-6, a multi-lobed slump located on a gentle north facing slope near the Eureka airstrip which features a two to three metre high headwall showing ice-rich permafrost in sandy silts and clays (Figure 4.7). The results of the 225 MHz surveys were further degraded by the presence of

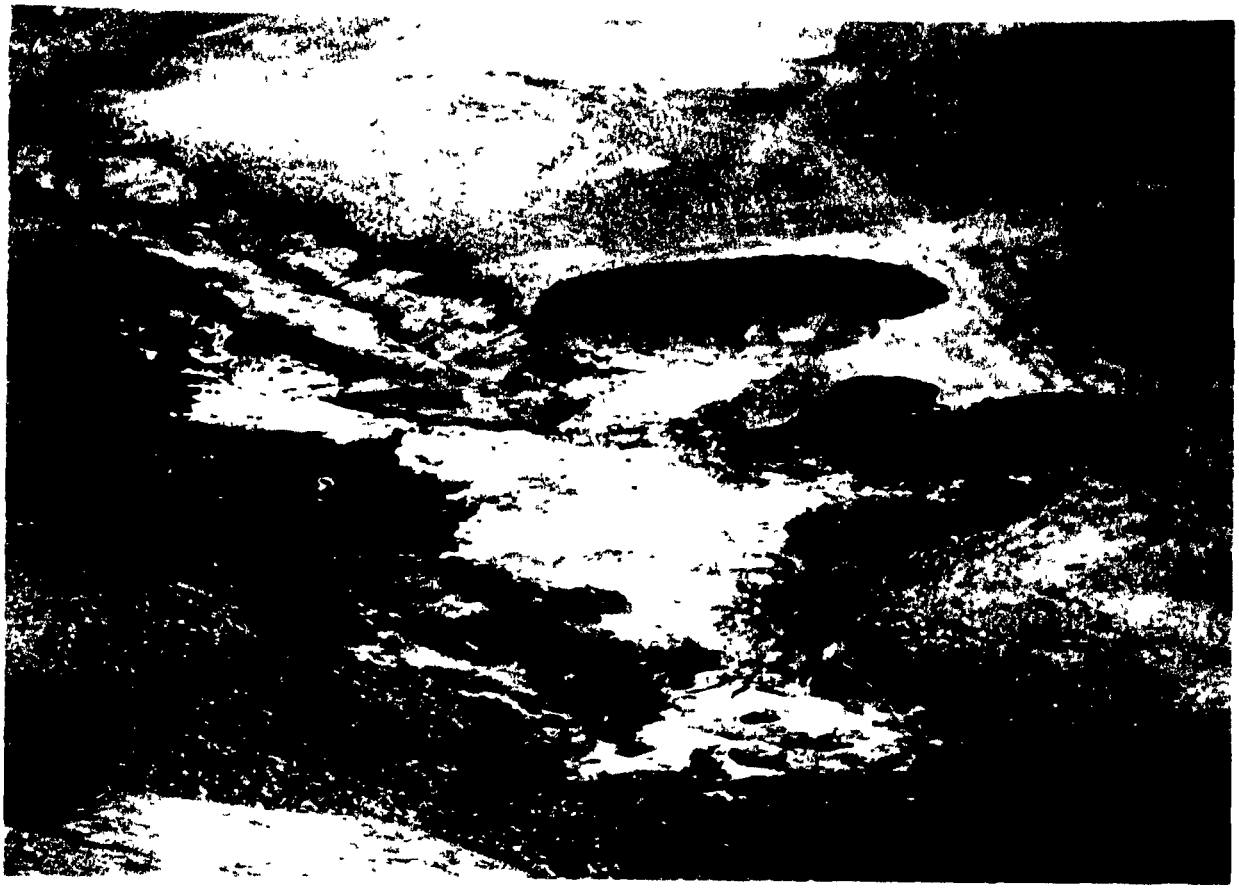

Figure 4 7 Site of the Eureka Air Strip GPR survey Survey grid was laid out above the slump headwalls Note presence of stream and vehicle tracks which predate the slump

between 15 and 100 cm of dry, windpacked snow, over a very hummocky soil surface; however, several interesting features can be seen.

The base of the active layer in October can clearly be seen on the profiles as a strong, continuous reflector at about 8 ns corresponding to a depth of about 40 cm, assuming a radar wave velocity of .10 m/ns. The base of the surface frozen layer is not visible as it is interfered with by the direct ground wave arrival at 5 ns, corresponding to the 50 cm antenna separation.

The top of an ice-rich layer containing massive ice in one of the lobes of the slump can be traced from the headwall along the length of a 25 m profile as it varies in depth from 1.25 m to 1.0 m (Figure 4.8). Several internal reflections in this layer are also evident which are caused by bands of sediment and gas bubbles. The base of the ice layer is not visible in the profile which only extends to a depth of 3 m due to a problem with the radar system.

Also shown in Figure 4.8 are the patterns created by reflected and direct wave arrivals through the air, snow, and soil. The velocity of radar waves in dry snow is only slightly slower than that through air, thus the direct air and snow waves arrive almost simultaneously, with the reflected wave from the snow base arriving next. These are followed by the direct wave through the soil (the "ground wave").

Another profile which runs from east to west across the slope above the slump shows evidence of an earlier erosional feature, possibly a mud flow (Figure 4.9). The top of the icy layer mentioned above is visible at a depth of

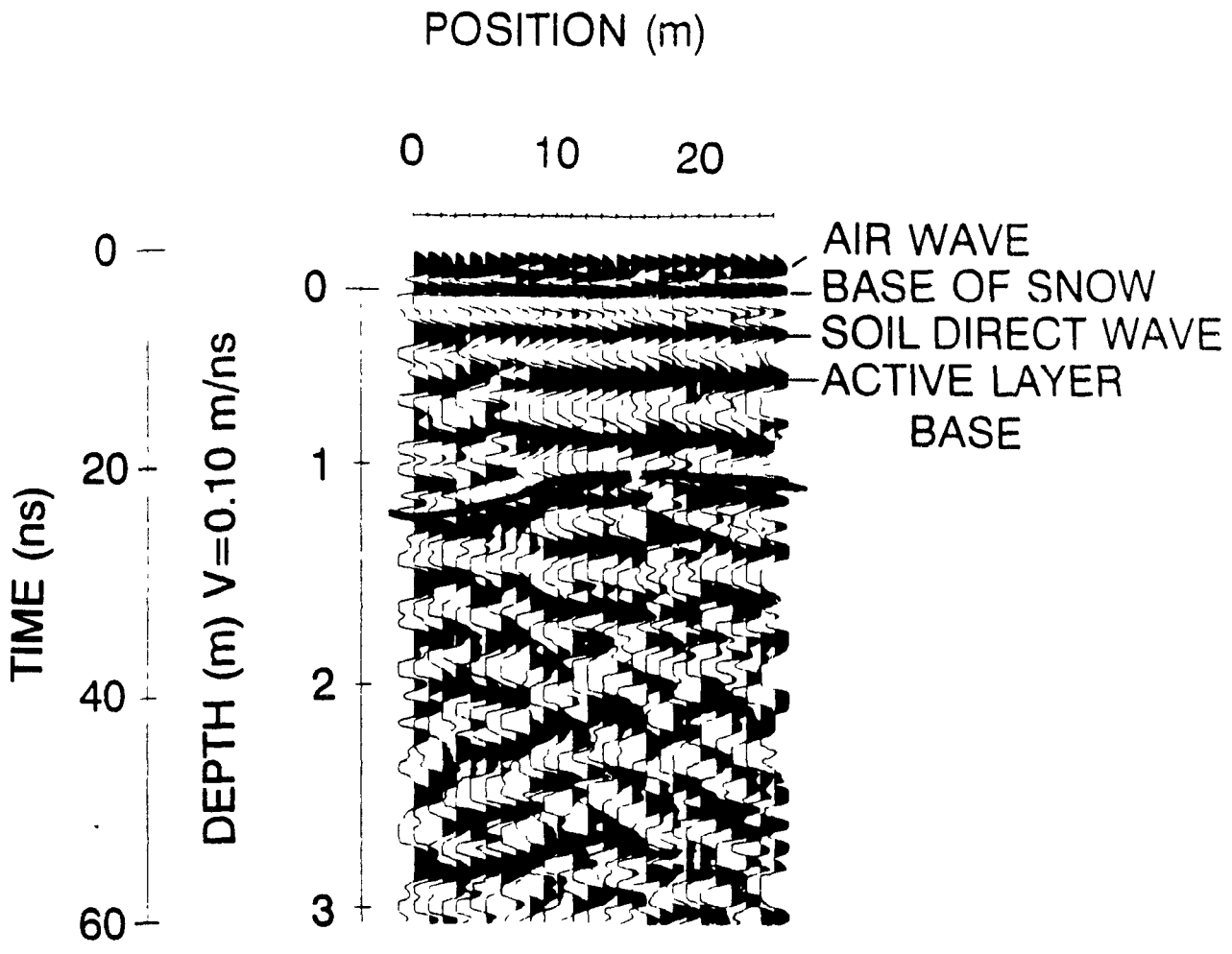

Figure 4.8 A 225 MHz profile from the Air Strip site showing the pattern created by direct and reflected waves through the air, snow, and soil, and from ice lenses in silt below the base of the maximum summer depth of thaw.

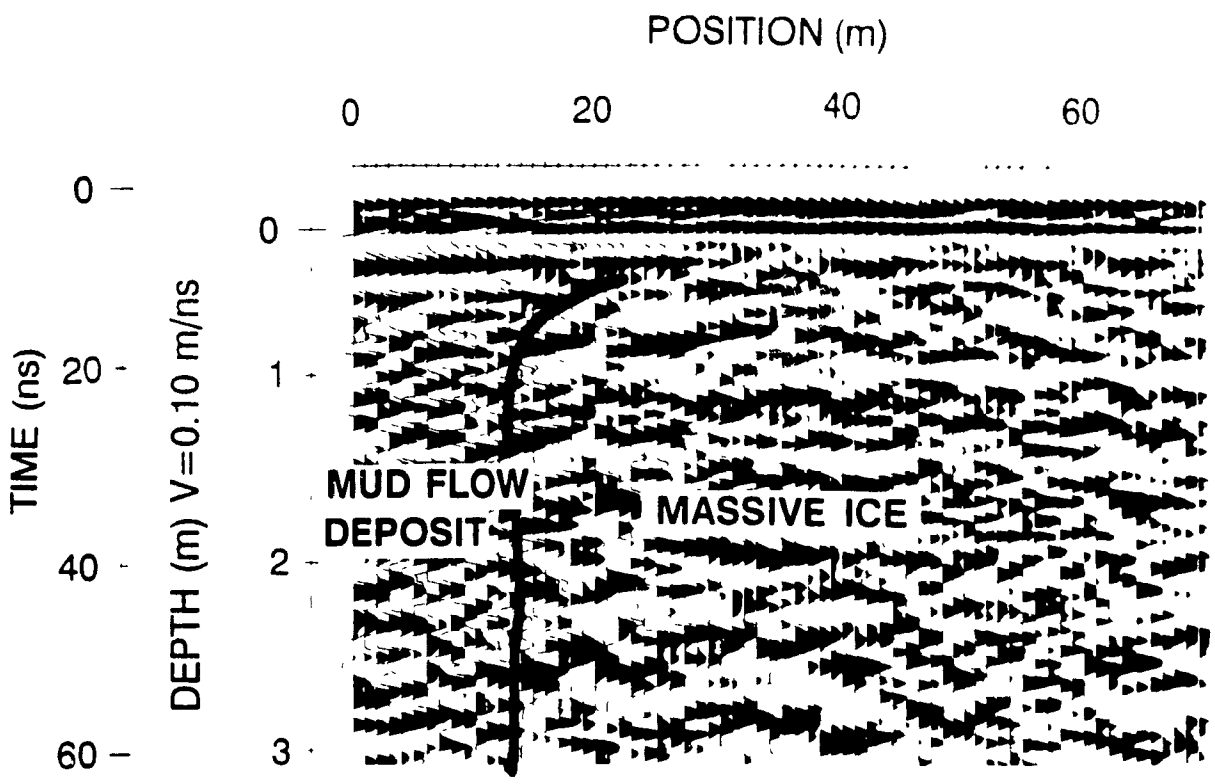

Figure 4.9 A 225 MHz profile showing a mud flow deposit which was visible as massive silty clay in one of the slump lobe headwalls at the Airstrip site.

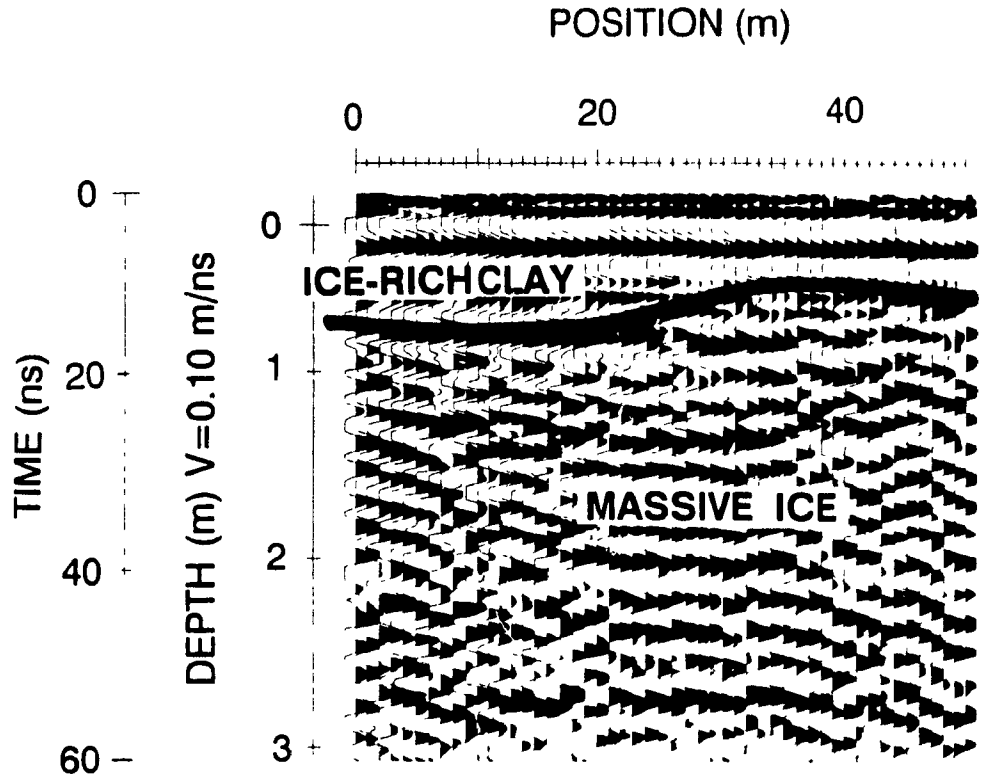

Figure 4.10 A 225 MHz profile diplaying internal layering in the massive ice, with ice-rich clay overlying the gradational boundry at the top of the massive ice.

about a metre, and is fairly flat, but it does not appear to extend into an apparently disturbed area between stations 0 and 12. This part of the profile lacks any coherent structure and may represent a massive silt and clay flow deposit.

Internal layering in the massive ice is visible in most of the profiles of this area (Figure 4.10). The thin, well defined boundaries about 15 to 25 cm apart form a wavy, sub-parallel pattern which often extends to the base of the profile without any significant discontinuities. This pattern is markedly different from that observed at Hot Weather Creek and seems to indicate that this ice body has not been disturbed thermally. There are no cross-cutting reflectors that would suggest a thermal erosion surface, and no such features were seen in the exposed headwalls of this slump. This is also true of the top of the ice layer, which seems to grade into the ice-rich clay layer above it.

4.3 GEOLOGICAL FIELD SURVEY

Twenty-eight retrogressive thaw slumps were identified by helicopter and ground reconnaissance within the study area. These slumps were found to occur in five areas, and were therefore identified by this grouping (Figure 4.11). The areas were labelled Hot Weather Creek, Eureka, South Slidre, and South Fosheim 1 and 2. Several parameters were measured at each site, including ALTITUDE, LENGTH, WIDTH, CIRCUMFERENCE, HEADWALL HEIGHT, HEADWALL SLOPE, and the slopes ABOVE, BESIDE, and on the FLOOR, of the

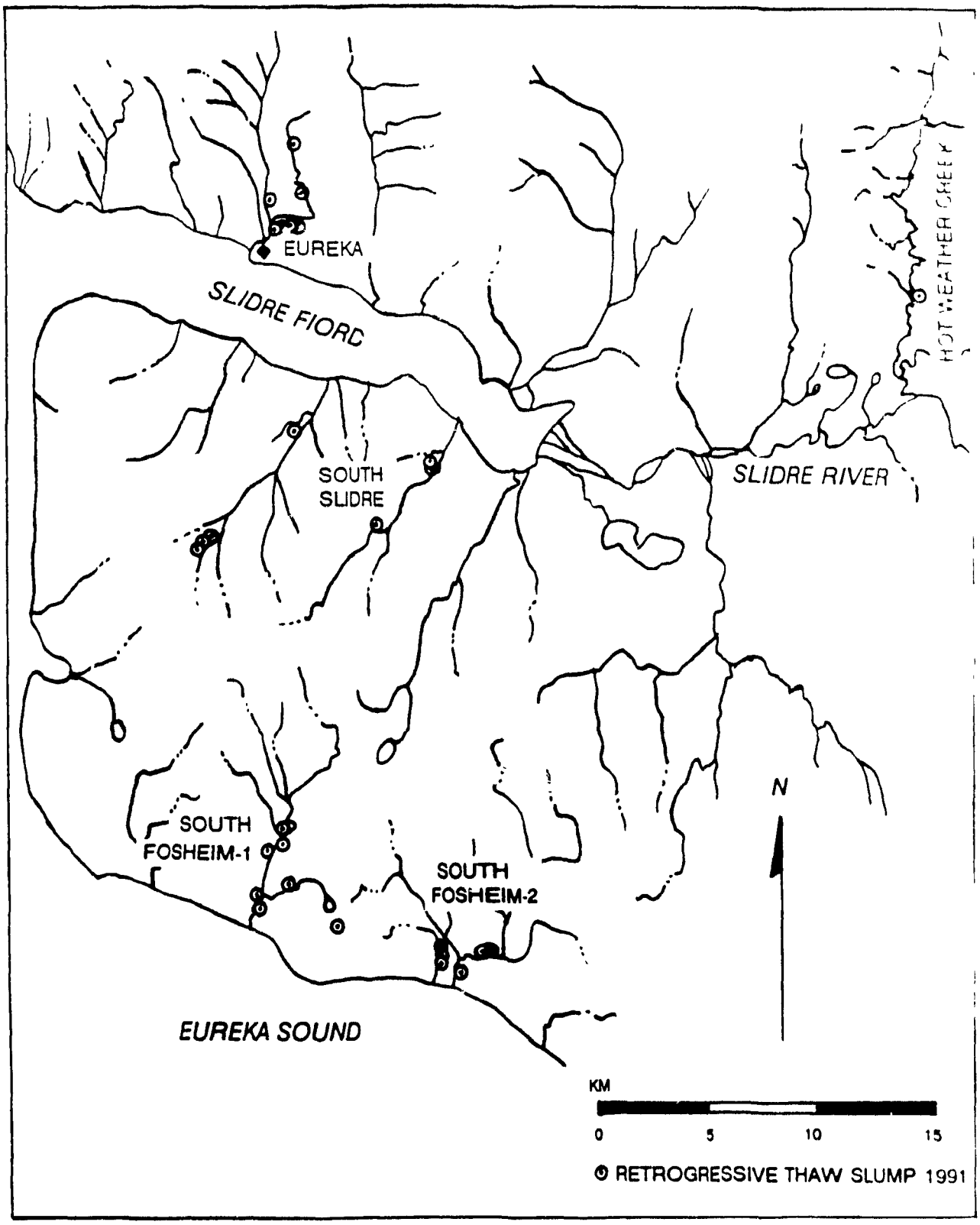

Figure 4.11 Location map of 1991 active thaw slumps.

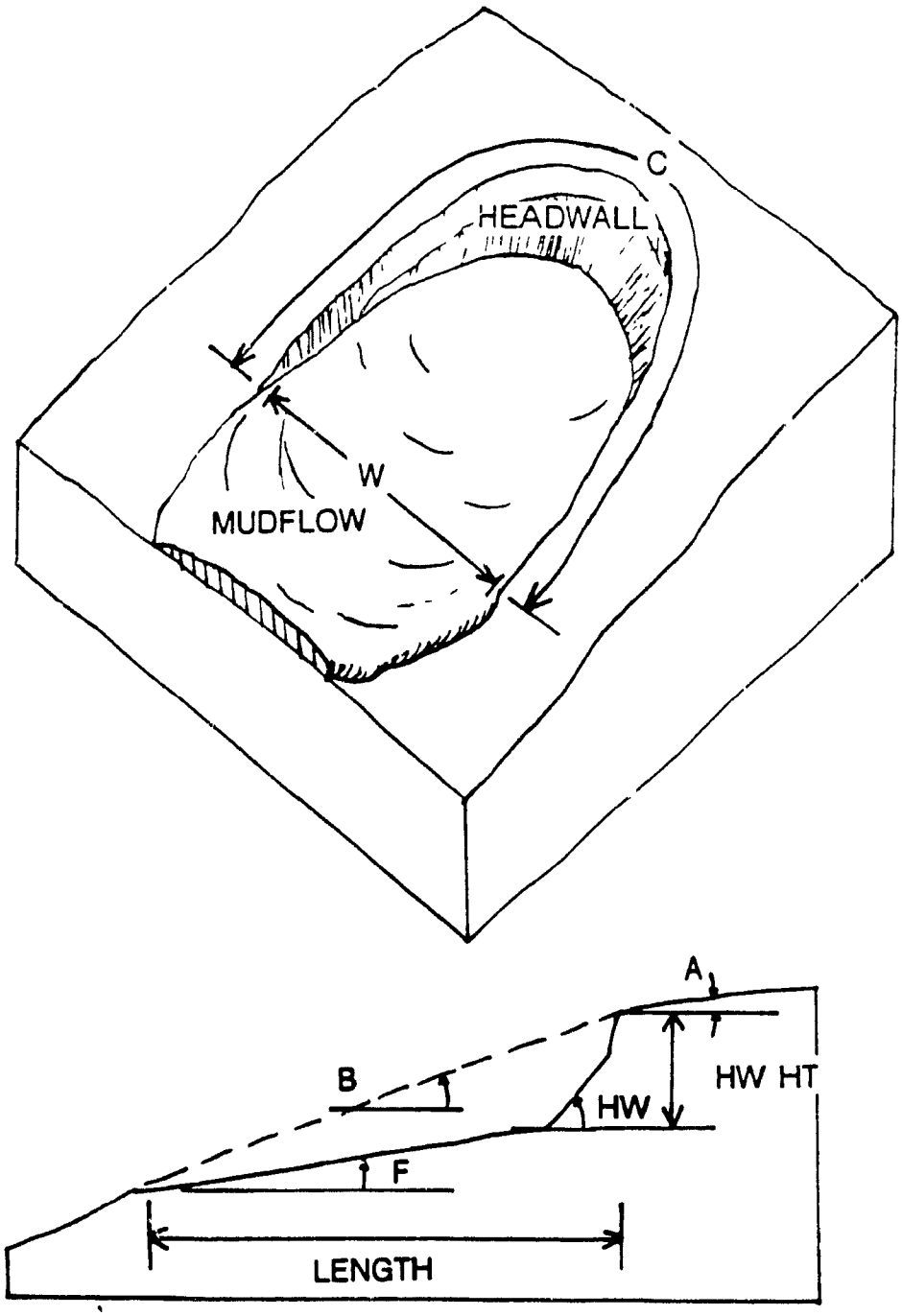

Figure 4.12 Measured thaw slump parameters.

W - Width
C - Circumference
HW HT - Headwall Height
L - Length

Slopes: A - Above
B - Beside
F - Floor
HW - Headwall

TABLE 4.1
THAW SLUMP DIMENSIONS, 1991

Slump	Altitude (m asl)	Length (m)	Width (m)	Circumference (m)	Headwall Height (m)
SF-1A	101	50	34	124	7
SF-1B	38	30	30	102	5
SF-1C	40	46	49	130	7 8
SF-1D	73	33	25	104	4
SF-1E	40	50	90	210	3
SF-1F	51	20	22	49	2
SF-1G	51	24	24	58	
SF-2AI	45	51	30	100	5
SF-2AII	45	20	20	64	10
SF-2B	41	30	40.5	76	6 5
SF-2C	41	50	40	134	3 5
SF-2D	48	25	28	68	2 5
SF-2E	55	18	18	40	2 5
SF-2FI	60	24	17	55	1 5
SF-2FII	60	26	30	60	1 5
SS-1	61				5
SS-3	94	55	40	43	3.8
SS-4	98	28	40		2 4
EU-1	40		35		14
EU-2	82		20		6
EU-3	29	13	20		1.5
EU-4	62		25	47	2
EU-6	46				
EU-7	41	10	15	25	0 75
EU-8	38	10	11		
EU-9		48	31		3 5
HWC-W	76	30	40		
HWC-E	76	40	35		

NB. SF-1 = South Fosheim-1 SF-2 = South Fosheim-2
SS = South Slidre EU = Eureka
HWC = Hot Weather Creek (measured in 1990)

TABLE 4.2
THAW SLUMP SLOPE PARAMETERS, 1991

Slump	Headwall	Floor	Above	Beside
SF-1A	80°	10°	22°	32°
SF-1B	22	5	6	8
SF-1C	39	5	0	8
SF-1D	30	5	5	8
SF-1E	65	5	7	7
SF-1F	70	8		
SF-1G	50	10	0	
SF-2AI	80	5	25	10
SF-2AII	87	10	0	40
SF-2B	80	5	10	15
SF-2C	80	10	7	13
SF-2D	70	10	10	20
SF-2E	50	5	10	17
SF-2FI	45	2	10	10
SF-2FII	35	5	2	
SS-1	62	0	5	8
EU-1	60	5	26	27
EU-2	75			
EU-3	35		10	
EU-4		10		
EU-6	35	0	5	
EU-7	20	0	8	8

NB. SF-1 = South Fosheim - 1
SF-2 = South Fosheim - 2
SS = South Slidre
EU = Eureka

slumps (Figure 4.)

In addition to the 1990 and 1991 sites which were investigated directly several sites were identified from airphotos taken in 1959 of the entire study area at 1:60 000 scale, and from others taken in 1982 and 1986 in the Eureka area at about 1:40000 scale. From these photos and from 1:50 000 scale topographic maps, measurements of ALTITUDE, LENGTH, and WIDTH were obtained.

4.3.1 RETROGRESSIVE THAW SLUMPS

4.3.1.1 PAST THAW SLUMP DISTRIBUTION

Analysis of 1959 airphotos with a scanning stereoscope at 4.5x magnification revealed several apparently active slumps. The relatively low resolution of these reconnaissance mapping photos coupled with their small scale (1:60 000 nominal) made identifying these features very difficult and biased the survey towards larger slumps. The easiest dimension to measure in the photo was the width of the slumps, owing to the contrast between the dark slump floor and the light, dry ground above the headwall. Thus when these parameters are compared for 1959 and 1991, it can be seen (Figure 4.13) that the larger slumps (image size over 1.5 mm or 90 m width) tend to occur in about the same abundance in both years. The smaller ones are understandably under-represented in the 1959 sample, but if the larger slumps are an indication, the total number of active slumps in the two years is about

TABLE 4 3
THAW SLUMP DIMENSIONS, 1959 - 1986

Slump	Altitude (m asl)	Length (m)	Width (m)
SF1-1-59	91	30	15
SF1-2-59	91	30	30
SF1-3-59	43	60	120
SF1-4-59	38	30	30
SF2-1-59	30	30	15
SF2-2-59	30		60
HWC-59	76	120	90
EU-10-59		45	60
EU-1-82	38	14	14
EU-2-82	38		
EU-A-86	61	11	16
EU-1-86	46	13	17
EU-2-86	61	13	43
EU-3-86	38	27	20
EU-4-86	76	20	20
EU-5-86	76	20	20
EU-6-86	38	14	14
EU-7-86	53	7	13
EU-8-86	53	13	13

NB. SF1 = South Fosheim - 1
SF2 = South Fosheim - 2
EU = Eureka
HWC = Hot Weather Creek

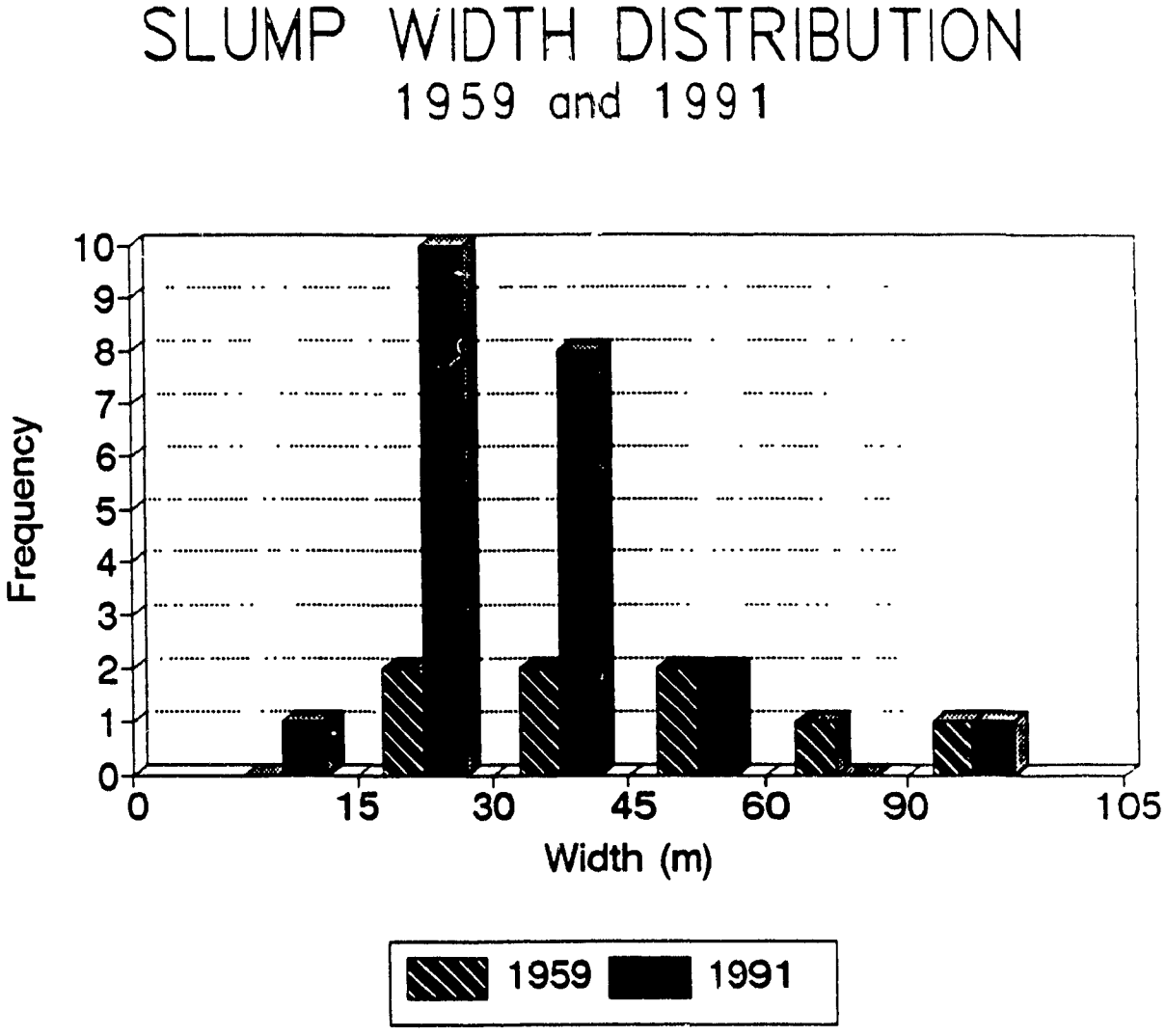

Figure 4.13 1959 and 1991 observed thaw slump widths indicate that smaller slumps are under-represented in the 1959 airphotos. Judging by the larger slumps (45+ m), the probable number of thaw slumps active in 1959 is comparable to 1991.

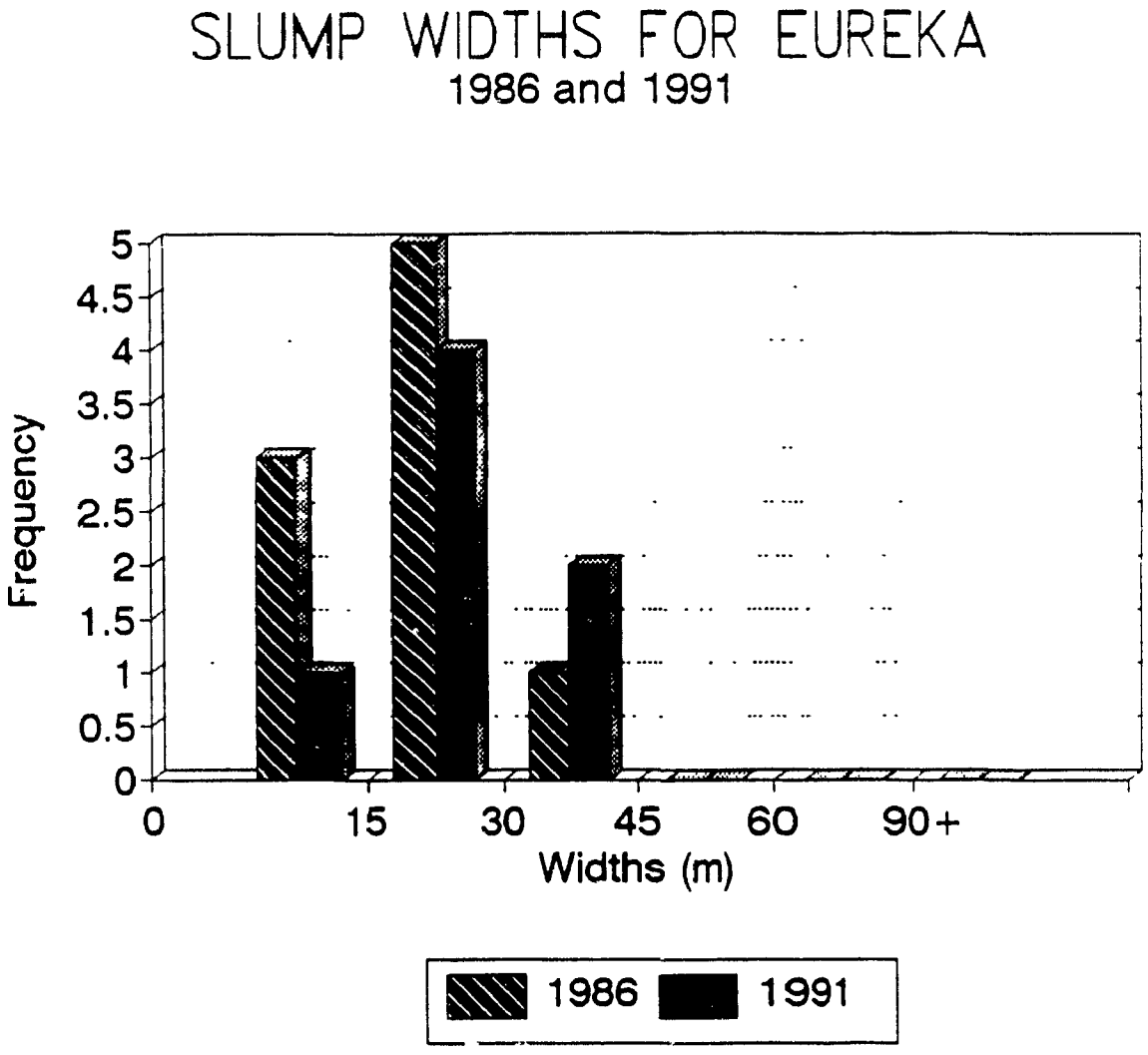

Figure 4.14 Thaw slump widths at Eureka determined from 1986 airphotos and 1991 field observations indicate little change in slump size distribution.

the same. This assumes that the size distribution in both years is similar, and that all of the active slumps over 90 m in width were detected in the 1959 airphotos. Features only 1 mm (60 m) in width on the airphotos were much more difficult to discern than those 1 5 mm across The larger slumps were rather easy to locate on the photos, which lends confidence to the data Of course there is no way to be sure, and with such a small sample a small error would be significant, but these results seem to agree with observations made in 1991.

Inactive slump scars were not counted or measured as the emphasis was on ground ice exposures. However, there were few scars in the study area The greatest concentration of scars was in the South Fosheim-1 area in close proximity to the presently active slumps. These scars were of comparable size and shape to the active sites, and appeared to occur with similar frequency Whether or not these scars date from the 1950s is unknown, but few appeared to have any vegetation within them.

When slump widths for the Eureka site are compared between 1986 and 1991 using 1:4000 scale 1986 photos, one can see that there has been little change in either the overall number of slumps or their size distribution (Figure 4.14). Here the main problem is small sample size, not under-estimation. The photos are of such high quality that one can easily see active layer detachment scars, ice wedge polygons, and vehicle tracks; all of which are smaller than the smallest observed slump in 1991. Interestingly, only two sites were detected

in this area on the similar quality 1982 photos, indicating that most of the 1991 Eureka sites are less than nine years old, but greater than five.

4.3.1.2 PRESENT THAW SLUMP DISTRIBUTION

As one can see in the study area map (Figure 4.11), most of the 1991 thaw slumps occur along rivers and streams. About half of these sites actually contact the streams, and may have been initiated by bank erosion. Other slumps occur at the tops of very steep slopes which are part of asymmetrical valley systems, while the rest are located on gentle slopes.

Given that bank collapse and erosion may well be a trigger mechanism for slumping, it was thought that perhaps slump initiation might be linked to river gradient with more rapid stream flow causing greater bank erosion. Several rivers, both with and without slumps, were measured from 1:50 000 scale photomaps and profiles of each were constructed. No relationship was found when slump occurrences along rivers were compared to gradients. This is not surprising when one examines the distribution of river gradients. Almost 90% of the river segments measured show gradients below 4%. Such little variation is unlikely to influence slump distribution, especially when dealing with such a small number of slumps to begin with.

River gradients tend to increase gently with altitude between sea level and 120 m altitude. These segments tend to show a more dendritic pattern and lie within areas of marine and fluvial sediments. Above approximately 120

m a.s.l, sediment cover is reduced and drainage patterns are influenced more by the underlying geologic structure, becoming increasingly rectangular and showing greater variation in gradient.

Figure 4.15 shows the distribution of thaw slump altitudes derived from 1959, 1982, and 1986 airphotos and from 1991 field observations for the entire study area. One can see that there are no slumps observed above marine limit (140 m a.s.l.) and that two thirds of the sites occur between 30 and 60 m a.s.l. No obvious factor which affects or is affected by altitude was discovered (other than the lack of marine sediments above 140 m a s l.). The altitudinal distribution may reflect ground ice distribution or it may simply be a function of the distribution of land elevation in this area. However, there is no correlation between average ice contents in the slumps and their altitudes, nor was slump length or width found to vary with altitude.

Retrogressive thaw slump orientations are profiled in Figure 4.16 This sample includes all slumps visited in 1990 and 1991 and all those seen in 1959, 1982, and 1986 airphotos. The strongest control here is the orientation of the valleys in which the slumps occur Even in areas showing a predominantly dendritic pattern, most drainage is north-south due to the geological structure of the Fosheim Peninsula. Therefore one would expect east and west facing slumps to dominate Why there are so few west facing slumps may be linked to the asymmetrical cross-section of the valleys which tend to have their shallow slopes on their west sides facing east. These

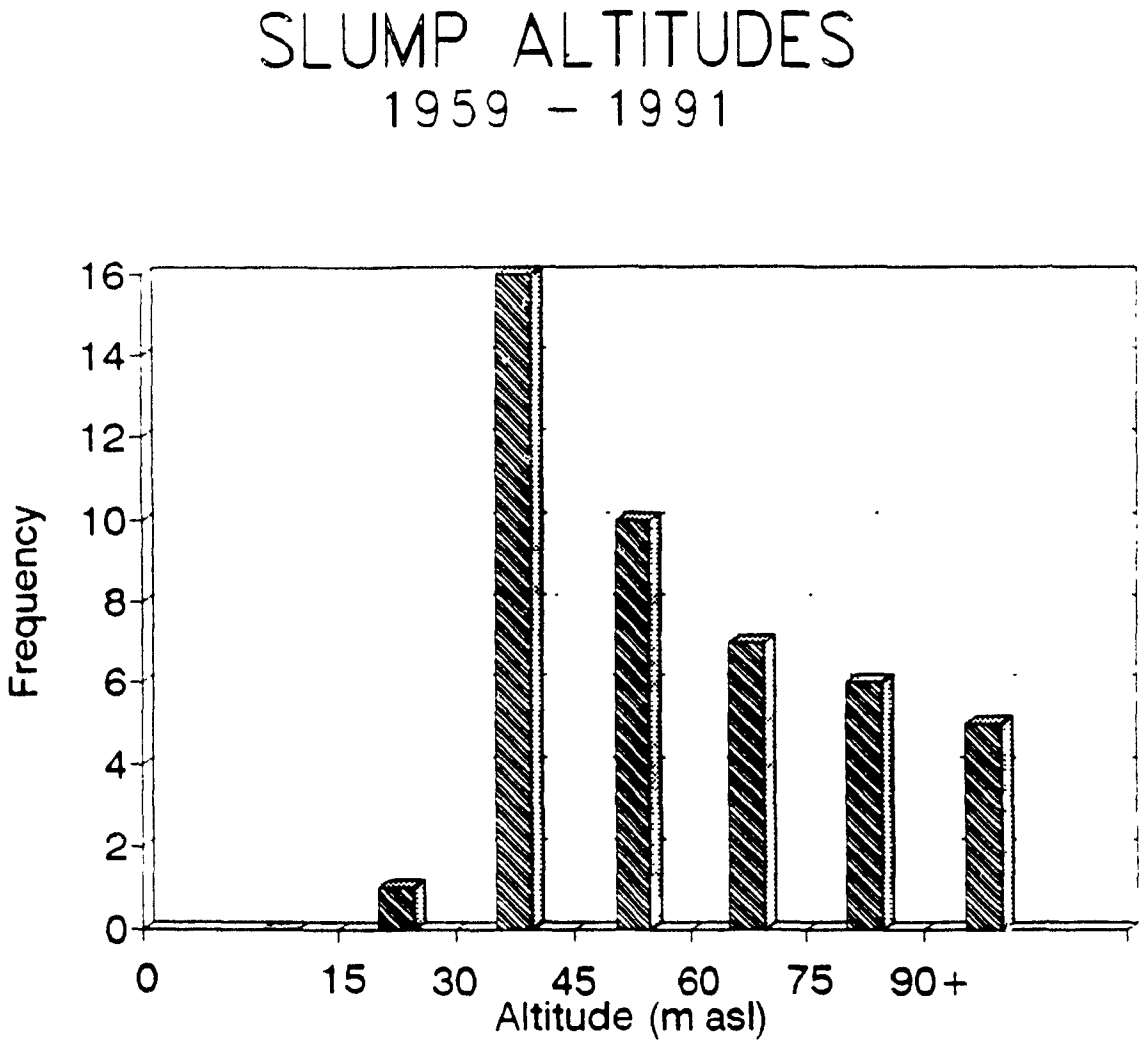

Figure 4.15 Thaw slump altitude distribution derived from airphotos from 1959, 1982, and 1986; as well as from field observations in 1991. No thaw slumps were seen above marine limit (140 - 145 m asl.)

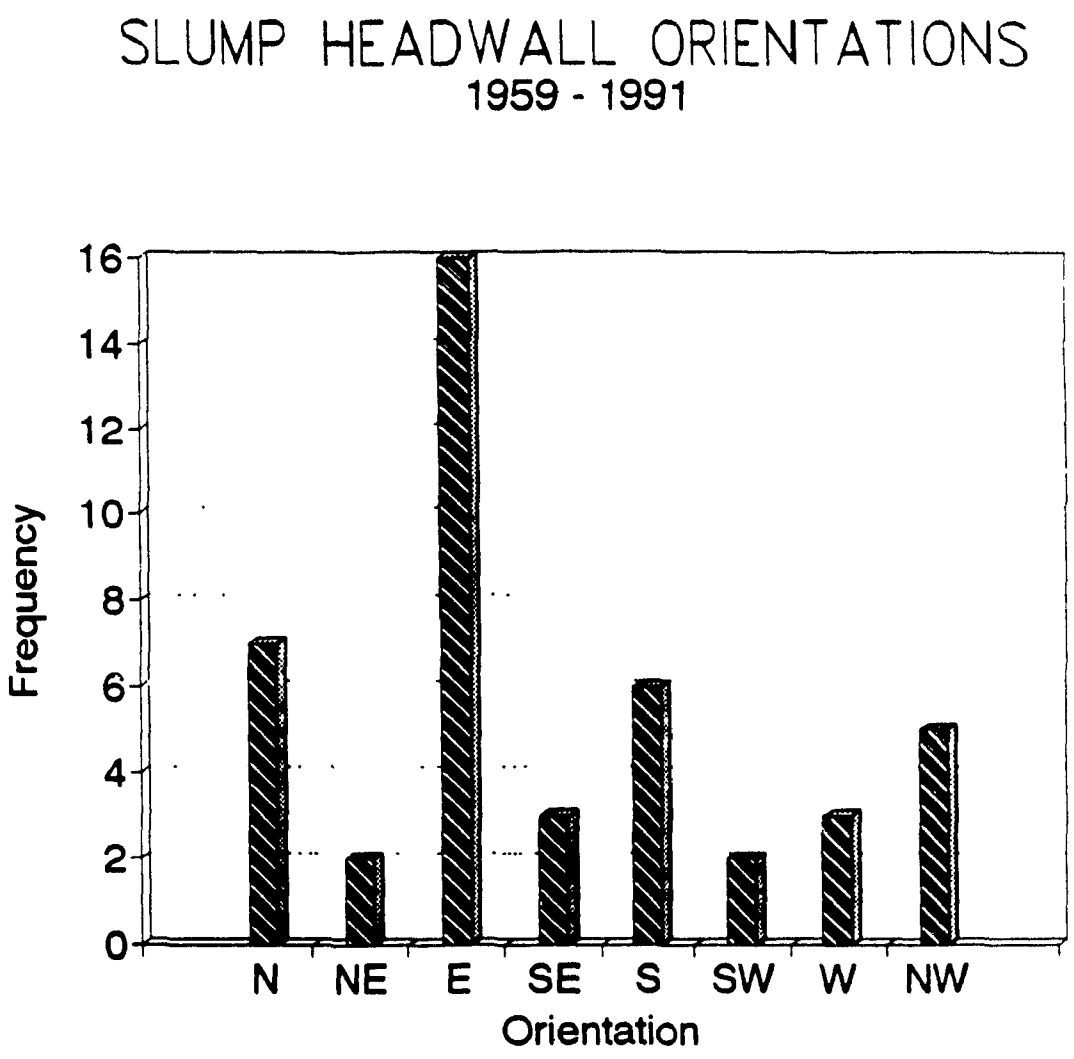

Figure 4.16 Slump headwall orientations for slumps observed in 1991 as well as on airphotos from 1959, 1982, and 1986. Main controls on orientation are structurally controlled drainage and the predominance of east facing shallow slopes of asymmetrical valleys.

shallow, east facing slopes tend to show more slump activity than the steep valley sides, possibly due to reduced drainage and greater snow accumulation in winter providing more insulation (late season snow banks tended to be located on these slopes).

4.3.1.3 THAW SLUMP MORPHOLOGICAL RELATIONSHIPS

Thaw slump length is measured from the apparent origin of the slump to the top of the headwall, while width is measured across the widest part of the slump bowl. In irregular slumps the slump shape was visually averaged while multi-lobed slumps were treated as separate sites.

When the lengths and widths of all of the slump features seen in 1991 and in all of the airphotos from 1959 to 1986 are compared, a 1:1 relationship is revealed (Figure 4.17). Lengths and widths tend to be equal, especially for slumps less than 40 m wide. The small number of slumps larger than 40 m makes it difficult to describe a relationship for large slumps.

Most thaw slumps are relatively shallow, usually two to four metres in height, typically exposing 1.5 to 3.5 m of ice and icy sediments. Some slumps were observed with 10+ m headwall heights, but these were rare. Given this predominance of shallow slumps, opportunities for observing deeper strata, especially for the purpose of interpreting GPR profiles, were very limited. Natural exposures over any sizeable area could only be used to map the top few metres of permafrost. Deeper exposures tended to be isolated from each

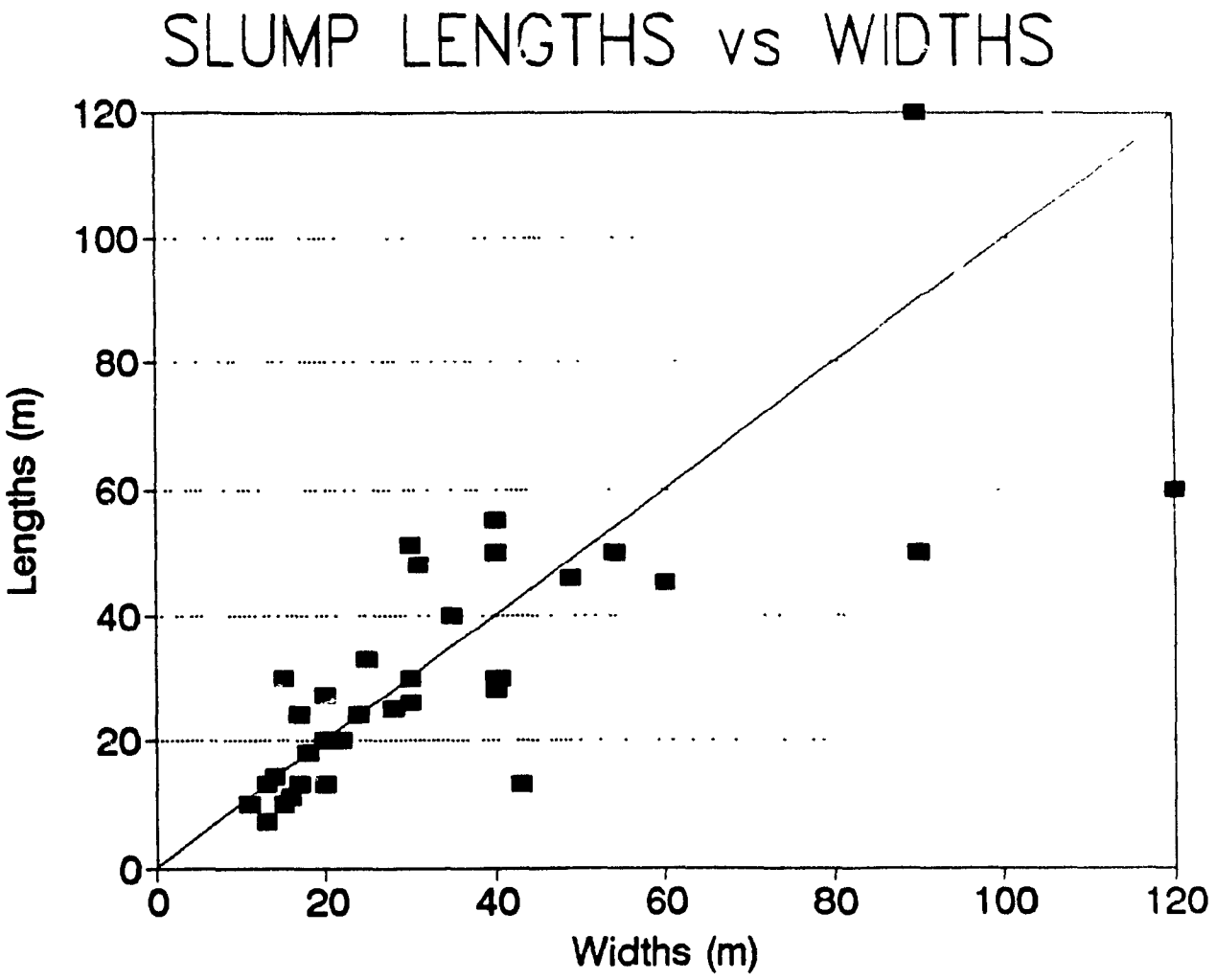

Figure 4.17 Lengths and widths of slumps observed in the field in 1991 and in 1959, 1982, and 1986 airphotos show a virtual 1:1 relationship for small to medium sized thaw slumps

other, making interpolation between them impossible. There is no apparent relationship between headwall height and either slump length or width.

Initially, headwall height appeared to be linked to ice content in the headwall, as it was assumed that greater ice contents would lead to the formation of deeper slumps. This was found not to be the case. Headwall height does not correlate with average ice contents for the slumps, but it is influenced by the local slope upon which the slump is found (r^2 = .36) with steeper slopes naturally giving rise to higher headwalls, regardless of ice content (Figure 4.18). This relationship becomes an almost obvious consequence when one considers the surface angle of the saturated mud found in the floor of an active slump. This angle was never seen to be more than 10° in fifteen slumps in 1991, and was commonly less than 5°, even in areas of steep local slope.

Undisturbed slope angles measured adjacent to active slumps in 1991 show a dominance of shallow (0°-20°) angles (Figure 4.19). In fact, two thirds of the 1991 sites occur on slopes of between 5° and 15°. These angles are similar to the 12° and 14° angles given as the average slopes for active layer detachment slides at Black Top Creek and Big Slide Creek respectively (Lewkowicz, 1990). Given that detachments slide scars were often seen in association with slumps, it seems likely that active layer detachments may be a trigger mechanism for retrogressive thaw slumps.

Interestingly, more than half of the slopes above the slump headwalls

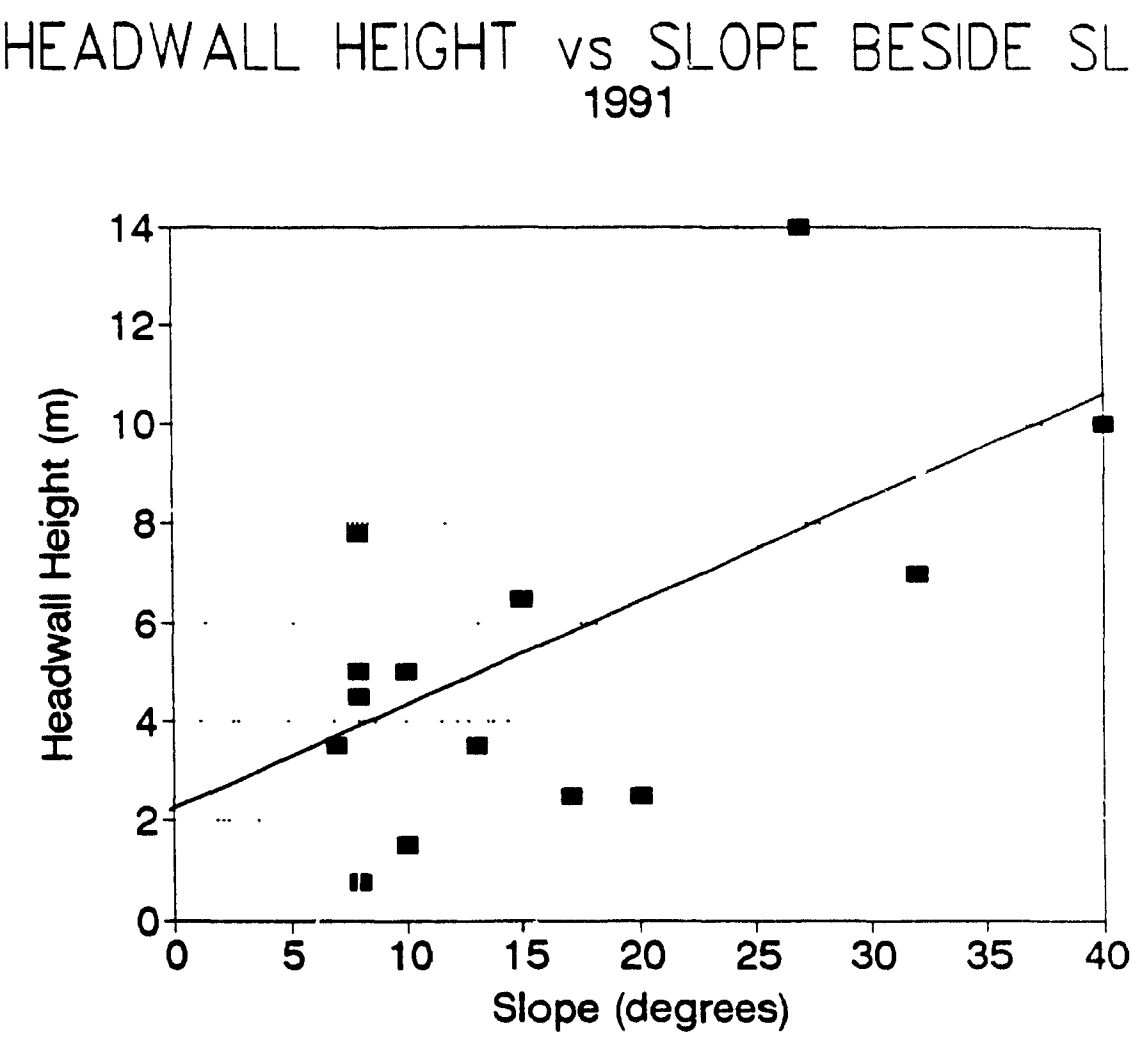

Figure 4.18 A weak relationship is revealed between headwall height and the slope upon which the slump occurs with steeper slopes producing higher headwalls where sufficient ice is present.

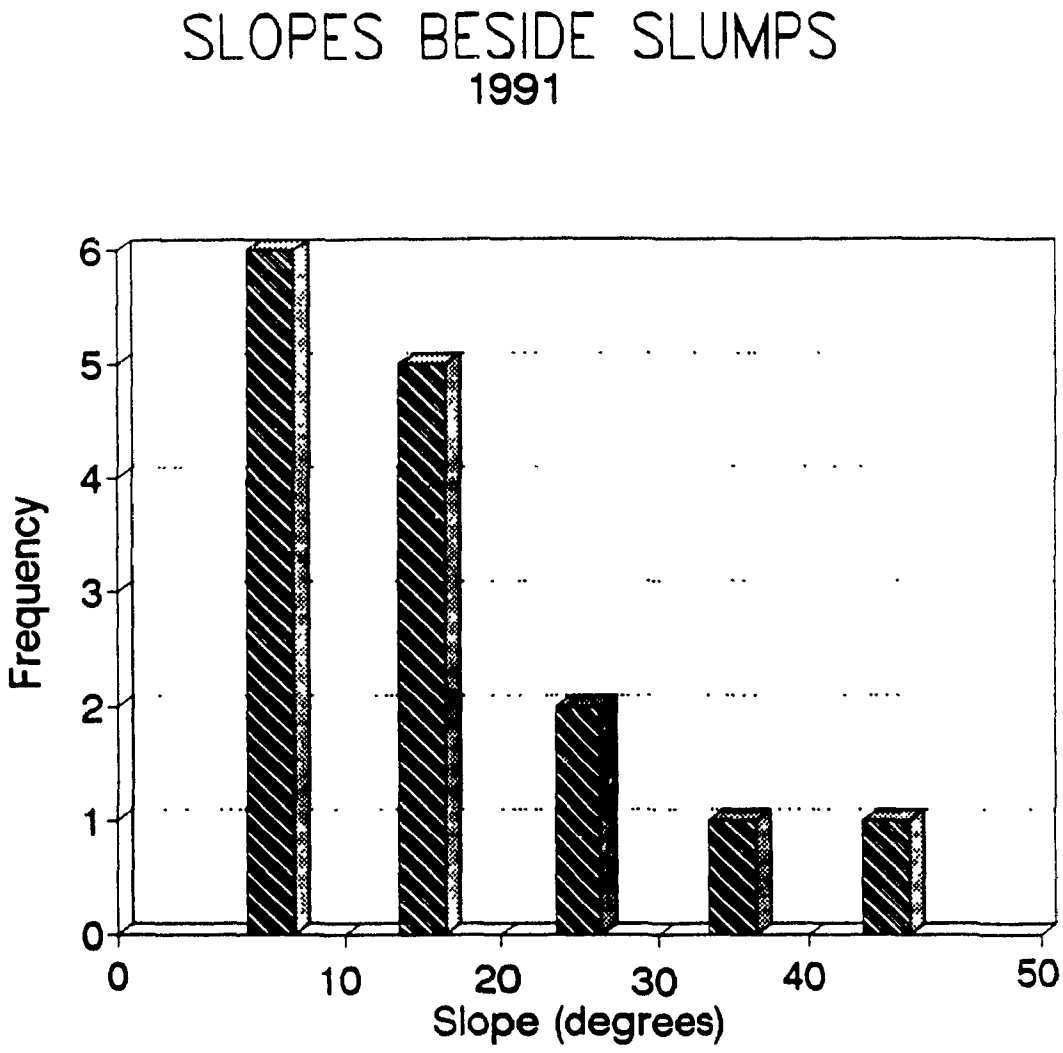

Figure 4.19 Slopes adjacent to active thaw slumps are taken as the local slope prior to modification by the slump. The majority of these slopes are comparable to those associated with active layer detachments, implying a relationship between slumps and detachments.

were less than those measured beside the slumps, and in only one case was the slope above steeper. Many of the slumps appear to be located towards the tops of the local grades. Of these, many are found part of the way up shallow valley sides while others are found at the tops of steep valley walls.

A comparison of angles of slump floors with local slopes at each site indicates that retrogressive thaw slumps tend to reduce slope gradients to about one third their former values. Thus these features do contribute to the ongoing process of planation in the Arctic, but to what overall extent is unclear as yet.

Headwall slopes shown in Figure 4.20 reveal a bimodal distribution. These slopes, while unaffected by headwall height or average ice content, may be influenced by soil characteristics such as cohesiveness. Less cohesive soils may detach and slide down an exposed ice face more easily, exposing underlying layers at the top of the headwall before the rest of the headwall can melt back,resulting in a shallower headwall slope. More cohesive soils tend to protect the ice at the headwall top while the headwall melts back, producing a steeper slope.

4.3.2 ICE WEDGES

Ice wedge polygons are ubiquitous on the Fosheim Peninsula. The large size of the polygons and the widths of the ice wedges suggest a gradual cooling period quite some time ago, possibly during the early Holocene marine

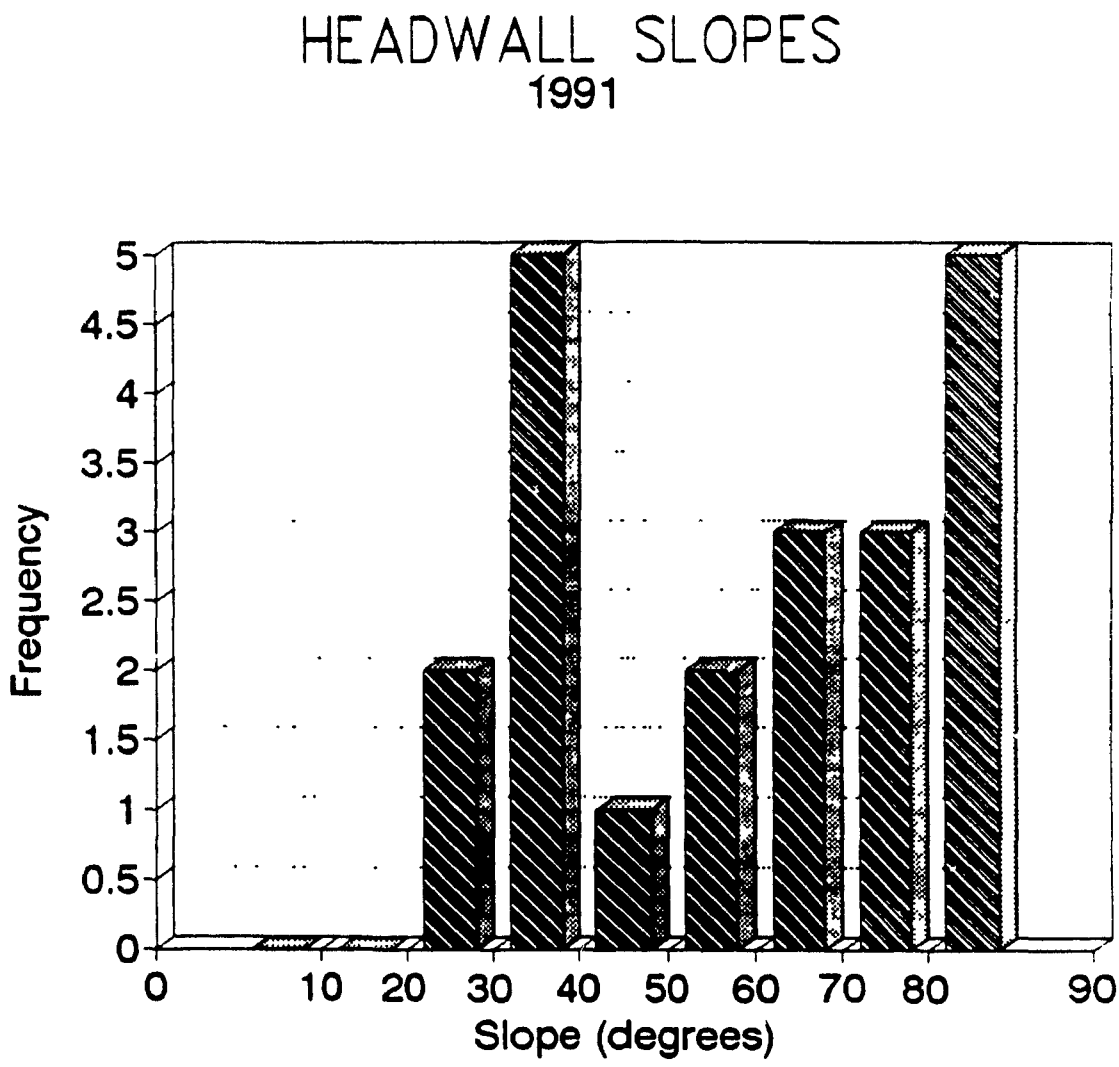

Figure 4.20 The bi-modal distribution of average headwall slopes may be due to soil characteristics such as cohesiveness, with more cohesive soils protecting the tops of headwalls longer and leading to steeper slopes.

regression. Large orthogonal polygons even appear on river flood plains in sands and gravels and on shallow slopes which appear to be undergoing solifluction, indicating that erosion, which would obscure the polygons, operates at an extremely slow pace.

4.3.3 SOIL MECHANICS

Plastic and Liquid limits for several soil samples from eight thaw slumps were tested and Plasticity Indices computed. Values of PI ranged from 3 to 20, averaging 10. These relatively low numbers were derived from plastic and liquid limits that averaged 20% and 31% moisture by dry weight respectively. When the samples were plotted along the A-Line on the Plasticity Chart for the USCS system, they clustered in the areas defined by slightly plastic clays and sand with fines or clay binder. The low values for some of the Plasticity Indices combined with low liquid limits implies that some soils would fail suddenly, with little advance deformation, even with the addition of small amounts of water.

The ice content values are, in most cases, sufficient to exceed the liquid limits of these soils, causing liquid flow. Where they are not, plastic flow can develop, but additional water from ice rich layers in other parts of the exposed headwalls is usually available to exceed the liquid limit in thaw slumps.

Even liquid limits as low as 3% would not allow liquid flow to occur due to rain fall or late season snow, as this water would simply disperse in the

active layer. Precipitation levels on the Fosheim Peninsula are insufficient to wet the active layer enough to liquify the soil, although gully erosion is common on steep slopes. However, the melting of ice-rich layers at the base of the active layer could easily supply the necessary moisture to cause liquid flow at this depth. Observations made by Edlund (personal communication) and Lewkowicz (1990) to the effect that active layer detachment slides occur more often in warm, sunny weather than in cool, wet weather seem to bear this out. Thus, an increase in summer warmth rather than precipitation could lead to increased active layer detachments, while an increase in precipitation could lead to greater gully erosion.

4.3.4 STRATIGRAPHIC RELATIONSHIPS

Ground ice occurs in two stratigraphic settings. First as shallow layers of ice interbedded with icy silt and clay and layers of sandy silt beginning just below the active layer; and second as deep massive ice overlain by five to ten metres of marine clay showing a reticulate cryotexture (Figure 4.21). Both settings exist at the Eureka and South Fosheim-2 areas, and representative stratigraphic columns are given in Figure 4.22.

The silt and sandy silt with minor gravel in which the shallow ground ice occurs is of possible near shore marine or deltaic origin (Bell, 1992). Generally, silt occurs as a shallow surface cover over ice-rich clay and silt showing reticulate or laminated ice lensing, with a gradational contact at the base of the

Figure 4 21 Massive clay with a reticulate cryotexture lies unconformably over massive ice in the Station Creek slump (EU-1) in the Eureka area The contact is marked in this instance by a thin (1 - 2 mm) layer of red sand, possibly reflecting the presence of sand beneath the massive ice

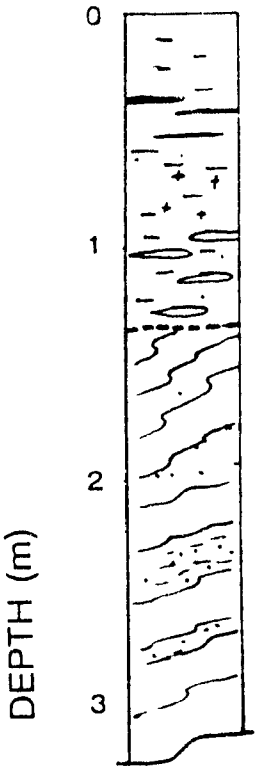

Silt and silty sand with some clay layers.

Ice veinlets and lenses in silt sandy silt.

Contact is gradational with sharp contacts in some areas.

Ice rich silt - sediment and gas bubble laminae contorted to varying degrees.

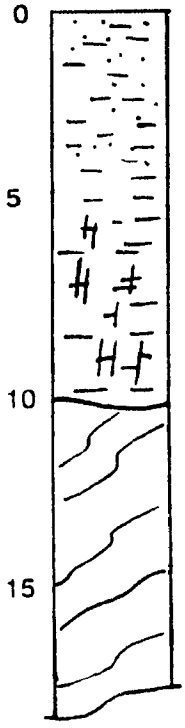

Silt and clay.

Massive clay with reticulate cryotexture.

Sharp undulating contact with thin layer of sand observed at one location.

Massive ice with contorted laminae of silt and gas bubbles.

Figure 4.22 Ground ice occurs in two general settings: 1) As shallow ice-rich silt overlain by silt and silty sand (top), and 2) As deep massive ice overlain by massive clay topped with silt (bottom).

surface silt.

GPR observations at Hot Weather Creek indicate that the top of the ice rich layer is marked by a thaw unconformity which follows the surface topography while the base may be gradational and undulating. In contrast, GPR profiles at Eureka show a gradational upper contact which varies in depth.

Massive ice which occurs beneath deep clay layers may show a sharp, undulating contact at the top of the ice, possibly indicating a thermal erosion discontinuity. In two cases a very fine layer of oxidized sand was found at the clay/ice boundary, hinting at the possible existence of a sandy layer below the massive ice. Such a structure reflects Mackay's (1971) model for the segregational formation of massive ice beds.

In many cases, both the massive ice and the icy sediments show folded and contorted laminae (both bubble trains and sediment bands) suggestive of differential loading or unloading, or tangential pressures due to creep or thrusting. As this is observed even in some shallow ground ice, it is reasonable to suppose that the ice was formed at a greater depth, or was buried after formation, and the surface was then eroded to its present level. In some slumps the degree of deformation varies markedly across the width of the headwall while in others the banding dips uniformly. Perhaps this is an indication of the scale of the disturbance, with the greater variation due to local, more intense pressure changes.

Shell fragments were seen on the surface and within the active layer as

well as in frozen sediments at several locations. While most of these could have undergone transport, articulated shells were found intact in growth position within the marine clay above the massive ice in slump EU-1 located approximately 500 metres north of Eureka on Station Creek (Pollard, personal communication)

Twenty shallow holes were drilled in 1973 at the old Eureka airstrip located a few kilometres north of the current strip on a gently rolling plain with ice wedge polygons west of Black Top Creek. Most holes were one to two metres deep with the two deepest at almost six metres. Clays and silts were predominant, with minor fine sand also encountered. Ice ranged from individual crystals to stratified ice and massive ice. Some ice may have been observed in bedrock shale, but due to the poorly lithified state of the rock and its further degradation by the ice, it was difficult to be sure that the material was actually bedrock.

Ground ice was observed in bedrock at Hot Weather Creek in 1992 by Pollard and others (personal communication), but it was of limited extent and may have been linked to the close proximity of the creek.

In general, ground ice appears to occur in two situations; one as a shallow ice-rich layer in silt and clay with an often gradational or conformable upper boundary, and the other as a deeper massive ice layer overlain unconformably by massive clay showing a reticulate ice pattern which sometimes contains shells in growth position. Both types occur in

unconsolidated shallow marine and deltaic sediments of Holocene age (Bell, personal communication to Pollard).

4.3.5 ICE CONTENT AND CHEMISTRY

An ice content profile developed from 1991 data (Figure 4.23) shows gravimetric ice contents with depth. The profile is bimodal, with a second ice occurrence below ten metres depth. Since this profile is obtained from natural exposures, few of which are deeper than eight metres, it is difficult to make generalizations about the distribution of deeper ground ice.

Samples from slump headwalls were taken at intervals of 50 cm to create ice content profiles. However, one can see in Figure 4.24 that the samples are not evenly distributed by depth. In part this due to the relative abundance of shallow slumps, but it is also due to the physical limitations of sampling inside an active slump. In the deeper slumps, the headwall could be sampled from the base up to the top of the ice face using crampons to climb on the ice. However, this was often several metres below the top of the headwall, which might contain as much as ten metres of frozen clay forming a vertical face. This face could not be climbed for sampling as it was too soft, and the continual fall of clay blocks weighing a kilogram or more made spending any time below it quite hazardous. Despite these difficulties, deep exposures showing massive ice were sampled, but those parts of the headwalls of deep slumps without massive ice were not sampled. Because of this, the

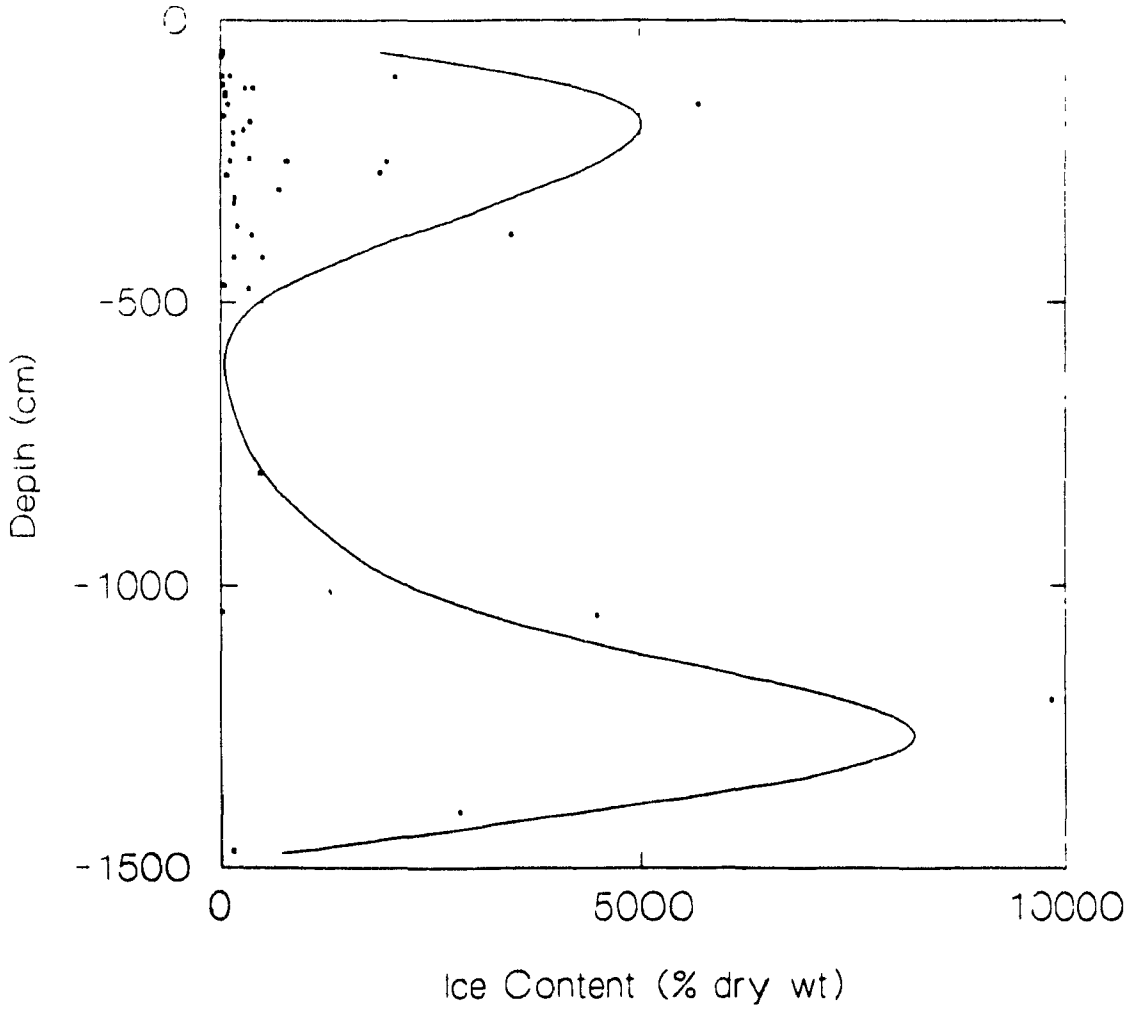

Figure 4.23 Ice content profile indicates the existence of two separate ice units with possibly different origins and histories.

SAMPLING FREQUENCY WITH DEPTH
1991

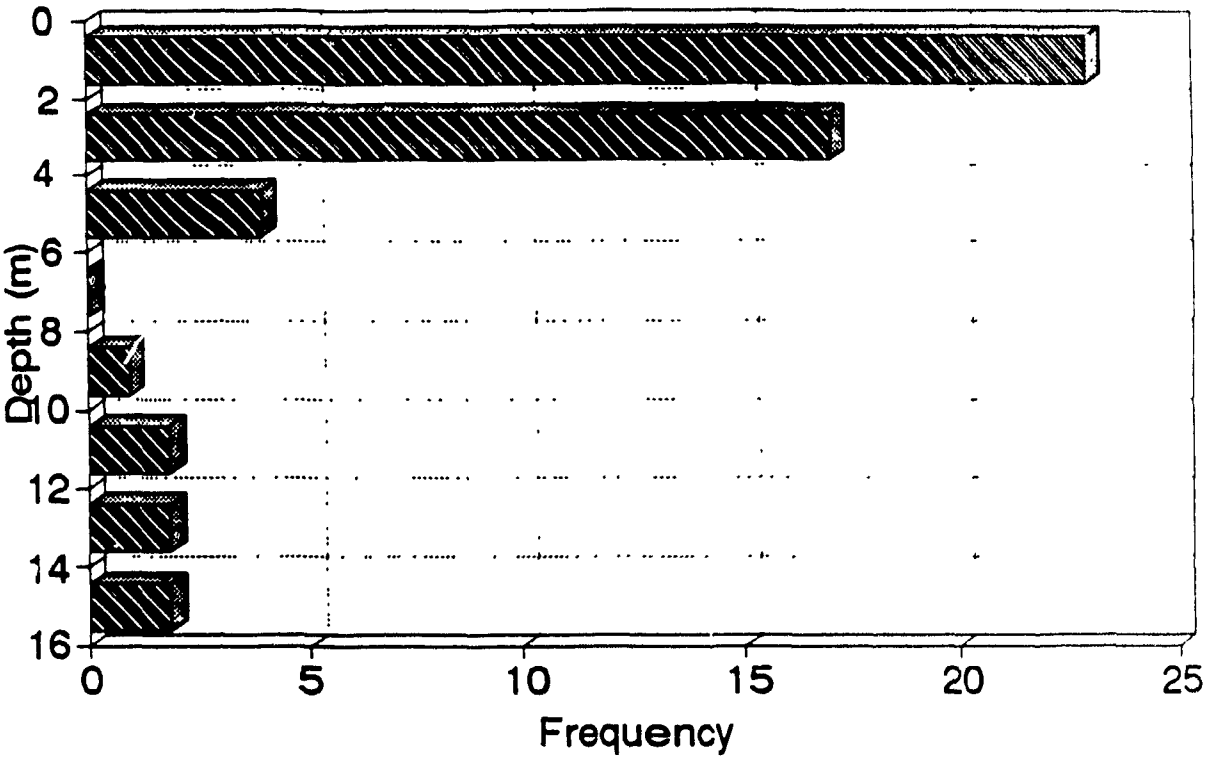

Figure 4.24 Samples are not distributed evenly with depth due to the predominance of shallow slumps and the difficulty in scaling the headwalls of larger slumps which restricted sampling to their bases. The effect on the ice content profile is minimized by the fact that the inaccessible layers contained little visible ice.

VOLUMETRIC ICE CONTENT VS DEPTH

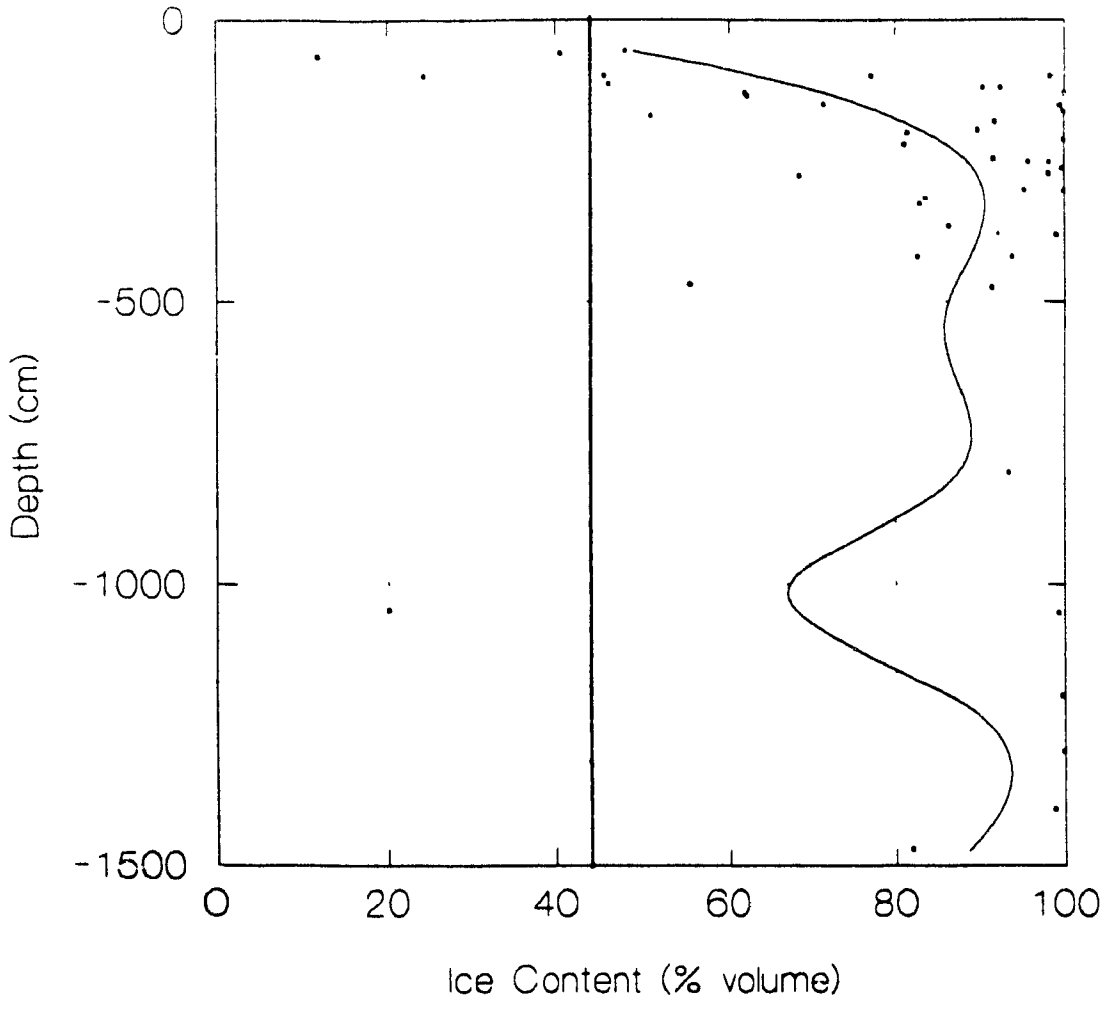

Figure 4.25 Volumetric ice profile indicating the predominance of excess ice in the study region. Average void space is assumed to be 44% for silt (Kezdi, 1974), which comprises a major portion of the surficial material.

TABLE 4.4
ICE SAMPLE CHEMISTRY

Sample	TDS (ppm)	pH
20	470	7.6
21	420	7.4
22	3300	7.7
23	2480	7.5
24	10720	7.5
24a	1870	7.8
40	270	7.4
42	110	8.2
54	200	7.4
55	≤10	6.8
72	2800	7.2
75	340	7.3
80	3960	7.2
81	2640	7.2
83	3060	7.0
84	3740	7.5
86	5640	7.2
89	15040	7.6
90	820	7.2
99	1020	7.7
100	370	7.6
101	980	7.8
111	1760	7.7

exact amounts of ice with depth might be biased slightly, especially with increased depth, but the overall shape, particularly the bimodal nature of the profile, is correct.

A depth profile of volumetric ice contents calculated from gravimetric moisture values is shown in Figure 4.25. Here the bimodal pattern seen in the gravimetric moisture profile is less evident, with the ice content for the soil column averaging about 85% by volume. Those samples with over 90% ice by volume comprise over half of the 1991 samples, while 84% contain excess ice (greater than 44% ice by volume).

Water from twenty-three ice samples taken from eight ground ice slumps was analyzed for pH and total dissolved solids (TDS). Despite the fact that the sample sites were widely distributed over the study area, there was very little variation in the results.

Typically, the water samples were neutral to basic, with pH's ranging from 6.8 in one case to 8.2, and averaging 7.4. This likely reflects the presence of carbonates in the bedrock derived sediments which were dissolved in the ground water from which the ice formed.

The level of dissolved solids in the water was found to be in the range of 10 to 15040 ppm, with most values occurring between 110 and 5640 ppm and averaging 2696 ppm. Two samples with the highest values were salty to taste, while the others were not. Given that salt encrustations on the soil surface are common in this area (likely due to their marine origin), it is

reasonable to suppose that the dissolved solids are dominated by salts.

4.4 SUMMARY

Ground probing radar results indicate that ground ice is widespread at Hot Weather Creek and that the upper contact of the ice-rich layer is abrupt and follows the terrain, indicating that it may be a thaw unconformity. Such a feature was not seen in GPR profiles from the Eureka area. Internal layering was also detected in the ground ice at both locations.

Ice wedges were detected by the GPR and served as "windows", increasing penetration depths from 10 m to 15 m in many places.

Ground ice was found to be widespread elsewhere in the study region, given the distribution of thaw slumps.

Conventional investigations of thaw slumps revealed many morphological relationships, but failed to find any clear link between ice content and slump morphology. Most controls on slump form seem to involve the local topography and soil characteristics. Controls on slump distribution are largely geological, in the form of structurally controlled river valleys and the various factors affecting asymmetrical valley development.

Ground ice was found to occur in two distinct stratigraphic settings at different depths, with ice content generally increasing with depth, and most areas having excess ice near the surface. Samples of this ice were found to be neutral to basic in pH, and to contain approximately 3000 ppm total dissolved solids, mostly as salt.

CHAPTER 5 DISCUSSION AND CONCLUSIONS

5.1 INTRODUCTION

Three central conclusions are drawn from this project:

1) Ground ice is an important component of permafrost on the Fosheim Peninsula and has been widely observed in marine sediments of Holocene age. Furthermore, ground ice appears in two distinct stratigraphic settings: as shallow icy sediment layers interbedded with sandy silt and silty clay, and as deep massive ice bodies often overlain by several metres of marine clay.

2) Ground probing radar can detect the physical differences between ice and sediment, as well as changes within the sediment itself, making this a useful and practical tool for permafrost investigation.

5.2 GROUND ICE ABUNDANCE

Ground ice was documented over a wide area in relatively high volumes and therefore and appears to be relatively widespread on the Fosheim Peninsula below marine limit. The distribution of active thaw slumps and slump scars suggests that shallow ground ice occurs in nearshore marine and deltaic silts and fine sands. Very minor occurrences in bedrock have been noted at Hot Weather Creek and in a drill core near Eureka, but the latter observation is uncertain. Given the poor state of lithification of the bedrock and the

shattering caused by frost, it is often difficult to differentiate bedrock from overburden. Since the two are so similar in character, why should ground ice not occur in both? Perhaps it does, but, given the depth of overburden on much of the peninsula, it is not widely exposed.

Deeper bodies of ground ice appear to be associated with massive clay and could possibly be of a different age than the shallow ice. However, both types of ice deposits are probably Holocene given that older ice at such a depth would likely have been thawed during the marine transgression associated with the end of the Wisconsin glaciation. Numerous shells found in marine deposits confirm a Holocene age for most of the ice bearing sediments (Hodgson, 1985).

Although deep drill data is not available, several shallow holes have been drilled at and near Eureka as well as at Hot Weather Creek. All of these have encountered varying amounts of ice, often as ice-rich layers but also as pure ice strata. These are the only other available data on ice occurrences which are not associated with thermokarst. Obviously, there is a need for a systematic drill program in this area. A drilling program by the Terrain Sciences Division of the GSC is possible in the near future, but it seems unlikely to be immediately realized given the current scarcity of funding in the federal government.

The presence of a thaw unconformity at depths of several metres may indicate an episode of deep thaw which disrupted the permafrost. This may have been a local phenomenon or a regional one, the evidence is inconclusive.

Both deep and shallow ground ice are contorted in places, possibly as the result of differential loading or unloading. Loading might be difficult to explain in such an environment if the ground ice postdates the last glaciation, but unloading due to erosion and removal of overlying sediments is certainly possible. Lateral forces due to creep appear to have also distorted the ice fabric.

Other large bodies of ground ice exist southeast of Hot Weather Creek and were investigated in 1992 by Pollard. Airphotos of that study area show isolated hills with smooth, brightly shaded tops and steep, irregular sides along the Slidre River. Similar features are visible south of the Slidre Fiord and near Eureka. These hills show a fine network of hexagonal ice wedge polygons suggestive of a rapid cooling event in well graded, ice-rich, fine grained sediments. Several researchers have commented on the possibility that these hills are ice cored or at least contain ground ice, but only recently has any ice been observed, and it is overlain by several metres of sediment (Pollard, personal communication). These hills will have to be made priority targets for drilling and/or deep radar profiling.

5.2.1 POSSIBLE CONSEQUENCES OF CLIMATE CHANGE

Predictions of warming and increased precipitation in arctic areas (Houghton *et al.*, 1990) have lead to speculations about the potential for increased terrain disturbance in areas underlain by ice-rich permafrost and

massive ground ice. An increase in average air temperature would warm the permafrost, leading to a more thaw-sensitive situation. This could result in the partial thawing of ice-rich sediments over a large portion of the study area. Enhanced active layer thicknesses can be very roughly estimated using the following equation:

$$z = (\alpha P/\pi)^{1/2} (\ln \mid A_o/T_o \mid) \qquad [5.1]$$

where z = Active layer thickness (cm)

α = soil thermal diffusivity (1.67×10^{-3} cm^2/sec)

P = period of thermal wave (1 year = 31 536 000 sec)

π = pi

A_o = surface temperature amplitude (°C)

T_o = mean annual surface soil temperature (°C)

(For an example see Gold and Lachenbruch, 1973)

Given monthly mean air temperature increases of 4.8°C for winter and 1.8°C for summer on Ellesmere Island as predicted by equilibrium Global Circulation Models for a doubling of CO_2 concentration (Houghton *et al.*, 1990), active layer thicknesses can be expected to increase from an average present value of about 54 cm to a new depth of 78 cm, or by about 45%. Of course, this estimate does not allow for changes in precipitation regimes, of which snow cover is as important as air temperature. However, one can see that active layer growth will likely affect soil which is currently ice-rich, and that

there is the potential for substantial subsidence and terrain disturbance.

5.3 UTILITY OF GROUND PROBING RADAR

Ground probing radar is probably the geophysical tool best suited for ground ice investigations. It responds relatively well to the conditions created by the presence of ground ice, can be used to detect freeze/thaw boundaries, and provides information on shallow geologic structures as well. Recent hardware and software developments have greatly streamlined the process of producing a final product from the initial data. Interpreting the data, however, requires considerable skill and experience in order to fully utilize all of the information provided by this system. Fortunately, rudimentary interpretations can be carried out by researchers with only basic knowledge of GPR analytical techniques. One need not be a specialist to successfully use this system.

Like all highly sophisticated electronic equipment designed for use in the field, GPR units work best indoors. Also, shipping the components thousands of kilometres to the field area, and then transporting them to the survey sites can rival the rigors of actual field use. In fact, the potential for damage from transportation in the field restricts surveys to those which can be reached by foot or by helicopter. In October 1991, a two kilometre trip cross country in a half-track truck rendered the Pulse EKKO IV-H useless despite the extensive precautions taken to protect it. This is not to say that the unit was poorly made, but that the terrain was very rough. Transporting the system by a small

"All Terrain Vehicle" would simply not be worth the risk. Thus flying the unit to a site or backpacking it are the only alternatives.

If transportation damage can be avoided, and it usually can be, the GPR tends to perform well in the field. Two units by Sensors and Software Inc., a Pulse EKKO III and a Pulse EKKO IV-H prototype, were used for this project. They were used in both summer and in late fall (-20°C average temperature with blowing snow) conditions and both units proved to be reliable in the field, save for some minor design and software problems with the prototype. However, after two or three weeks of use, both units failed (coincidentally) on the final day of field work, suggesting a short life between repairs. Fortunately, this did not affect the project in a major way. Other researchers have used the Pulse EKKO IV production unit for extended periods without any mishaps (Judge, personal communication).

A major advantage to using GPR over many other geophysical methods is the speed and ease with which surveys can be carried out. A two person team with little special training can cover several kilometres per day in good conditions. This is especially true on open tundra where there are few, if any, obstructions. Thus a large amount of data can be gathered in a short field excursion. The method is also non-surface disruptive, so environmental impact is negligible.

Of the centre frequencies used, 25 and 50 MHz provided results with the greatest combination of depth penetration, resolution, and lack of interference

The 50 MHz profiles revealed details of the ground ice and near surface structure while the 25 MHz profiles were used to interpret the deeper structures. However, interpretation would be greatly aided with the addition of drill data to depths of ten metres or more. Natural exposures in the GPR survey areas only provided two to three metres of stratigraphic control.

5.4 FUTURE RESEARCH

The Fosheim Peninsula will remain an important area for permafrost and other fields of research because of its varied environments and the access to logistical support through the Polar Continental Shelf Project (PCSP) facilities at Eureka, as well as the weather station there.

Much work remains to be done on ground ice occurrences to determine the history of formation of the ice-rich and massive ice bodies, as well as on the quaternary geology of the region. Such work is currently being carried out, and would definitely benefit from a drilling program. A systematic drilling program would greatly improve the understanding of this area, and the data it generated would serve as an enticement to other researchers who are discouraged from working in the region due to the lack of background information. Such a program must be carried out by a combination of government and universities, because, unlike the western Arctic, private resource exploration companies are not attracted to the area. This fact has been largely responsible for the lack of research in the high Arctic.

Another area of permafrost research which has been overlooked in this region is the formation of ice wedges. While extensive data exists for the western Arctic, it is practically non-existent in the high Arctic. Given that ice wedge polygons are widespread on the Fosheim, this would be a significant area of research.

Remote sensing applications are being explored in permafrost regions with a view to monitoring global change. The CRYSYS Project (CRYosphere SYStems) was begun in 1991 by the Canada Centre for Remote Sensing to bring together researchers from government and universities to study various aspects of the cryosphere, including permafrost, using the latest generation of satellite remote sensing platforms. This long term project will greatly expand the state of knowledge on high Arctic permafrost if ways can be found to collect the necessary ground truth data. The high cost of research in this region will remain a major hinderance to workers for quite some time to come, but it is hoped that as more information becomes available in the literature, more researchers will be encouraged to go to the Fosheim Peninsula.

REFERENCES

A - Cubed, Inc. 1986. Development of the Pulse EKKO III Profiling Radar System. UP - 352 Final Report (unpublished).

AES Environment Canada, 1982. Canadian Climate Normals 1951-1980 Temperature and Precipitation -- The North - Y.T. and N.W.T. Atmospheric Environment Service, Environment Canada.

Annan, A.P., Davis, J.L. and Scott, W.J. 1975. Impulse Radar Wide Angle Reflection and Refraction Sounding in Permafrost. *In:* Report of Activities Part C, Geological Survey of Canada, Paper 75-1C.

Annan, A.P. and Davis, J.L. 1976. Impulse Radar Sounding in Permafrost. Radio Science v 11, 4; pp. 383-394.

Arcone, S.A., Sellmann, P.V. and Delaney, A.J., 1982. Radar detection of ice wedges in Alaska. CRREL Report 82-43, US Army Corps of Engineers, Cold Regions Research and Engineering Laboratory.

Balkwill, H.R. and Bustin, R.M. 1975. Stratigraphic and structural studies, central Ellesmere Island and eastern Axel Heiberg Island, District of Franklin. *In:* Report of Activities, Part A, Geological Survey of Canada, Paper 71-1A, p. 513-517.

Barry, P.J. and Pollard, W.H. in press. Ground probing radar investigations of ground ice on the Fosheim Peninsula, Ellesmere Island, N.W.T. The Musk-Ox. Department of Geological Sciences, University of Saskatchewan, Saskatoon.

Bell, T. 1992. Glacial and Sea Level History, Western Fosheim Peninsula, Ellesmere Island, High Arctic Canada. Unpublished PhD. thesis, University of Alberta, Edmonton, Alberta.

Blake, W., Jr. 1970. Studies of glacial history in Arctic Canada. I. Pumice, radiocarbon dates, and differential postglacial uplift in the Eastern Queen Elizabeth Islands. Canadian Journal of Earth Sciences. v. 7, p. 634-664.

Bostock, H.H 1970. Physiographic Regions of Canada. Geological Survey of Canada map 1245A. Scale 1:5 000 000.

Brown, R.J.E. 1974. Some Aspects of Airphoto Interpretation of Permafrost in Canada. National Research Council of Canada, Division of Building Research Technical Paper No. 409.

Bustin, R.M. 1982. Beaufort Formation, eastern Axel Heiberg Island, Canadian Arctic Archipelago. Canadian Petroleum Geology, Bulletin, v. 30, p. 140-149.

Dallimore, S.A. and Davis, J.L., 1987. Ground probing radar investigations of massive ground ice and near surface geology in continuous permafrost. *In:* Current Research, Part A, Geological Survey of Canada, Paper 87-1A, pp. 913-918.

Davis, J.L., Scott, W.J., Morey, R.M. and Annan, A.P. 1976. Impulse Radar Experiments on Permafrost Near Tuktoyaktuk, Northwest Territories. Canadian Journal of Earth Sciences v 13; pp. 1584-1590.

EBA Engineering Consultants Ltd. 1990. Mackenzie Valley Geotechnical Database Phase 1 Final Report (unpublished).

Edlund, S.A. 1983. Bioclimatic zonation in a high Arctic region: Central Queen Elizabeth Islands. *In:* Current Research, Part A, Geological Survey of Canada, Paper 83-1A, pp. 381-390.

Edlund, S.A., Taylor, B.A. and Young, K.L. 1989. Interaction of climate, vegetation and soil hydrology at Hot Weather Creek, Fosheim Peninsula, Ellesmere Island, N.W.T. *In:* Current Research, Part D, Paper 89-1D, pp. 125-133.

England, J. 1976. Late Quaternary glaciation of the Eastern Queen Elizabeth Islands, N.W.T., Canada: alternative models. Quaternary Research, v. 6, pp. 185-202.

England, J. 1978. The glacial geology of Northeast Ellesmere Island. Canadian Journal of Earth Sciences, v. 15, p. 603-617.

England, J. 1983. Isostatic adjustments of a full glacial sea. Canadian Journal of Earth Sciences, v. 20, p. 895.

England, J. and Bradley, R.S. 1978. Past glacial activity in the Canadian high Arctic. Science, v. 200, p. 265.

French, H.M. and Harry, D.G. 1990. Observations on buried glacier ice and massive ice, western Arctic coast, Canada. Permafrost and Periglacial Processes, v. 1, pp. 31-43.

Goodwin, C.W., Brown, J. and Outcalt, S.I. 1984. Potential responses of permafrost to climatic warming. *In:* Carbon Dioxide-Induced Climatic Changes in Alaska, McBeath, J.M., ed., pp. 92-105.

Gold, L.W. and Lachenbruch, A.H. 1973. Thermal Conditions in Permafrost - A review of North American literature *In:* Proceedings of the Second International Conference on Permafrost. Yakutsk, USSR, National Academy of Sciences, Washington, D.C., pp.3-25.

Gowan, R.J. and Dallimore, S.R. 1990. Ground ice associated with granular deposits in the Tuktoyaktuk coastlands area, N.W.T. *In:* Permafrost Canada, Proceedings of the Fifth Canadian Permafrost Conference, Collection Nordicana, Centre d'études nordiques, Université Laval, pp. 283-290.

Hall, D.K., McCoy, J.E., Cameron, R.M., van Etten, P. and Stamm, M. 1980. Remote Sensing of Arctic Hydrologic Processes. Proceedings of the Third Colloquium on Planetary Water, Niagara Falls, N.Y., Oct. 27-29, 1980.

Hatton, L., Worthington, M.H. and Makin, J. 1986. Seismic Data Processing - Theory and Practice. Blackwell Scientific Publications.

Hodgson, D.A. 1985. The last glaciation of west-central Ellesmere Island, Arctic Archipelago, Canada. Canadian Journal of Earth Sciences, 22, 347-368.

Hodgson, D.A. 1989a. Surfic[illegible]terials, (Queen Elizabeth Islands). *In:* Chapter 6 of Quaternary Geology of Canada and Greenland, R.J. Fulton, ed.; Geological Survey of Canada, Geology of Canada, no. 1, (also Geological Society of America, The Geology of North America, v. K-1).

Hodgson, D.A. 1989b. Introduction (Quaternary Geology of the Queen Elizabeth Islands). In: Chapter 6 of Quaternary Geology of Canada and Greenland, R.J. Fulton, ed.; Geological Survey of Canada, Geology of Canada, no. 1, (also Geological Society of America, The Geology of North America, v. K-1).

Houghton, J.T., Jenkins, G.J. and Ephraums, J.J. (eds.) 1990. Climate Change: The IPCC Scientific Assessment. Published for the Intergovernmental Panel on Climate Change. Cambridge University Press, Cambridge, 364 p.

Judge, A.S., Taylor, A.E., Burgess, M. and Allen, V.S. 1981. Canadian geothermal data collection - Northern wells 1978-1980. Geothermal Series, No. 12, Earth Physics Branch, Energy Mines and Resources.

Kezdi, A. 1974. Handbook of Soil Mechanics, Volume 1: Soil Physics. Elsevier Scientific Publishing Co., Amsterdam, Holland, 294 p.

Kerr, J.W. 1981. Evolution of the Canadian Arctic Islands: a transition between the Atlantic and Arctic Oceans. *In:* The Ocean Basin Margin, Volume 5, The Arctic Ocean. Nairn, Churkin, and Stehli, eds. Plenum Press, N.Y., pp. 115-199.

Kinney, R.P. 1986. Massive ice detection by earth resistivity. *In:* Proceedings of the Fourth International Conference on Cold Regions Engineering, Ryan, W.L., ed. pp. 472-481.

Kovacs, A. and Morey, R.M. 1979. Remote Detection of Massive Ice in Permafrost Along the Alyeska Pipeline and the Pump Station Feeder Gas Pipeline. CRELL Report reprinted from: Proceedings of the Specialty Conference on Pipelines in Adverse Environments. ASCE, New Orleans, Jan. 15-17, 1979.

LaFleche, P.T., Judge, A.S., Moorman, B.J., Cassidy, B. and Bedard, R. 1988. Ground probing radar investigations of gravel roadbed failures, Rae Access road, N.W.T. *In:* Current Research, Part D, Geological Survey of Canada, Paper 88-1D, pp. 129-135.

Lambe, W.T. 1951. Soil Testing for Engineers. John Wiley and Sons New York, 165 pp.

Leschack, L.A., Morse, F.H., Brinley, W.R., Ryan, N. and Ryan, R. 1973. Potential use of airborne duel-channel infrared scanning to detect massive ice in permafrost. *In:* Permafrost, Second International Conference, Yakutsk, U.S.S.R., July 13-28, 1973, pp. 542-549.

Leschack, L.A. and Del Grande. 1976. A duel wavelength thermal infrared scanner as a potential airborne geophysical exploration tool. Geophysics, v. 41, no. 6, pp. 1318-1336.

Lewkowicz, A.G. 1990. Morphology, frequency, and magnitude of active-layer detachment slides, Fosheim Peninsula, Ellesmere Island, N.W.T. In: Permafrost Canada, Proceedings of the Fifth Canadian Permafrost Conference, Collection Nordicana, Centre d'études nordiques, Université Laval, pp. 111-118.

Lougeay, R. 1973. Detection of buried glacial and ground ice with thermal infrared remote sensing. *In:* Advanced Concepts and Techniques in the Study of Snow and Ice Resources. Santeford H., Smith H.L. (eds.). National Academy of Sciences, Washington, DC. pp. 487-493.

Lougeay, R. 1981 Potentials of mapping buried glacier ice with Landsat thermal imagery. *In:* Satellite Hydrology. (Deutch, Wiesnet, Rango. eds.) Proceedings of the 5th Annual William T. Pecora Memorial Symposium on Remote Sensing, 10-15 June, 1979. American Water Resources Association, Minneapolis, MN. pp. 189-192.

Mackay, D., Charles, M. and Phillips, C. 1974. Physical Aspects of Crude Oil Spills on Northern Terrain (second report). Task Force on Northern Oil Development report no. 74-25.

Mackay, D., Ng, T. W., Shiu, W. Y. and Reuber, B. 1979. The Degradation of Crude Oil in Northern Soils. Department of Indian and Northern Affairs, Environmental Studies report no. 18.

Mackay, J.R. 1963. The Mackenzie Delta area, N.W.T. Geographical Branch, Department of Mines and Technical Surveys, Ottawa, Memoir 5, 202p.

Mackay, J.R. 1971. The origin of massive icy beds in permafrost, western Arctic, Canada. Canadian Journal of Earth Sciences, 8: pp. 397-422.

Mackay, J.R. 1972. The world of underground ice. Annals of the Association of American Geographers, v. 62, no. 1, pp. 1-22.

Mackay, J.R. 1975a. The stability of permafrost and recent climatic change in the Mackenzie Valley, N.W.T. Geological Survey of Canada, Paper 75-1, Part B. *In:* Report of Activities, Part B.

Mackay, J.R. 1975b. Some resistivity surveys of permafrost thickness, Tuktoyaktuk Peninsula, N.W.T. *In:* Report of Activities, Part B, Geological Survey of Canada, Paper 75-1B, pp. 177-180.

Mackay, J.R. 1977. Changes in the active layer from 1968 to 1976 as a result of the Inuvik fire. *In:* Report of Activities, Part B, Geological Survey of Canada, Paper 77-1B, pp. 273-275.

Mackay, J.R. 1982. Active layer growth, Illisarvik experimental drained lake site, Richards Island, Northwest Territories. *In:* Current Research, Part A, Geological Survey of Canada, Paper 82-1A, pp. 123-126.

Mackay, J.R. 1989. Massive ice: some field criteria for the identification of ice types. *In:* Current Research, Part G. Geological Survey of Canada, Paper 89-1G, pp. 5-11.

McCann, D.M, Jackson, P.D., Fenning, P.J. 1988. Comparison of the seismic and ground probing radar methods in geological surveying. IEE Proceedings v. 135, Part F, #4, pp. 380.

O'Connor Associates Environmental Inc. 1990. Preliminary Report: Environmental Investigation, Eureka, Ellesmere Island, N.W.T. (unpublished).

Ostercamp, T.E. 1984. Potential impact of a warmer climate on permafrost in Alaska. *In:* Carbon Dioxide-Induced Climatic Changes in Alaska, McBeath, J.H., ed., pp. 106-113.

Patterson, D.E. and Smith, M.W. 1981. The Measurement of Unfrozen Water Content by Time Domain Reflectometry: Results from Laboratory Tests. Canadian Geotechnical Journal, v 18, 1; pp.131.

Permafrost Subcommittee. 1988. Glossary of Permafrost and Related Ground-Ice Terms. Associate Committee on Geotechnical Research, National Research Council of Canada Technical Memorandum No. 142.

Péwé, T.L. 1983. Alpine permafrost in the contiguous United States. Arctic and Alpine Research, 15, 145-156.

Pollard, W.H. 1990. The nature and origin of ground ice in the Herschel Island area, Yukon Territory. *In:* Permafrost Canada, Proceedings of the Fifth Canadian Permafrost Conference, Collection Nordicana, Centre d'études nordiques, Université Laval, pp. 23-30.

Pollard, W.H. 1991. Observations on massive ground ice on Fosheim Peninsula, Ellesmere Island, Northwest Territories. *In:* Current Research, Part E, Geological Survey of Canada, Paper 91-1E, pp. 223-231.

Pollard, W.H. and French, H.M. 1980. A first approximation of the volume of ground ice, Richards Island, Pleistocene Mackenzie delta, NWT. Canadian Geotechnical Journal, 17, pp. 509-516.

Pollard, W.H. and Dallimore, S.R. 1989. Petrographic characteristics of massive ground ice, Yukon Coastal Plain, Canada. *In:* Permafrost, Fifth International Conference Proceedings, v.I,, Tapir Publishers, Trondheim, Norway, pp. 224-229.

Prakla - Seismos. 1978. Migration. Prakla - Seismos Digest Volume 1, Extracts from reports 1971 - 1977, Hannover, Germany.

Rampton, V.N. and Walcott, R.I. 1974. Gravity profiles across ice cored topography. Canadian Journal of Earth Science, v. 11, pp. 110-122.

Shamanova, I.I. and Parmuzin, S.Y. 1988. Some aspect of the impact of climate on the development of thermokarst in the low-temperature cryolithozone of northern Yakutia. *In:* Polar Geography and Geology, vol. II, Winston & Sons, pub., pp.306-312.

Smith, M.W. and Riseborough, D.W. 1983. Permafrost sensitivity to climatic change. *In:* Permafrost, Fourth International Conference Proceedings, pp. 1178-1183.

Solomatin, V.I. 1986. Petrogenesis of Underground Ice Types. Academy of Sciences of U.S.S.R. Siberian Branch, Novosibirsk, Nauka. 215 p. (Translated excerpt courtesy of Pollard from Solomatin).

Stewart, T.G. and England, J. 1983. Holocene sea-ice variations and paleoenvironmental change, northernmost Ellesmere Island, N.W.T., Canada. Arctic and Alpine Research, v. 15, pp. 1-17.

Taylor, A.E. 1991. Holocene paleoenvironmental reconstruction from deep ground temperatures: a comparison with paleoclimate derived from the $\delta^{18}O$ record in an ice core from the Agassiz Ice Cap, Canadian Arctic Archipelago. Journal of Glaciology, v. 37, no. 126, pp. 209-219.

Thorsteinsson, R. 1971. Geology of Slidre Fiord, District of Franklin. Geological Survey of Canada map 1298A, scale 1:50 000.

Thorsteinsson, R. and Tozer, E.T. 1970. Geology of the Arctic Archipelago. *In:* Geology and Economic Minerals of Canada, R.J.W. Douglas, ed. Geological Survey of Canada Economic Geology Report 1, 5th edition, pp. 548-590.

Ulriksen, C.P. 1982. Application of Impulse Radar to Civil Engineering. Doctoral Thesis, Department of Engineering Geology Lund University of Technology, Sweden.

Wray, W.K. 1986. Measuring Engineering Properties of Soils. Department of Civil Engineering, Texas Technical University. Prentice-Hall International Series in Civil Engineering and Engineering Mechanics. Prentice-Hall Inc., Englewood, NJ. 276 pp.